An Investigation of the Integrity of Two Components of the Cerebellar Neurocircuitry Involved in Classical Eyeblink Conditioning in Children Prenatally Exposed to Alcohol: A Magnetic Resonance Spectroscopy and Functional Magnetic Resonance Imaging Study

Lindie du Plessis

Department of Human Biology

University of Cape Town

Thesis presented for the degree of

Doctor of Philosophy

October 2014

Abstract

An Investigation of the Integrity of Two Components of the Cerebellar Neurocircuitry Involved in Classical Eyeblink Conditioning in Children Prenatally Exposed to Alcohol: A Magnetic Resonance Spectroscopy and Functional Magnetic Resonance Imaging Study

Impairment in classical eyeblink conditioning (EBC) has previously been reported in children with fetal alcohol spectrum disorders (FASD) (Jacobson et al., 2008). The deep cerebellar nuclei and cerebellar cortex are critical elements of the cerebellar-brainstem circuitry that mediates EBC (Green et al., 2002a; Yeo and Hardiman, 1992; Perret et al., 1993). In this study, we used magnetic resonance spectroscopy (MRS) and functional MRI (fMRI) to assess the effects of prenatal alcohol exposure on brain metabolism in the cerebellar deep nuclei and brain function in the cerebellar cortex, respectively.

We found that higher levels of prenatal alcohol exposure were associated with lower levels of both N-Acetylaspartate (NAA) and choline-containing metabolites, and with higher levels of glutamate plus glutamine (Glx), suggesting a disruption of the glutamate–glutamine cycling involved in glutamatergic excitatory neurotransmission. Since the interpositus nucleus is one of the most crucial structures in the acquisition of the EBC response, abnormal metabolism in this region could be responsible for altered synaptic plasticity in children with FASD.

Of the four cerebellar regions that were identified as being activated more by control children during rhythmic vs. non-rhythmic finger tapping, smaller differences in BOLD (blood oxygenation level dependent) activation were observed in children with FASD in two, namely vermis IV-V and right Crus I. Increasing levels of prenatal alcohol exposure were, however, associated with smaller differences in activation in all four regions, all of which have previously been linked to timed responses.

In the paced/unpaced finger tapping fMRI study, we found four regions where increased BOLD activation during unpaced tapping compared to rest was associated with improved ability to maintain rhythm as evidenced by lower intertapping variability – right VIIIa and b, left VIIIa and right VI. These regions have previously been implicated in motor control with additional evidence of timing in lobule VI. In three of the regions, all except right VIIIa, increasing alcohol exposure was related to smaller increases in activation during unpaced tapping, with the strongest relations seen in the dosage dependent variable. Interestingly, the location of the activation in right VI is similar to a region that has been implicated in studies of EBC (Blaxton et al., 1996; Cheng et al., 2008).

Our results point to altered metabolic levels in the deep nuclei and reduced functioning of several cerebellar cortical regions in children with FASD, highlighting the extensive damage caused by prenatal alcohol exposure. Although we did not find associations of EBC performance with either metabolite levels or activity in these regions, suggesting that damage to these areas are not primarily responsible for the observed EBC deficit, the extent of this damage could play a role in the impaired EBC performance seen in these children.

Acknowledgements

Firstly, I need to thank and acknowledge the support, encouragement and advice from my supervisor, Associate Prof Ernesta M. Meintjes, who has assisted me in transferring from a chemical background to medical imaging - not an easy feat! Without too much elaboration, I can truly say that I could not have asked for a better mentor in the department.

To all the co-authors of my articles, I am very grateful for their input and suggestions. Especially to Joseph and Sandra Jacobson, I express my gratitude for allowing me to assist in their study.

Thank you to the NRF for funding my studies, and the NRF and NIH for funding the project as a whole

Very importantly, I also need to thank my parents, Johan and Joey du Plessis, my sister and brother-in-law, Elmarie and Stian Mouton, as well as their children Kian and Linmarie for their constant support during all my endeavours.

List of Abbreviations

Abbreviation	Description
AA	absolute alcohol
ALE	activation likelihood estimate
AMPA	α-Amino-3-hydroxy-5-methyl-4-isoxazolepropionic acid
ANCOVA	analysis of covariance
ANOVA	analysis of variance
ARBD	alcohol-related birth defects
ARND	alcohol-related neurodevelopmental disorders
BOLD	blood oxygenation level dependent
CBF	cerebral blood flow
CBV	cerebral blood volume
$CMRO_2$	cerebral metabolic rate of oxygen
Cho	glycerophosphocholine plus phosphocholine
CR	conditioned response
CS	conditioned stimulus
CSF	cerebrospinal fluid
CUBIC	Cape Universities Brain Imaging Centre
DGG	ɣ-D-glutamylglycine
EBC	eyeblink conditioning
emf	electromagnetic field
EPI	echo planar imaging
FAS	fetal alcohol syndrom
FAS/PFAS	combined FAS and PFAS
FASD	fetal alcohol spectrum disorder
fMRI	functional magnetic resonance imaging
FWHM	full-width at half maximum
GABA	Gamma-aminobutyric acid
GLM	general linear model
Gln	glutamine
Glu	glutamate
Glx	glutamate plus glutamine
GM	gray matter
GPC	glycerophosphocholine
H	hydrogen

Abbreviation	Description
HE	heavily exposed
Hz	Hertz
Ins	myo-Inositol
IOM	Institute of Medicine
IQ	intelligence quotient
ISI	inter-stimulus interval
ITI	inter-tapping interval
JSAIS	Junior South African Intelligence Scale
kHz	kilohertz
LTD	long term depression
LTP	long term potentiation
MHz	megahertz
mM	millimolar
MNI	Montreal Neurological Institute
MPRAGE	magnetization-prepared rapid gradient echo
MR	magnetic resonance
MRI	magnetic resonance imaging
MRS	magnetic resonance spectroscopy
ms	milliseconds
Na	sodium
NAA	N-acetyl aspartate
NMDA	N-methyl-D-aspartate
NMR	nuclear magnetic resonance
oz	ounces
P	phosphorus
PCh	phosphocholine
PET	positron emission tomography
PFAS	partial fetal alcohol syndrome
PPVT	Peabody Picture Vocabulary Test-Revised
PRESS	point-resolved spectroscopy
PTX	Picrotoxin
rCBF	regional cerebral blood flow
RF	radiofrequency
ROI	region of interest
s	seconds
SD	standard deviation
SNR	signal-to-noise-ratio

Abbreviation	Description
SPM	Statistical Parametric Mapping
SUIT	spatially unbiased atlas template
SVD	singular value decomposition
tCr	creatine plus phosphocreatine
TE	echo time
TR	repetition time
UR	unconditioned response
US	unconditioned stimulus
VOI	volume of interest
WISC-IV	Wechsler Intelligence Scale for Children-IV
WM	white matter

Table of Contents

List of Figures

List of Tables

Preface

This thesis presents a neuroimaging study of two key components of the cerebellar circuit associated with classical eyeblink conditioning (EBC) in children with fetal alcohol spectrum disorders (FASD). Previous studies have found that children prenatally exposed to alcohol are unable to acquire a reflex response requiring millisecond accuracy, while control children are able to do so (Jacobson et al., 2008; 2011). Millisecond timing has been shown to be, at least in part, mediated by the cerebellum (Diedrichsen et al., 2007; Ivry et al., 1998; 2002; Ivry and Keele, 1989; Jueptner et al., 1995; Penhune et al., 1998; Schlerf et al., 2007; Spencer et al., 2003).

This thesis includes three independent articles using different methodologies to identify cerebellar anomalies that may play a role in the observed EBC deficit. These articles are found in chapters four to six. Although the overall motivation of the study was the impaired performance of children with FASD in EBC, these articles were not compiled as such, but focused on altered metabolism in the cerebellar deep nuclei and altered functioning in the cerebellar cortex – neurocircuitry previously implicated in EBC. Outcomes were not compared to EBC measures, but instead, individually investigated different aspects that could contribute to the overall study. In all three articles, my contribution to the papers was assistance with data acquisition, analysis of the data and writing of the articles. The combination of three independent articles into the thesis does, however, lead to necessary repetition as each article in itself consists of an introduction, methods, results and discussion.

In chapter one a complete background for the motivation of the study is given. FASD and its manifestations are firstly described to familiarize the reader with the subject group. Classical EBC and the deficient performance seen in the alcohol exposed children is then

elaborated on, followed briefly by an explanation of the neuroimaging procedures we used to assess specific aspects of the neurocircuitry involved in EBC.

The second chapter contains a description of the cerebellum on a gross and histological scale and then proceeds to discuss previous studies of cerebellar-mediated timing. The specific neurociruitry in the cerebellum responsible for successful EBC is then covered.

Chapter three briefly describes the neuroimaging methods employed in this study – magnetic resonance spectroscopy (MRS) and functional magnetic resonance imaging (fMRI).

The first article, which has been published in the journal Alcoholism: Clinical and Experimental Research, is in chapter four with the permission of John Wiley and Sons, Ltd. In this article, MRS was used to assess possible differences in the chemical environment between children with FASD and control children in a structure previously identified as crucial for EBC – the cerebellar deep nuclei.

This article was co-authored by Joseph L. Jacobson, Sandra W. Jacobson, Aaron T. Hess, André van der Kouwe, Malcolm J. Avison, Christopher D. Molteno, Mark E. Stanton, Jeffry A. Stanley, Bradley S. Peterson and Ernesta M. Meintjes.

Chapter five contains the first of two fMRI studies assessing functional activity during a finger tapping task. In this task, the children were required to press a button in synchrony with an auditory metronome emitting sounds either at a steady pace or randomly. The goal of this study was to evaluate activity in cerebellar cortical structures associated with timing by studying activations during actions where a rhythm is learned compared to actions that are randomly assigned. It is assumed that the internal timing mechanism used during this task is the same as that required for an EBC response.

This article is has been submitted to the journal Neuroimage: Clinical and is currently under review. The co-authors of this article are Joseph L. Jacobson, Frances C. Robertson, Sandra W. Jacobson, Christopher D. Molteno and Ernesta M. Meintjes.

The second fMRI article forms chapter six. In this task, the children were asked to tap their fingers in synchrony with a steadily-paced auditory metronome and keep tapping at the same speed once the metronome stops after emitting 12 tones. Once again, it is assumed that the neurocircuitry used in this task is also used in EBC and possible differences in activation patterns between the diagnostic groups were investigated when the children were required to maintain a steady pace of motion with no metronome. However, the contrast of self-paced finger tapping was compared to rest and therefore contributions from motor control were to be expected. This article is currently under review by the co-authors, who are the same as for the article in chapter five.

Chapter seven consists of a discussion of the study as a whole. It takes the results from the three individual articles and highlights the extensive damage to cerebellar neurocircuitry caused be prenatal alcohol exposure.

Chapter One

Introduction

Fetal alcohol spectrum disorder (FASD) is the most widely encountered preventable form of mental retardation worldwide and is caused by maternal drinking during pregnancy. In the United States the incidence of FASD is one to three per 1000 live births, while that in the Cape Coloured (mixed ancestry) population in the Western Case Province of South Africa has been estimated to be 18 to 141 times greater than that – the highest reported incidence in the world (May et al., 2000; 2007). The Western Cape is known for its vineyards and wine production and a very large portion of the Cape Coloured community works on these wine farms. Farm labourers used to be paid, in part, with wine – a remuneration method called the *dop* system. Socioeconomic deprivation combined with the easy access to alcohol, lead to excessive maternal drinking and therefore a high prevalence of FASD in these communities (Croxford and Viljoen, 1999). Even though the *dop* system has since been declared illegal, heavy alcohol consumption persists in both the urban and rural Cape Coloured communities (Jacobson et al., 2006).

Although alcohol consumption during pregnancy has been known to harm the unborn fetus for centuries, it was only in 1968 that these effects were published in the medical literature (Lemoine et al., 1968). In 1973 the term 'fetal alcohol syndrome' or FAS was coined in a paper published by Jones and Smith (1973), but it is only after three further publications by these authors that this condition became widely recognized.

Ever since the initiation of these studies there have been challenges associated with the classification of the condition as it became clear that the degree of neurological damage varies with the level and timing of alcohol exposure (Calhoun and Warren, 2007).

Today the term 'fetal alcohol spectrum disorder' (FASD) is used to cover the whole spectrum of conditions that may arise from prenatal exposure to alcohol. The range of disorders covered by the term FASD were defined in 1996 by the Institute of Medicine (IOM) and elaborated on in 2005 (Hoyme et al., 2005). The different forms of FASD are:

- Fetal alcohol syndrome (FAS) with confirmed maternal alcohol exposure
- Fetal alcohol syndrome (FAS) without confirmed maternal alcohol exposure
- Partial fetal alcohol syndrome (PFAS) with confirmed maternal alcohol exposure
- Partial fetal alcohol syndrome (PFAS) without confirmed maternal alcohol exposure
- Alcohol-related birth defects (ARBD)
- Alcohol-related neurodevelopmental disorders (ARND)

Each of these classifications has a specified list of criteria that has to be met for a positive diagnosis.

FAS is the most severe form of FASD. These children are characterized by a distinctive craniofacial dysmorphology, including a flat philtrum, thin upper lip and small palpebral fissures (Hoyme et al., 2005). They also have smaller head circumferences and are subject to growth retardation.

A partial FAS (PFAS) diagnosis requires the presence of two of the three facial features as well as either a small head circumference, signs of retarded growth or signs of neurological damage. The third group afflicted with alcohol-related neurodevelopmental disorders (ARND) does not have any of the characteristic facial features, but it is known that these children were exposed to alcohol prenatally and there are signs of neurobehavioral deficits. In this group, the lack of the characteristic facial features associated with FAS and PFAS often lead to improper diagnoses and treatment (Streissguth and O'Malley, 2000).

The Cape Town longitudinal cohort employed in our study was recruited during the period from 1999 to 2002 at an antenatal clinic in Cape Town in an area where there is known to be heavy alcohol consumption (Jacobson et al., 2008). Pregnant woman who

admitted to consuming alcohol during pregnancy were invited to participate in the study. A child born to a mother consuming at least 14 drinks a week or who partakes in binge drinking was considered to be heavily exposed. The next mother who visited the clinic and who drank less than one drink per day or seven drinks per week, and who did not binge drink, was invited to participate as a control subject.

The FASD diagnoses were made according to the revised IOM criteria (Hoyme et al., 2005). Each child was examined for growth and FAS dysmorphology by two expert dysmorphologists during a clinic conducted in 2005; a subset who could not attend the clinic was examined by one dysmorphologist (Jacobson et al., 2008). There was substantial agreement among the examiners on the assessment of all dysmorphic features, including the three principal fetal alcohol-related features—philtrum and vermilion measured on the Astley and Clarren (2001) rating scales and palpebral fissure length (median $r = 0.78$).

The cohort was subsequently divided into four groups – FAS, PFAS, heavily exposed non-syndromal (HE) and non- or minimally exposed controls. The mothers of the HE group were known to consume at least 14 drinks per week and/or partook in binge drinking, but these children did not have any of the characteristic facial features associated with FASD.

The main motivation for conducting this study is the reduced performance observed by children prenatally exposed to alcohol in the classical eyeblink conditioning (EBC) paradigm (Jacobson et al., 2008; 2011). The standard short delay EBC incorporates a conditioned stimulus (CS), a tone lasting for 750 ms combined with an unconditioned stimulus (US), a puff of air to the eye during the last 100 ms of the tone, which elicits a reflexive eye blink. Repeatedly pairing the CS with the US leads the eye blink to become a conditioned response (CR) where subjects blink at exactly the right time to avoid the puff of air to the eye.

As opposed to short delay EBC, trace EBC has a brief stimulus free interval (typically 500 ms) between the CS and US. Figure 1.1 shows a schematic diagram of the two task variants of EBC.

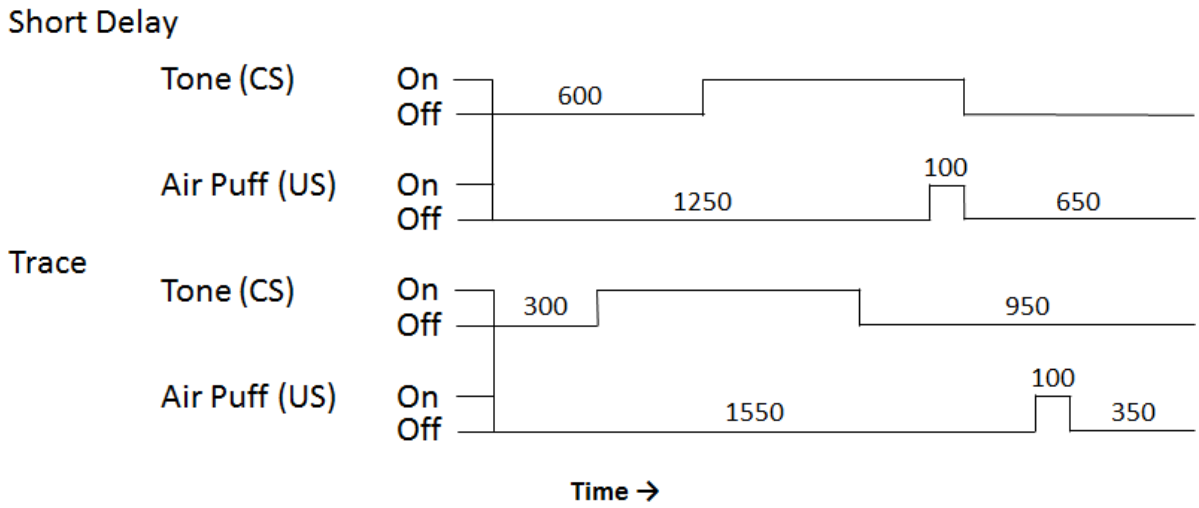

Figure 1.1: Schematic diagram of short delay and trace conditioning (Jacobson et al., 2011)

Figure 1.2 shows a typical EBC setup. It has been shown that the EBC response could be elicited in children as young as five months, with healthy control children achieving the same level of conditioning as adults (Herbert et al., 2003).

Figure 1.2: Experimental EBC setup

In the 5-year old follow-up of the Cape Town longitudinal cohort, a remarkably striking EBC deficit was noted in children with prenatal alcohol exposure (Jacobson et al., 2008).

None of the children with full FAS met criteria for conditioning at the end of three sessions of short delay EBC. Children with at least 40% conditioned responses were deemed to have successfully conditioned. Only 33.3% of the PFAS children and 37.9% of the HE children met criteria for conditioning at the same time, compared to 75% of the control children (Table 1.1).

Table 1.1: Comparison of the number of children that met criteria during short delay EBC for conditioning as a function of diagnosis at age 5 (Jacobson et al., 2008)

	Alcohol Exposed			Non-exposed		Total
	FAS	**PFAS**	**Heavily Exposed**	**Control**	**Microcephalic**	
Session 1	0 (0.00%)	2 (11.1%)	3 (10.3%)	4 (20.0%)	1 (25.0%)	10 (12.3%)
Session 2	0 (0.00%)	3 (16.7%)	2 (6.9%)	9 (45.0%)	2 (50.0%)	16 (19.8%)
Session 3	0 (0.00%)	1 (5.6%)	6 (20.7%)	2 (10.0%)	0 (0.0%)	9 (11.1%)
Total Conditioned	0 (0.00%)	6 (33.3%)	11 (37.9%)	15 (75.0%)	3 (75.0%)	35 (43.2%)
Total N	10	18	29	20	4	81

Values are number of children (%) who met the criterion of at least 40% conditioned responses (CR) in a session. Each child is shown in the session in which s/he first met the criteria for conditioning.

It was also striking that 75% of the microcephalic children, who have IQ's similar to those of the children with FAS, did meet criteria for conditioning after three sessions.

A follow up study using delay conditioning on the same children supported the findings for the 5-year old data at a mean age of 11.3 years (63 children) and trace conditioning (32 children) 1.5 years later at a mean age of 12.8 years (Jacobson et al., 2011). All the children performed better during short delay conditioning at this age after four

sessions (66.7% FAS, 60.7% HE, 89% control), but the alcohol exposed children needed more sessions than the control children to achieve this performance (Table 1.2). All the children had greater difficulty with the trace conditioning, but, once again, the alcohol exposed children required more sessions to achieve conditioning and overall poorer performance was still seen after four sessions (33.3% FAS, 57.1% PFAS, 66.7% control). Children with PFAS were not mentioned in this study.

Table 1.2: Comparison of the number of children that met criteria during short delay and trace EBC for conditioning as a function of diagnosis at school age (Jacobson et al., 2011)

	Short Delay Conditioning			
	FAS	**HE**	**Control**	**Total**
Session 1	0 (0.0%)	6 (21.4%)	12 (41.4%)	18 (28.6%)
Session 2	2 (33.3%)	6 (21.4%)	11 (37.9%)	19 (30.2%)
Session 3	1 (16.7%)	4 (14.3%)	3 (10.3%)	8 (12.7%)
Session 4	1 (16.7%)	1 (3.6%)	0 (0.0%)	2 (3.2%)
Total Conditioned	4 (66.7%)	17 (60.7%)	26 (89.7%)	47 (74.6%)
Total N	6	28	29	63
	Trace Conditioning			
	FAS	**HE**	**Control**	**Total**
Session 1	1 (16.7%)	2 (14.3%)	3 (25.0%)	6 (18.8%)
Session 2	0 (0.0%)	1 (7.1%)	5 (41.7%)	6 (18.8%)
Session 3	1 (16.7%)	4 (28.6%)	0 (0.0%)	5 (15.6%)
Session 4	0 (0.0%)	1 (7.1%)	0 (0.0%)	1 (3.1%)
Total Conditioned	2 (33.3%)	8 (57.1%)	8 (66.7%)	18 (56.3%)
Total N	6	14	12	32

Values are number of children (%) who met the criterion of at least 40% conditioned responses (CR) in a session. Each child is shown in the session in which s/he first met the CR criterion.

It has been previously established that the EBC response is, at least in part, mediated by the cerebellum (Dimitrova et al., 2002; Gerwig et al., 2007) and the effect of prenatal alcohol exposure on EBC has been reported in several studies (Jacobson et al., 2008; 2011, Green et al., 2002a; 2002b). Green et al. (2002a; 2002b) noted disrupted EBC in rat weanlings and adults that were exposed to alcohol postnatally during the period equivalent to the human third trimester. Cell loss, as well as altered neuronal activity was found in the cerebellar deep nuclei of the rats. Loss of Purkinje and granule cells was linked to prenatal binge drinking in similar studies (Dunty et al., 2001; Hamre and West, 1993). Apoptosis also lead to degeneration of cells in various cerebellar regions, even after only a single binge exposure (Dikranian et al., 2005).

Our study makes use of two magnetic resonance imaging (MRI) techniques – magnetic resonance spectroscopy (MRS) and functional MRI (fMRI) - to assess the integrity of two cerebellar components known to be critical for successful EBC in children prenatally exposed to alcohol.

The first part of the study assesses the chemical composition of the cerebellar deep nuclei, which has been shown to be critically involved in EBC (Aksenov et al., 2004; 2005). Alterations in metabolite levels in this cerebellar region could indicate that prenatal alcohol exposure adversely affects neuronal integrity or neurotransmission in this region.

The second part of the study is based on the assumption that a timing deficit is responsible for the poor EBC performance seen in children with FASD. Two finger tapping tasks, requiring millisecond accuracy, were performed while fMRI data were acquired. Analysis of the performance of the children during these tasks could indicate whether this assumption rings true. In addition to this, the fMRI data would allow for the identification of specific cerebellar regions where activation is altered by prenatal alcohol exposure.

Chapter Two

The Role of the Cerebellum in Timing and Classical Eyeblink Conditioning

2.1 Cerebellar Anatomy and Histology

The cerebellum, aptly named after the Latin term meaning 'little brain', is situated beneath the cerebrum at the posterior base of the skull and has been the focus of many studies dating as far back as the 16th century (Glickstein et al., 2009). Animal studies dating back to the beginning of the 19th century already pointed to the involvement of the cerebellum in motor control (Ferrier, 1886). Mounting evidence corroborating these findings, lead to the misconception that this brain structure is solely involved in motor functioning. More recently studies have shown that the cerebellum is also crucial for other non-motor functions (Watson, 1978; Berntson et al., 1973; Desmond et al., 1997; Leiner et al., 1993; 1994), and is involved in several intrinsic connectivity networks (Habas et al., 2009).

On a gross anatomical scale, the cerebellum is similar to the cerebrum in the sense that a grey matter cortex surrounds inner white matter. This white matter is commonly referred to as the *arbor vitae*, meaning 'tree of life', due to the highly convoluted surface of the grey matter, which creates branch-like effects seen in a cross-sectional view (Fig. 2.1). Imbedded in the white matter, a deeper cluster of grey matter, referred to as the cerebellar deep nuclei and consisting of four distinct nuclei - the fastigial, globose, emboliform and dentate – is found.

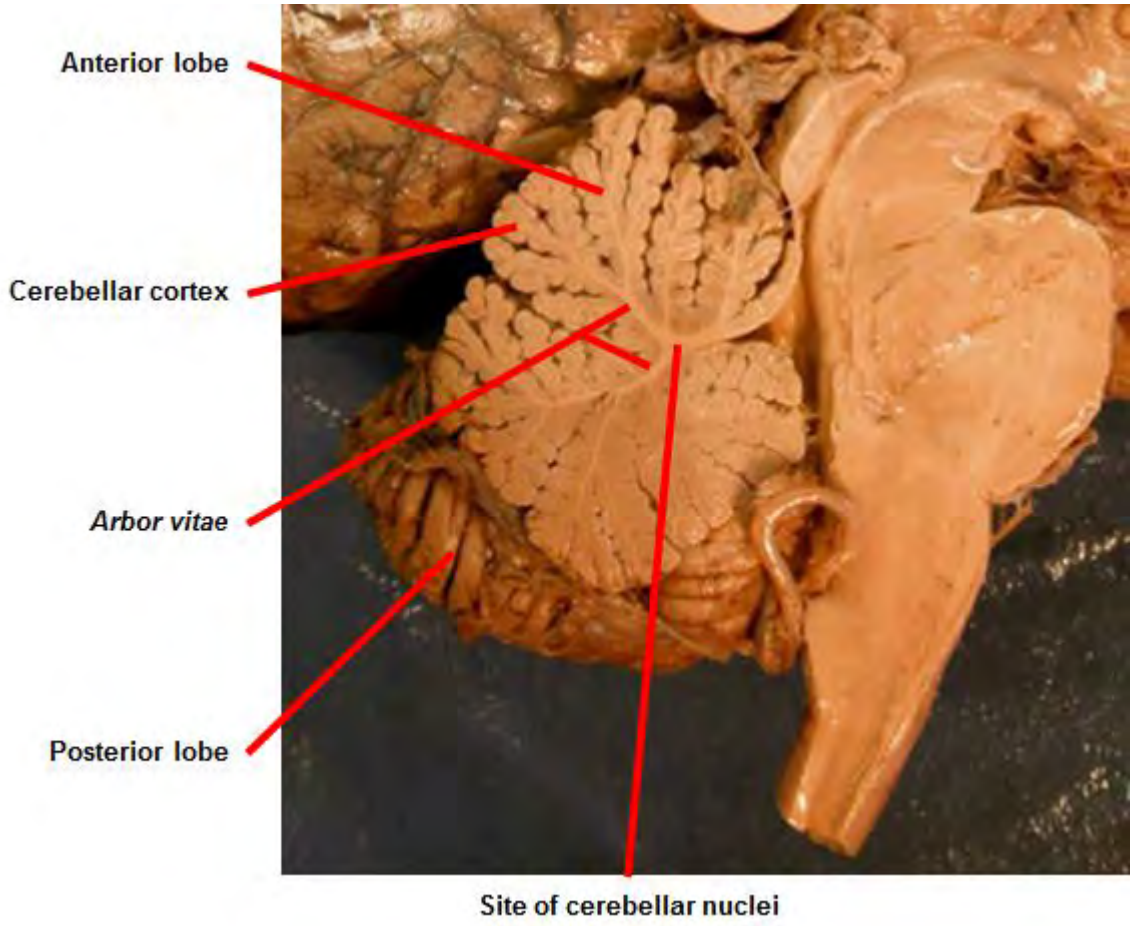

Figure 2.1: Cross sectional view of the cerebellum (reproduced and adapted with permission from Wissmann, P.)

A description of the gross anatomy of the cerebellum has been made difficult due to the different terminology used over the years. In this thesis, structures will be referred to according to the terminology suggested by Schmahmann et al. (2000). The cerebellum is divided sagittally into the vermis, situated most medially, the intermediate and the lateral zones (Fig. 2.2). It is also separated into an anterior and posterior lobe by the primary fissure, and a third, much smaller lobe, the flocculonodular lobe is separated from the other lobes by the posterolateral fissure.

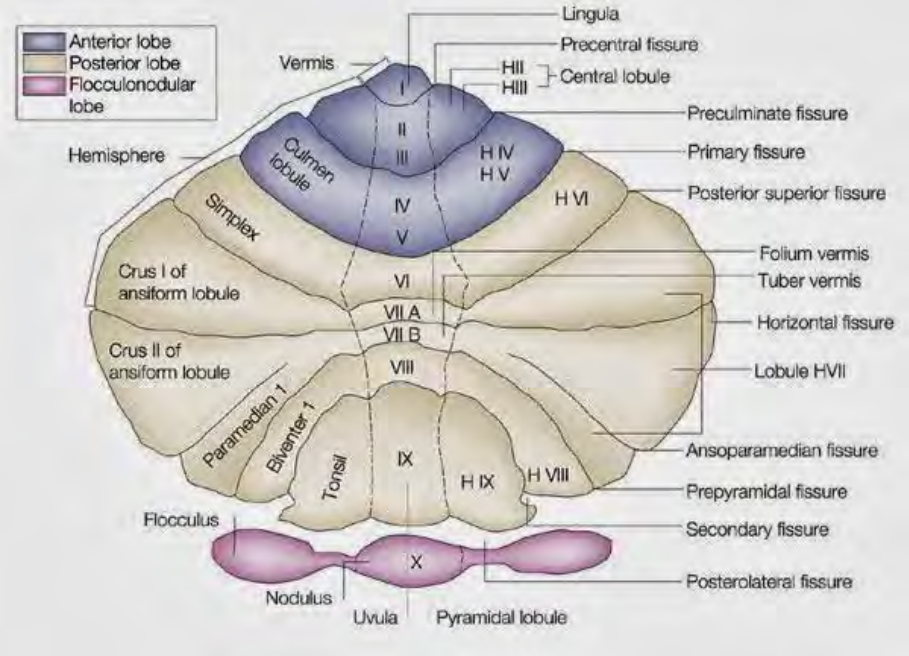

Figure 2.2: Cross sectional view of the cerebellum showing major structures and lobules (Rickson, 2013)

The anterior lobe is further divided into five lobules (I – V), while the posterior lobe consists of lobules VI to IX, as well as Crus I and Crus II. The floculonodular lobe is generally referred to as lobule X.

On a histological level (Fig. 2.3), the cerebellum is significantly different from the cerebrum (Fig. 2.3a). The grey matter cortex is divided into three layers – an outermost molecular layer, an intermediate Purkinje cell layer and an inner granule layer (Voogd and Glickstein, 1998).

Mossy fibers, so named due to the appearance of their synaptic terminals, relay sensory input from several sources and form glutamatergic excitatory synapses with hundreds of granule cells in the granule layer of the cerebellar cortex (Ito, 2006). Each granule cell, in turn, only synapses with four or five mossy fibers (Eccles, 1967).

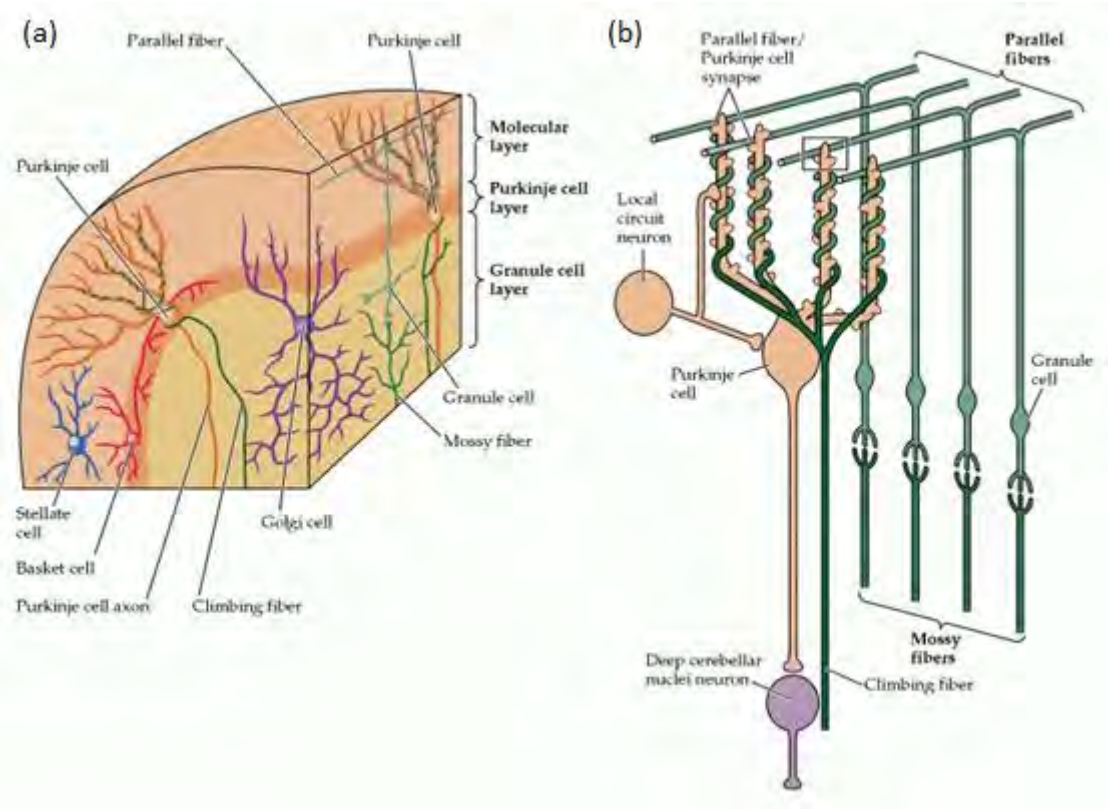

Figure 2.3: Histological structure of the cerebellum with (a) focusing on the location of cerebellar cells and (b) on the connectivity of these cells (reproduced with permission from Purves et al., 2012)

Granule cells are the smallest cells in the brain, although they are also the most abundant. Axons from these granule cells project upward into the molecular layer and bifurcate into parallel fibers to form excitatory synapses with the dendritic spines of hundreds of Purkinje cells (Eccles, 1967). The singly aligned cell bodies of Purkinje cells, forming the Purkinje cell layer, and an extensive network of dendrites, orientated perpendicularly to the direction of the parallel fibers, extend upward into the molecular layer. This arrangement allows each parallel fiber to form excitatory synapses with hundreds of Purkinje cells along the way.

As opposed to the mossy fibers projecting onto Purkinje cells via granule cells and parallel fibers, climbing fibers (originating solely from the inferior olive) form excitatory synapses with Purkinje cells by wrapping their axons around the dendrites of the Purkinje

cells (Fig. 2.3b). This configuration leads to the creation of multiple synapses between a Purkinje cell and a single climbing fiber (Purves et al., 2012).

In addition to projections to the cerebellar cortex, both mossy and climbing fibers also form direct excitatory synapses with the deep nuclei (Christian and Thompson, 2003).

Purkinje cells project to the cerebellar deep nuclei, as well as certain nuclei in the brainstem, but as opposed to the aforementioned neurons, Purkinje cells are GABAergic and therefore have an inhibitory effect on their targets (Voogd and Glickstein, 1998).

The cerebellar deep nuclei are the sole output from the cerebellum, which places them at the core of cerebellar functioning as previous studies have shown (Steinmetz, 1990; McCormick et al., 1982; Kleim et al., 2002; Nicholson and Freeman, 2004; Delgado-Garcia and Gruart, 2002; Choi and Moore, 2003; Green and Woodruff-Pak, 2000). They receive strong inhibitory GABAergic input from Purkinje cells and much weaker excitatory glutamatergic input from mossy and climbing fiber collaterals.

These nuclear cells fire spontaneously and it is the input from the Purkinje and collateral fibers that modulate the extent of firing.

Basket and stellate cells are located in the molecular layer of the cortex and both receive input from several sources including not only the parallel fibers, but collaterals from other neurons as well (Ito, 2012). Basket cells form inhibitory synapses at the soma of the Purkinje cell, whilst the stellate cells create inhibition at the Purkinje cell dendrites. This ultimately creates a feed-forward control system for successful inhibition of Purkinje cell firing.

The third inhibitory cell type, the Golgi cell, on the other hand creates a feedback loop. Golgi cells receive excitatory input from both the parallel fibers, as well as mossy fiber terminals and, in turn, create inhibitory synapses with granule cells, which do not excite the Purkinje cell.

Two types of timing have been identified – event and emergent timing (Zelaznik et al., 2005; Ivry et al., 2002). In event timing, specific temporal goals are set and tasks such as rhythmic finger tapping, EBC, discrete finger flexion/extension and discontinuous circle

drawing fall into this category. In contrast to this, emergent timing is employed during continuous tasks where timing is regulated by a motor component or trajectory control, such as seen in continuous circle drawing (Zelaznik et al., 2002; 2005).

The hypothesis that the cerebellum is involved in timing dates back to the 1960's and has been confirmed by multiple studies (Braitenbach, 1967; Ivry, 1993; Schlerf et al., 2007; Mauk et al., 2000; Ivry et al., 2002; Ohyama et al., 2003).

2.2 Cerebellar Mediated Timing

In studies of temporal learning and control, two main neural timing mechanisms have been proposed. The first is a dedicated mechanism in which specific neural circuitry are responsible for all timing responses. As Buonomano and Karmarkar (2002) point out, a centralized mechanism would mean that successful temporal discrimination between identical stimuli would also imply this ability between intermodal stimuli.

The second is an intrinsic mechanism, which suggests that timing is not specific to dedicated neural regions, but that all neurons have the ability to contribute to timing (Buonomano and Laje, 2010; Ivry and Schlerf, 2008). In this case, the same neuronal dynamics would apply in different brain regions according to the type of stimuli received.

At this point it should be noted that not all studies involving timing are applicable to our current study. Four timescales are referred to in these studies – microsecond, millisecond and second processing, as well as circadian rhythms (Mauk and Buonomano, 2004; Buonomano and Karmarkar, 2002).

Our study aims to probe the timing mechanism involved specifically in EBC as a potential explanation for the EBC deficits seen in children with FASD. Since EBC requires millisecond timing, in the range 10 to 500 ms (Buonomano and Karmarkar, 2002; Mauk and Buonomano, 2004), our discussion here focuses specifically on cerebellar timing in this range.

In the study of dedicated and intrinsic neural mechanisms, several different models of timing have been proposed.

Oscillator models imply that an accumulator integrates the pulses of a central pacemaker and is classified as one of the dedicated timing models (Spencer et al., 2009). However, based on neural physiology the oscillator model appears to not be applicable to the processing of millisecond intervals, required for the current study (Buonomano and Karmarker, 2002).

Population clock models, an intrinsic model, suggest that groups of neurons fire at different time intervals in response to a given stimulus (Buonomano and Laje, 2010). Once the combined strength of firing in this group of neurons is sufficient, the neuron responsible for motor output would fire.

Labelled line models, also classified as a dedicated timing model, suggest that neurons can selectively respond to certain intervals i.e. the neurons have specific temporal properties (Buonomano and Karmarkar, 2002). The selectivity is mainly attributed to several biological mechanisms of neurotransmission.

Interval discrimination tasks have been widely used to study timing in humans. The experiment basically requires the subject to discriminate whether the interval between two stimuli is at a standard interval or not ($T + \Delta t$).

Wright et al. (1997) performed experiments where subjects were trained in an auditory discrimination task (1 kHz) with a standard interval of 100 ms. This training consisted of daily one hour sessions over a period of ten days. Their first finding was that discrimination accuracy improved significantly with practice. In addition to this, when a 4 kHz tone was used, instead of the 1 kHz tone used for training, high performance was still seen in temporal discrimination performance. However, the success of the task for the trained interval was not translated to discrimination intervals of 50, 200 or 500 ms. These findings support a labelled line model and suggest that temporal learning is interval specific.

In another study using tactile stimuli, Nagarajan et al. (1998) trained subjects with a standard interval of 125 ms at a certain skin location. Post-training their results showed that

performance on this task at the standard interval was comparable independent of the location of the stimulus. When compared to other base intervals, some generalization was seen in the task using 75 ms, but not with the greater 225 ms standard intervals. Using the auditory discrimination task proposed by Wright et al. (1997) they also found that the sensory training at 125 ms generalised to an auditory discrimination task.

The question is how these findings would translate to tasks where a timed motor response is required. Keele et al. (1985) showed that performance in interval discrimination tasks were correlated with the ability to maintain rhythmic motor components, even when different effectors were used. These findings suggest that the results from the interval discrimination tasks would translate to the tasks included in our study – EBC and rhythmic finger tapping.

Mauk and Buonomano (2004) performed a comprehensive review of temporal processing focussing on millisecond timing. They proposed that the cerebellum functions as a feed-forward mechanism in tasks requiring millisecond timing. In contrast to feed-back systems which adjust outputs in response to inputs, feed-forward systems allow the anticipation of the input after some learning regarding the association between certain stimuli.

Feed-forward timing systems therefore create an interval-specific temporal delay of the motor response once the mossy fiber input has arrived (Ohyama et al., 2003). This delay is learned from the repetitive combination of input from the mossy fibers followed by the input from the climbing fibers, which is referred to as the error signal when discussing this feed-forward control. The time delay in the actual signal transmission via the mossy fibers requires that the error signal should be separated from the mossy fiber input by at least 100 ms for learning to occur. Efferent pathways driven by activity in the neurons of the interpositus nucleus is then responsible for the actual motor component involved in the timed response.

2.3 Role of the Cerebellum in EBC

While the previous section reviewed the role of the cerebellum in maintaining millisecond timing, this section reviews previous studies specifically aimed at investigating the cerebellar mechanisms involved in EBC at a neuronal level.

Each of the deep nuclei is involved in different aspects of cerebellar control, but the interposed nuclei, consisting of the emboliform and globose nuclei, have been shown to be crucial elements of the EBC circuitry (Steinmetz, 1990; McCormick et al., 1982; Kleim et al., 2002; Nicholson and Freeman, 2004; Delgado-Garcia and Gruart, 2002; Choi and Moore, 2003; Green and Woodruff-Pak, 2000). As previously mentioned the strong inhibitory GABAergic input from Purkinje cells and much weaker excitatory glutamatergic input from mossy and climbing fiber collaterals modulate the extent of firing in the nuclei.

Pharmacological studies have been used to study the degree to which the two different inputs modulate firing in the interpositus nucleus during acquisition of the EBC response. One study by Aksenov et al. (2004) used Pictrotoxin (PTX), an antagonist of GABA that blocks calcium channels, and Muscimol, an agonist of GABA receptors, to study the involvement of the inhibitory input from Purkinje cells on the interpositus nucleus in CR's during EBC. As would be expected, the GABA agonist completely abolished CR's due to the effective inhibition of the nuclear cells by the Purkinje cells. However, infusion of dose dependent PTX also adversely affected CR's in the rabbit. Baseline activity increased which reduced, and at high doses, even abolished activation during the CS. At these levels, CR's were completely suppressed.

The second study by the same author assessed the extent of involvement of the excitatory glutamatergic input from the mossy and climbing fibers on the interpositus nucleus and effectively on the CR's (Aksenov et al., 2005). In this study, ɣ-D-glutamylglycine (DGG), an antagonist of both α-Amino-3-hydroxy-5-methyl-4-isoxazolepropionic acid (AMPA) and N-methyl-D-aspartate (NMDA) receptors, and therefore excitatory glutamate transmission, was infused in the interpositus nuclei of rabbits. Even at the highest doses, the CR's were not

abolished, although there was decreased CR incidence and increased CR latency. Adding PTX to the DGG infusion gave the same results as was seen in the previous study (Aksenov et al., 2004) – dose dependent CR incidence and complete abolishment of CR's. These results show that the Purkinje cell component of neurotransmission to the interpositus nucleus has a much greater effect on learning of the EBC response. It is also clear that very specific modulation of the nuclear cells in the interpositus nucleus is required for the learning of the correct EBC response as both over- and underactivity adversely affects CR's. It also indirectly implicates the involvement of the cerebellar cortex in the learning of the EBC response.

Mediation of the correct level of activity in the interpositus nucleus is achieved by two mechanisms, namely long-term potentiation (LTP) and long-term depression (LTD). The dynamics at the synapse between the Purkinje cell and the neurons of the interpositus nucleus is a good example of LTD. Many cellular mechanisms induce these responses which either strengthen (LTP) or weaken (LTD) connectivity between synapses (Daniel et al., 1998). The brain's ability to perform controlled LTP and LTD is generally referred to as synaptic plasticity, which is crucial for the acquisition and retention of learned responses.

The consensus is that synaptic plasticity is required at the cerebellar cortex and in the interpositus nucleus for the acquisition of the EBC response (Gerwig et al., 2007; Christian and Thompson, 2003; Mauk, 1997; Yeo, 1991; Kim and Thompson, 1997; Woodruff-Pak and Disterhoft, 2008; Lindquist et al., 2013). A generic diagram that has been adapted from other literature is shown in Figure 2.4 (Christian and Thompson, 2003).

The involvement of the cerebellar cortex has been implicated in that the LTD at the parallel fiber-Purkinje cell synapse is mediated by conjunctive stimulation of climbing fibers and parallel fibers (Ekerot and Kano, 1989; Karachot et al., 1994). More specifically it was found that postsynaptic LTD at the parallel fiber-Purkinje cell only occurs in the presence of climbing fiber input, while absence of input from climbing fibers leads to LTP at this synapse (Ito, 2006; Medina et al., 2000; Hirano, 1990). Ultimately the Purkinje cells then act as a coincidence indicator (Delgado-Garcia and Gruart, 2002). In the event of EBC, mossy fiber

inputs from the CS activates the Purkinje cells via the granule cells and parallel fibers, but once firing of the climbing fibers from the US takes place, this firing leads to LTD of the parallel fibre-Purkinje cells synapse and ultimately reduces inhibition to the interpositus nucleus (Ito, 2006). More specifically, one study found that this LTD was most successful when activation of the parallel fiber occurred 50 to 200ms before activation of the climbing fiber, which is a typical inter-stimulus interval (ISI) used in eyeblink conditioning (Wang et al., 2000).

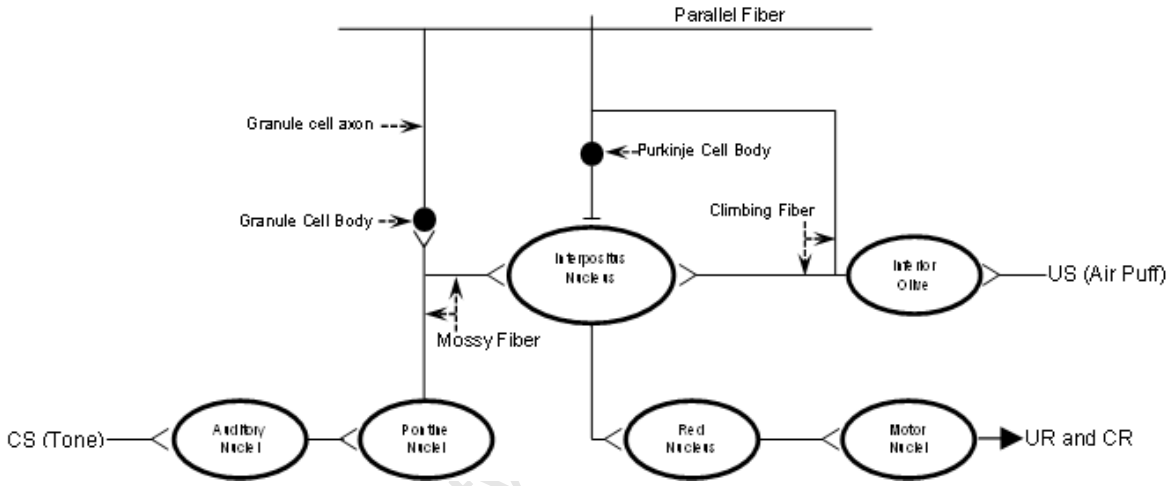

Figure 2.4: Neural circuitry involved in the acquisition and retention of the EBC response

These aforementioned versions of synaptic plasticity at the parallel fiber-Purkinje cell and Purkinje cell-interpositus nucleus neurons are very simplified as many other cellular mechanisms are at play. The other cell types present in the cerebellum (basket, stellate and Golgi cells) have not been taken into account, although they may also play an important role in the LTD and LTP required for EBC.

Interestingly, Aksenov et al. (2005) found that suppression of the glutamate receptors at the interpositus nucleus also lead to reduced inhibition by the Purkinje cells. This is counterintuitive, but the authors suggest that it could be due to other regulatory feedback systems, which would implicate the involvement of the three aforementioned cells.

Altogether, for the learning the of the EBC response, specific levels of excitation of neurons in the interpositus nucleus is required. This in turn, implicates the involvement of the cerebellar cortex, as the neurons from the interpositus nucleus receive the strongest input from Purkinje cells.

Chapter Three

Magnetic Resonance Imaging Techniques

Prior to advances in neuroimaging, the neural manifestations of FASD were studied post mortem. These examinations noted prominent anomalies in several brain structures (Clarren et al., 1978; Jones et al., 1973). With new available non-invasive techniques, we are able to study, amongst others, the human body's structure (MRI), chemical composition (MRS) and functional activity (fMRI) *in vivo*.

3.1 Nuclear Magnetic Resonance (NMR) and Magnetic Resonance Imaging (MRI)

In 1946, both Bloch et al. (1946) and Purcell et al. (1946) discovered that when a sample is placed in a magnetic field, a resonance phenomenon is seen. Through NMR, specific quantum mechanical magnetic properties of the atomic nuclei in the sample can be detected.

The most commonly used nucleus in MRI is hydrogen (^{1}H) due to the abundance of water in the human body (Jezzard and Smith, 2009). In this study only ^{1}H imaging, also called proton imaging, was used. Other nuclei also visible in MRI include sodium (^{23}Na) and phosphorus (^{31}P).

During magnetic resonance imaging these nuclei are placed in a large magnetic field B_0. This aligns the spins to precess either parallel or anti-parallel to the B_0 field. The rate of precession of these spins is called the Larmor frequency, which is the product of the gyromagnetic ratio (a constant specific to the nuclei) and the magnitude of the B_0 field.

$$\omega_0 = \gamma B_0 \qquad \text{(Eq. 3.1)}$$

Spins precessing parallel to B_0 are at a lower energy state (α-state) than spins opposing the main magnetic field (β-state). The small temperature-dependent excess of spins in the lower α-energy state is given by the Boltzmann equation (Hashemi et al., 2012)

$$\frac{n_\alpha}{n_\beta} = e^{\Delta E/kT} = e^{\hbar\omega_0/kT} \qquad \text{(Eq 3.2)}$$

where

n_α is the number of spins in the lower energy state

n_β is the number of spins in the higher energy state

ΔE is the energy difference between the two states

k is the Boltzmann constant

T is the absolute temperature in Kelvin

$\hbar$ is Planck's constant divided by 2π

ω_0 is the Larmor frequency.

The direction of the B_0 field is typically denoted by the z-direction of Cartesian coordinates, while the xy-plane represents the transverse field.

A steady-state, net magnetization vector (M_0) aligned with the B_0 field is created by the excess spins in the α-state.

Application of a radiofrequency (RF) pulse with a frequency equal to the precessional frequency of the spins imbues energy into the atoms in the lower energy state, causing these atoms to 'flip' away from the longitudinal axis. The strength and duration of the RF pulse determines to which extent the longitudinal magnetization is 'flipped' and this is referred to as the 'flip angle'. The application of the RF pulse therefore results in a transverse (M_{xy}) and longitudinal (M_z) magnetization vector. The termination of the RF pulse causes these spins to return to the lower energy state, which releases the energy previously absorbed. This released energy induces an electromagnetic field (emf) in the scanner's receiver coil, situated perpendicularly to the B_0 field, which gives rise to the MR signal.

The relaxation of the spins from the higher to the lower energy level is characterized by two time constants, T_1 and T_2, characteristic to the tissue being imaged.

T_1 relaxation, also known as spin-lattice or longitudinal relaxation represents the time required for the M_z magnetization vector to regrow to 63% of its equilibrium value. The term spin-lattice relaxation refers to the fact that this process occurs as a result of interactions of the spins with the surrounding 'lattice'.

T_2 relaxation, also called spin-spin or transverse relaxation represents the time for M_{xy} to decay to 37% of its original value. After the application of the RF pulse, the spins are aligned in the same direction in the xy-plane. This is referred to as the spins being 'in phase'. Due to interactions between the spins and field inhomogeneities the spins start to precess at different rates and therefore the amplitude of the transverse magnetization decays as these spins become 'out of phase'. Larger scale field inhomogeneities such as is seen at tissue/sinus interfaces leads to much more rapid decay of the transverse signal and is represented by T_2*. The T_2 value for tissue is therefore a constant, while the value of T_2* changes with the uniformity of the magnetic field.

MRI makes use of gradient magnetic fields to allow for spatial localization of the MR signal to obtain structural information. However, the details of this technique are not within the scope of this study.

3.2 Magnetic Resonance Spectroscopy (MRS)

Magnetic resonance spectroscopy (MRS) is an analytical method to determine the chemical composition of a substance *in vitro* or of tissues *in vivo* and is based on the same NMR principles as MRI.

MRS has a wide range of possible applications, such as the development of more effective and reliable drugs for treatment through a better understanding of the chemical composition of tissues associated with specific diseases, as well as non-invasive biopsies.

Chemical shielding forms the basis of MRS. According to the atomic model as presented by Bohr, all protons are surrounded by electrons and the motion of these charges create a very small counter magnetic field, B_e, opposing the main applied magnetic field, B_0 (Fig. 3.2) (De Graaf, 2008). This opposing magnetic field is so small that it is neglected in typical MRI studies, but in MRS the resulting field relays critical information regarding the chemical environment of the protons.

The effective local magnetic field (B_{eff}) experienced by the protons in the chemical compound is therefore not equal to B_0, but to the difference between the two resulting magnetic fields.

$$B_{eff} = B_0 - B_e \qquad \text{(Eq 3.3)}$$

As a result, the effective magnetic field is directly related to the local chemical environment of the proton being studied and according to the Larmor equation the rate of precession (ω_{eff}) will change with the effective magnetic field (B_{eff}) and is given by:

$$\omega_{eff} = \gamma B_{eff} \qquad \text{(Eq 3.4)}$$

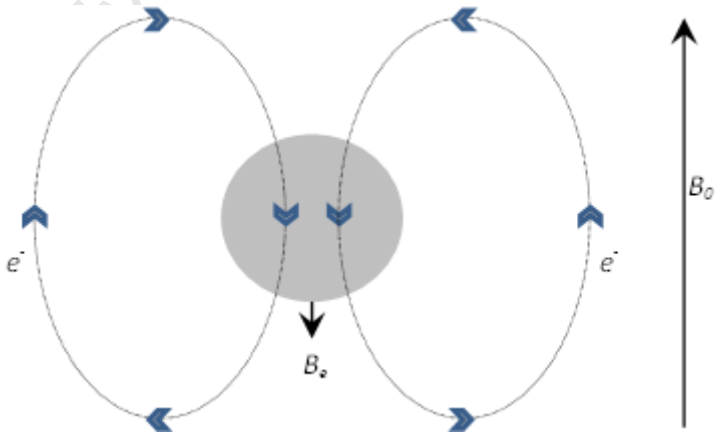

Figure 3.1: Opposing magnetic field (B_e) generated by electron flow

In order to normalise the effect of different B_0 field strengths, chemical shift (δ) is defined as the relative increase or decrease of the precessional frequency of a proton (ω_{eff}) compared to that of a proton in a reference substance (ω_{ref}) and is given by

$$\delta = \frac{\omega_{eff} - \omega_{ref}}{\omega_{ref}} \quad . \qquad \text{(Eq 3.5)}$$

In vivo MRS usually uses water as a reference. As mentioned before, the change in precessional frequency is very small – typically a few Hertz (Hz), while precessional frequencies are of the order of tens of MHz for magnetic field strengths typically used in MR scanners. For this reason, chemical shift is reported in the dimensionless parts per million (ppm) unit.

Protons in different chemical environments will resonate at different frequencies, i.e. have different chemical shifts. For molecules containing more than one proton in dissimilar chemical environments, the spectra will contain multiple peaks representing the respective proton types.

As seen before, very small forces such as electron flow in chemical shielding, affects the chemical shift of a proton. Different protons in the same molecule will also have a magnetic effect on each other. This is a phenomenon referred to as spin-spin splitting.

Figure 3.2 shows two identical molecules with both protons in the α-state in (a) and proton A in the α-state and proton B in the β-state in (b).

In figure 3.2(a), the electrons surrounding the two protons move in a similar fashion due to the α-α configuration and the electrons essentially form an 'electron cloud'. This means that electrons are allowed to move farther away from the nucleus and therefore leads to less effective shielding of the protons. The opposing configuration in 3.2(b) forces the electrons to move closer to their respective nuclei, resulting in greater shielding of the proton.

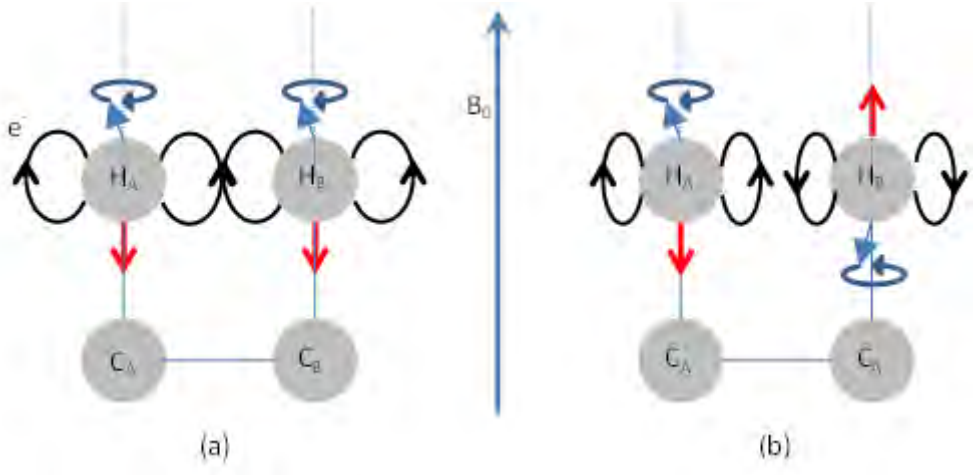

Figure 3.2: Diagram showing the creation of the different magnetic moments (μ_e) (red arrows) caused by electron flow (black lines) in the (a) α-α and (b) α-β spin states

The different configurations of the protons in the illustration therefore lead to:

- Smaller B_e and a larger B_{eff} for the α-α state
- Larger B_e and a smaller B_{eff} for the α-β state

From the Larmor equation, this translates to the fact that protons in the α-α configuration would have higher resonance frequencies than the protons in the α-β configuration. In turn, protons in the α-α and the α-β-states will precess at respectively higher and lower frequencies than a lone proton.

A typical spectrum obtained from *in vivo* proton MRS of the human brain is shown in figure 3.3 above. The chemical shift in ppm is plotted on the x-axis, while the y-axis represents quantitative data regarding each of the metabolites. The area under a specific metabolite peak corresponds to the concentration of that metabolite in the volume of interest.

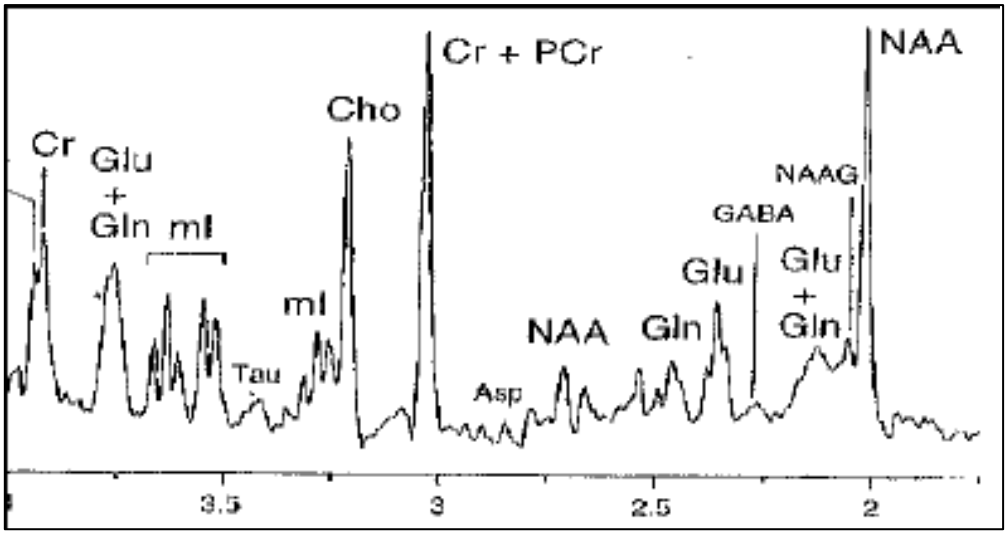

Figure 3.3: Typical chemical shift spectrum for brain tissue (De Graaf, 2008)
***Asp* = aspartate, *Cho* = choline, *Cr* = creatine, *GABA* = *γ*-aminobutyric acid, *Glu* = glutamate, *Gln* = glutamine, *mI* = myo-inositol, , *NAA* = N-acetylaspartate, NAAG = *N*-acetylaspartylglutamate, *Tau* = taurine**

3.3 Functional Magnetic Resonance Imaging (fMRI)

Blood oxygenation level dependent (BOLD) fMRI is an imaging method used to assess brain metabolic function by measuring changes in the MR signal arising from magnetic susceptibility changes that accompany brain function over different areas in the brain (Jezzard and Smith, 2009). Neural activation requires an increase in oxygen and glucose to the region as the neurons become more metabolically active. Oxygenated blood flows to the active region with oxygen levels exceeding the demand. This creates an oxygen gradient between the blood vessels and the cell mitochondria for sufficient diffusion of the oxygen to the required site. The iron-containing protein haemoglobin found in red blood cells facilitates this transport by binding to the oxygen to form oxyhaemoglobin. After diffusion the oxygen-poor haemoglobin, deoxyhaemoglobin, is transferred away from the active site. This reaction by the body to neural activity is referred to as the haemodynamic response.

It was back in 1936 that Pauling and Coryell found that oxyhaemoglobin molecules are diamagnetic (repelling any applied magnetic field) and deoxyhaemoglobin molecules are paramagnetic (attracting any applied magnetic field). Intuitively, the presence of these two

molecules would have a significant effect on the microscopic field inhomogeneities and therefore the T_2* value. BOLD fMRI exploits the differences in magnetic properties of the oxy- and deoxyhaemoglobin and the ratio of the two associated with neuronal activity. The paramagnetic properties of deoxyhaemoglobin leads to distortion of the magnetic field and therefore reduces the T_2 and T_2* in the blood vessels, causing signal loss. On the other hand diamagnetic oxyhaemoglobin does not really affect the signal. In T_2*-weighted images the altered magnetic fields caused by the presence of deoxygenated blood will reduce the signal intensity by an amount related to the relative concentration of deoxyheamoglobin and oxyhaemoglobin. With neural activation, the increased flow of oxygenated blood reduces the effect of deoxyhaemoglobin in the activated region so that we observe a signal increase (Ogawa et al., 1992; Kwong et al., 1992). This mechanism forms the basis of BOLD fMRI.

The design of the fMRI experiment ultimately relies on the information required from the experiment. In our study we made use of the blocked task paradigm where alternating tasks, requiring distinct brain responses, are performed for set periods. These blocks are usually interleaved with rest periods spanning the similar times as the active blocks. The relative change in the intensity of the signal is then measured either between the tasks or between the task and the rest condition (Amaro and Barker, 2006). Figure 3.4 represents the timing of a classic block design task.

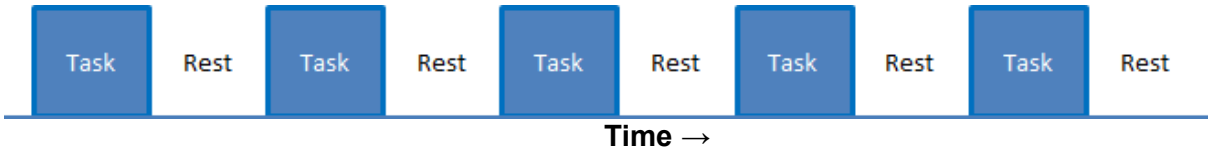

Figure 3.4: Typical block design showing interleaved periods of task performance and rest

Although variations in the standard haemodynamic response have been seen between individual subjects (Aguirre et al., 1998), Buxton et al. (2004) proposed a model for

the haemodynamic response taking cerebral blood flow and the BOLD response into consideration. An initial dip in the MRI signal is typically seen in the region of brain activation. These authors attribute this 'dip' to increased oxygen extraction prior to the delayed increase in cerebral blood flow in response to the activation. The positive BOLD effect following this initial dip is the body's response to the activation by increasing oxygenated blood flow to the region of activation. A third phase is also seen after termination of the stimulus and is referred to as the poststimulus undershoot. This phase is seen due to the slower recovery of cerebral blood volume compared to cerebral blood flow and cerebral rate of oxygen metabolism. Higher ratios of deoxyhaemoglobin then lead to the decreased signal. The graphical representation of the haemodynamics and BOLD response described in that article is shown in figure 3.5.

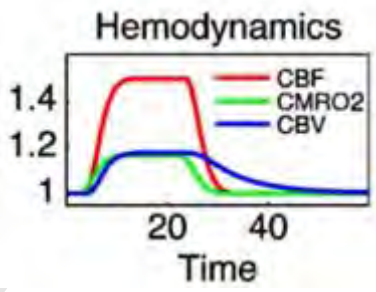

Figure 3.5: Modelling of the BOLD response signal in terms of cerebral blood flow (CBF), cerebral metabolic rate of oxygen ($CMRO_2$) and cerebral blood volume (CBV) (Buxton et al., 2004)

The different phases of the haemodynamic response should be taken into account in the design of the experimental paradigm. Task blocks should be of sufficient duration to capture the response, while the rest-blocks should be long enough for recovery of the poststimulus undershoot.

fMRI is particularly sensitive to motion as functional and structural data need to be aligned for optimal results. Also, any motion between measurements of successive MRI volumes may result in a signal change in a particular voxel that could incorrectly be attributed to neural activation. It is for this reason that motion correction is a crucial part of data pre-processing in fMRI. This is usually an automated algorithm incorporated into functional imaging processing packages such as Brainvoyager QX (Goebel et al., 2006) and SPM (Ashburner, 2012). Slice time correction is necessary since the functional data for all the slices are not captured simultaneously. Typically slices are acquired in an interleaved fashion. Low frequency noise resulting from physiological processes of the body may also be reduced by applying a high-pass filter.

The next step in analysing fMRI data is to ensure that the functional and structural data are aligned for each subject. In order to successfully analyse activation in multiple subjects, all data need to be normalized to a specific template, usually into Talairach space. Since the high-resolution structural data leads to improved inter-subject co-registration, these are typically normalised to a template for each subject. Each subject's functional data are then aligned to their own structural scan and re-sliced in normalised space.

The stimulation protocol defines the timing (onset and termination) of the different events/tasks performed during the fMRI data acquisition. A general linear model (GLM) is used to analyse the data, where each predictor corresponds to a specific task (i.e. left hand finger tapping). The time course of each predictor is created by convolving the timing blocks of the task with the theoretical haemodynamic response function.

Statistical analyses can then be performed by solving the GLM for every voxel in the brain. The beta value for each predictor indicates how much of the variance in the time course signal in that voxel is due to the task defined by the time course of the predictor. As such, high beta values indicate that a lot of the variance is associated with that specific task, while low betas indicate that the brain activity is not related to that task.

For determination of group effects, as was necessary in our study, a random effects GLM was first run for the time course data of each subject to create beta maps for each predictor or the contrasts of interest (i.e. left hand tapping minus right hand tapping) for each individual subject. Second-level analyses were then run, which involve performing various statistical analyses to compare the beta values on a voxel-by-voxel basis to identify regions where the betas of one group differ significantly from the betas of the other group.

It is important to choose the correct threshold when using voxel-by-voxel analysis, since the large number of voxels in the brain would lead to a multiple comparison problem. If a *p*-value of 0.05 is used, then for every 100 voxels tested, five would return false positive results. Since the human brain has an average volume greater than 1000 cm^3 and fMRI voxels are defined by millimetre dimensions, thousands of voxels will be included in the analysis, making the multiple-comparison problem very severe.

Several methods have been applied to compensate for multiple comparisons. A popular, yet exceptionally strict, method to control for this problem is Bonferroni correction (Narum, 2006). This method takes into account the number of tests performed (N) and an initial *p*-value of 0.05 would be reduced to 0.05/N. In an fMRI study incorporating, for instance, 20 000 voxels, activation would only be deemed significant at $p = 0.0000025$.

Another method to control for multiple comparisons is based on the hypothesis that a voxel would not activate individually, but rather in conjunction with its neighbours (Worsley et al., 1992). These methods are referred to as spatial extent methods. More specifically, in our study we used cluster size correction based on Monte Carlo simulations (Forman et al., 1995). This method ultimately calculates the minimum number of contiguous voxels in a cluster for statistical significance and a *global* error probability of the selected *p*.

Chapter Four

An *in vivo* ^{1}H Magnetic Resonance Spectroscopy Study of the Deep Cerebellar Nuclei in Children with Fetal Alcohol Spectrum Disorders

Lindie du Plessis[1,2], Joseph L. Jacobson [2,3,4], Sandra W. Jacobson[2,3,4,] Aaron T. Hess[1,2], Andre van der Kouwe[5], Malcolm J. Avison[6], Christopher D. Molteno[3], Mark E. Stanton[7], Jeffrey A. Stanley[4], Bradley S. Peterson[8], Ernesta M. Meintjes (PhD)[1,2]

Abstract

Prenatal alcohol exposure has been linked to impairment in cerebellar structure and function, including eyeblink conditioning. The deep cerebellar nuclei, which play a critical role in cerebellar-mediated learning, receive extensive inputs from brain stem and cerebellar cortex and provide the point of origin for most of the output fibers to other regions of the brain. We used in vivo ^{1}H magnetic resonance spectroscopy (MRS) to examine effects of prenatal alcohol exposure on neurochemistry in this important cerebellar region.

MRS data from the deep cerebellar nuclei were acquired from 37 children with heavy prenatal alcohol exposure and 17 non- or minimally-exposed controls from the Cape Coloured (mixed ancestry) community in Cape Town, South Africa.

[1] MRC/UCT Medical Imaging Research Unit, University of Cape Town, Cape Town, South Africa
[2] Department of Human Biology, University of Cape Town, Cape Town, South Africa
[3] Department of Psychiatry and Mental Health, University of Cape Town, Cape Town, South Africa
[4] Department of Psychiatry and Behavioral Neurosciences, Wayne State University School of Medicine, Detroit, MI, USA
[5] Department of Radiology and Athinoula A. Martinos Center for Biomedical Imaging, Massachusetts General Hospital, Boston, MA, USA
[6] Vanderbilt University Institute of Imaging Science, Nashville, TN, USA
[7] Department of Psychology, University of Delaware, Newark, Delaware, MD, USA
[8] Division of Child Psychiatry, Columbia College of Physicians and Surgeons, New York, NY, USA

Increased maternal alcohol consumption around time of conception was associated with lower NAA levels in the deep nuclei (r = -0.33, p < 0.05). Higher levels of alcohol consumption during pregnancy were related to lower levels of the choline-containing metabolites (r = -0.37, p < 0.01), glycerophosphocholine plus phosphocholine (Cho). Alcohol consumption levels both at conception (r = 0.32, p < 0.05) and during pregnancy (r = 0.35, p < 0.01) were related to higher levels of glutamate plus glutamine (Glx). All these effects continued to be significant after controlling for potential confounders.

The lower NAA levels seen in relation to prenatal alcohol exposure may reflect impaired neuronal integrity in the deep cerebellar nuclei. Our finding of lower Cho points to disrupted Cho metabolism of membrane phospholipids, reflecting altered neuropil development with potentially reduced content of dendrites and synapses. The alcohol-related alterations in Glx may suggest a disruption of the glutamate–glutamine cycling involved in glutamatergic excitatory neurotransmission.

4.1 Introduction

Fetal alcohol spectrum disorders (FASD) include a range of physical growth and neurobehavioral deficits in children whose mothers drank alcohol during pregnancy. We used magnetic resonance spectroscopy (MRS) to study effects of prenatal alcohol exposure on potential neurochemical indicators in the deep cerebellar nuclei of children. The incidence of FAS is estimated to be 18 - 141 times greater in the Cape Coloured (mixed ancestry) population in the Western Cape Province of South Africa (May et al., 2007) than in the United States. This which is among the highest reported incidences in the world. Fetal alcohol syndrome (FAS), the most severe FASD, is characterized by distinctive craniofacial dysmorphology, small head circumference, and pre- and/or postnatal growth retardation (Hoyme et al., 2005). A diagnosis of partial FAS (PFAS) requires the same facial dysmorphology as well as small head circumference, retarded growth, or neurobehavioral

impairment. A large proportion of exposed children lack the characteristic FAS facial features but exhibit a broad range of cognitive and/or behavioural deficits.

The earliest autopsy studies in humans reporting damaging effects of prenatal alcohol exposure identified errors in cell migration, agenesis or thinning of the corpus callosum, and anomalies in the cerebellum and brain stem (Jones and Smith, 1973; Archibald et al., 2001). Cerebellar structural anomalies (Clarren, 1977; Jones and Smith, 1973) have been consistently reported in FAS, and studies of effects on brain volume have reported disproportionate size reductions in the cerebellum (Clarren, 1977; Jones and Smith, 1973; Archibald et al., 2001; Chen et al., 2012). In addition, many of the behavioural deficits seen in individuals with FASD, including spatial recognition, motor learning, and fine motor control, are mediated, in part, by the cerebellum (Guerri, 1998). In the 5-year follow-up of our Cape Town Longitudinal Cohort, a remarkably striking deficit in delay eyeblink conditioning, a cerebellar-mediated nonverbal classical conditioning paradigm, in which the subject learns to associate a conditioned stimulus, typically a pure tone, with a brief air puff to the eye (unconditioned stimulus) that elicits a reflexive blink (Jacobson et al., 2008). None of the children in the Cape Town sample with full FAS met criteria for conditioning, compared to 75% of the healthy controls; only 33.3% of the children with PFAS and 37.9% of the heavily exposed nonsyndromal children met criteria for conditioning. These findings were subsequently confirmed in a school-aged cohort (Jacobson et al., 2011).

The deep cerebellar nuclei, which play a critical role in cerebellar-mediated learning (Christian and Thompson, 2003), receive extensive inputs from brain stem and cerebellar cortex, and most output fibers from the cerebellum to other brain regions, originate from this region. Neural plasticity in the deep nuclei is known to be essential to create the new neural pathways that mediate the conditioned response (Green et al., 2002a; Freeman and Nicholson, 2000). Neurodegeneration via apoptosis of cerebellar cells has been demonstrated in the deep cerebellar nuclei of alcohol-exposed rats (Dikranian et al., 2005), leading to decreased numbers of neurons in this region (Green et al., 2002b).

In the present study, we performed single-voxel *in vivo* ^{1}H MRS in the deep cerebellar nuclei of children with FASD and non- or minimally-exposed control children to assess biochemical alterations in this region. In contrast to previous studies that have examined the relation of prenatal alcohol exposure to MRS endpoints (Cortese et al., 2006; Astley et al., 2009), we performed both real-time motion and first-order shim correction to ensure accurate anatomical localization throughout acquisition and improved magnetic field homogeneity (Hess at el., 2011a). We report absolute metabolite concentrations using water scaling, calculated after adjustment for tissue fractions of gray matter (GM), white matter (WM) and cerebrospinal fluid (CSF) in the voxel. The metabolites measured reliably using this procedure were N-acetylaspartate (NAA), glycerophosphocholine plus phosphocholine (Cho), phosphocreatine plus creatine (tCr), myo-inositol (Ins), glutamate (Glu), and glutamate plus glutamine (Glx). Given that NAA is considered a marker of functioning in neuroaxonal tissue and that decreased numbers of neurons have been reported in the deep nuclei of alcohol-exposed rats (Green et al., 2002b), we hypothesized that prenatal alcohol exposure would be associated with lower levels of NAA in this region. The relation of prenatal alcohol exposure to the levels of the other metabolites was also examined. In addition, given that the children with full FAS were particularly vulnerable to impairment in eyeblink conditioning (Jacobson et al., 2008; 2011) and the findings of Green et al. (2002b) showing fewer neurons in their most heavily alcohol-exposed rats, we hypothesized that this group would show the greatest reduction in NAA compared to controls.

4.2 Methods

4.2.1 Participants

Pregnant women from the Cape Coloured community in Cape Town, South Africa, were recruited between 1999 and 2002 at their first antenatal clinic visit (Jacobson et al., 2008). The Cape Coloured, composed mainly of descendants of white European settlers, Malaysian slaves, indigenous Khoi-San aboriginals, and black Africans, have historically

comprised the large majority of workers on grape and fruit farms in the wine-producing region of the Western Cape. The Western Cape supports a large wine-producing industry, in which farm workers were traditionally paid, in part, with wine. Socioeconomic deprivation combined with easy access to alcohol has led to excessive maternal drinking, even during pregnancy, which has persisted in both the urban and rural Cape Coloured communities, leading to a high prevalence of FASD.

Cape Coloured pregnant women who reported consuming at least 14 standard drinks/week or binge drinking (≥ 5 drinks/occasion) were recruited into the study, as was a control group of pregnant women who abstained or drank minimally during pregnancy (< 7 drinks/week and no binge drinking). Excluded were women < 18 years of age and those with diabetes, epilepsy, or cardiac problems requiring treatment, and religiously observant Moslem women, whose religious practices prohibit alcohol consumption. Infant exclusionary criteria included major chromosomal anomalies, neural tube defects, multiple births, and seizures.

Maternal alcohol consumption was assessed using a timeline follow-back approach (Jacobson et al., 2002; 2008). At recruitment the mother was interviewed regarding incidence and amount of drinking on a day-by-day basis during a typical 2-week period at time of conception. She was also asked whether her drinking had changed since conception; if so, when the change occurred and how much she drank on a day-by-day basis during the preceding 2 weeks. This procedure was repeated in mid-pregnancy, and again at 1 month postpartum to provide information about drinking during the latter part of pregnancy. Volume was recorded for each type of beverage consumed each day, converted to absolute alcohol (AA) using multipliers proposed by Bowman et al. (1975), and averaged to provide three summary measures of alcohol consumption at conception and during pregnancy: average ounces of AA consumed/day, AA/drinking day (dose/occasion) and frequency (days/week). Number of cigarettes smoked on a daily basis and frequency of marijuana and other drug use (days/week) were also obtained.

Each child was examined for growth and FAS dysmorphology by two U.S.-based expert dysmorphologists following the revised Institute of Medicine criteria (Hoyme et al., 2005) during a 6-day clinic in 2005 (Jacobson et al., 2008). Five children who did not attend the clinic were assessed by a Cape Town-based dysmorphologist with expertise in FAS diagnosis. There was substantial agreement among the dysmorphologists on assessment of all dysmorphic features, including the three principal fetal alcohol-related characteristics—palpebral fissure length, and philtrum and vermilion measured using the *Lip-Philtrum* Guide (Astley and Clarren, 2001) (median $r = 0.78$). The dysmorphologists subsequently conducted a case conference to reach consensus regarding which children met criteria for the FAS and PFAS diagnoses (Jacobson et al., 2008).

IQ was assessed on the Wechsler Intelligence Scale for Children-IV (WISC-IV) at 9 years (see detailed description in Jacobson et al., 2011 and Diwadkar et al., 2013). The WISC-IV was administered in English or Afrikaans, depending on the language used in the child's elementary school classroom. The WISC-IV was translated into Afrikaans by a clinical psychologist whose first language is Afrikaans and back-translated by another native Afrikaans speaker. At the 5-year follow-up of this cohort, we had administered the Junior South African Intelligence Scale (JSAIS; Madge et al., 1981), which is available in Afrikaans and English and has been normed for South African children. Seventy-one of the children from that follow-up were administered the WISC-IV at 9 years. IQ scores obtained using the JSAIS at 5 years were strongly correlated with the 9-year WISC scores, $r = 0.79$, $p < 0.001$.

4.2.2 *In vivo* ^{1}H MRS Acquisition

MRS data were acquired from 72 right-handed children (age 8.8 - 12.0 years). Those with braces or metal implanted in their body or claustrophobia were not scanned. All scans were performed on a 3T Allegra (Siemens Medical Systems, Erlangen, Germany) scanner at the Cape Universities Brain Imaging Centre. The volume of interest (VOI) was localized in

the deep cerebellar nuclei (Fig. 4.1) using a T_2-weighted acquisition immediately preceding the spectroscopy.

Signal loss due to iron deposits in this region (Dimitrova et al., 2006) facilitates accurate localization on T_2-weighted images and reproducible positioning of the VOI. Iron deposits in the deep nuclei are low in children but increase with age (Aoki et al., 1989) and the deep nuclei were visible in 67% of the children scanned in this study.

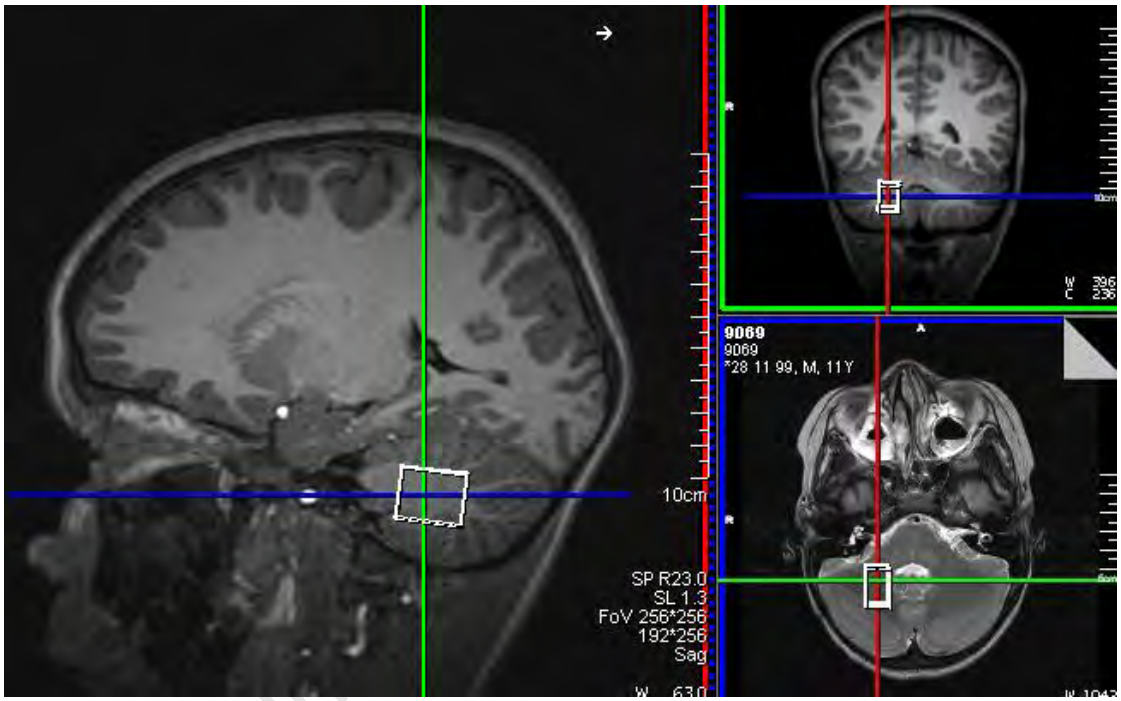

Figure 4.1: Voxel placement for MRS data acquisition

^{1}H MRS data for the 3.8 cm^3 voxel were obtained using an EPI volumetric navigated point-resolved spectroscopy (PRESS) sequence (Hess et al., 2011a) with real-time first-order shim and motion correction (TR = 2000 ms, TE = 30 ms, 128 measurements, vector size 1024, spectral bandwidth 1000 kHz). Water unsuppressed ^{1}H MRS measurements were acquired for seven different TE's (TE = 30 ms, 50 ms, 75 ms, 100 ms, 144 ms, 500 ms and 1000 ms, TR = 4000 ms; 2 averages) to estimate tissue fraction composition (Ernst et al., 1993).

All procedures were performed according to protocols approved by ethics committees at Wayne State University and University of Cape Town. All parents/guardians provided informed written consent, and the children provided oral assent.

4.2.3 ^{1}H MRS Pre-processing and Quantification

Individual measurements were recorded separately and frequency- and phase-corrected offline before averaging (Hess et al., 2011b). Briefly, this procedure involved convolving the spectrum from each measurement with a simulated spectrum to robustly detect the frequency shift of the metabolites, followed by singular value decomposition (SVD). The primary component of the SVD provides a set of complex weights that were used to recombine the spectra in a weighted and phase-coherent manner. A spectral range of -448 Hz to 128 Hz was used for both the convolution and SVD. This technique ensured narrower linewidths and higher signal-to-noise ratios (SNRs).

Metabolite levels of the resulting corrected water-suppressed spectra were quantified using LCModel (Provencher, 2008). The water signal of the water-unsuppressed spectra were also quantified using LCModel and modelled as a function of TE using a tri-exponential function (Sigma Plot; version 11) to estimate the tissue fraction of GM, WM and CSF in the voxel (Ernst et al., 1993). GM, WM, and CSF voxel content values, along with the other appropriate relaxation correction factors were then utilized to obtain absolute quantification values (Gasparovic et al., 2006; Kreis et al., 1993) from the frequency- and phase-corrected data (Hess et al., 2011b).

4.2.4 Exclusionary Criteria

Several exclusionary criteria were applied to ensure extraction of only the most reliable results. Spectra from nine children were excluded due to LCModel SNRs < 8; seven, due to full-width at half maximum (FWHM) linewidths of NAA > 9.6 Hz. SNR in LCModel is defined as the ratio of the maximum in the spectrum minus baseline over the

analysis window to twice the root mean square residuals (Provencher, 2008). Statistical analyses were performed only on the metabolite peaks with an overall mean Cramer-Rao Lower Bound value < 20%; namely, NAA, Cho, tCr, Ins, Glu and Glx. Two additional subjects were excluded as extreme outliers (> 2 standard deviations above or below the mean), one on the continuous alcohol exposure measures, the other on the metabolite concentrations.

4.2.5 Statistical Analyses

Statistical analyses were performed using SPSS (version 20). Nine control variables were considered as potential confounders: child's gender and age at assessment and maternal education (years), marital status (married/unmarried), verbal intellectual competence (Peabody Picture Vocabulary Test-Revised), nonverbal intellectual competence (Raven Progressive Matrices), smoking (cigarettes/day) and marijuana use (days/month) during pregnancy, and maternal age at delivery.

Each metabolite level was examined in relation to prenatal alcohol exposure at conception and during pregnancy in separate hierarchical multiple regression analyses. Prenatal alcohol exposure was entered in the first step of each analysis; all control variables related to the metabolite (at $p < 0.20$) were entered in the second step to determine if the effect of prenatal alcohol on the metabolite continued to be significant after statistical adjustment for potential confounders. Each metabolite was also examined in relation to FASD diagnosis using analysis of variance (ANOVA). In addition, given that the FAS group was particularly vulnerable to impairment in eyeblink conditioning and that Green et al. (2002b) found fewer neurons in the deep nuclei of the most heavily ethanol-exposed rats, we ran a planned contrast of NAA levels in controls vs. the FAS group, which is comprised of the most severely exposed and affected children.

4.3 Results

4.3.1 Sample Characteristics

After applying exclusionary criteria, we report data for 54 (34 male, 20 female) right-handed children. Table 4.1 summarizes demographic information for the children included in the study.

Table 4.1: Sample characteristics (*N* = 54)

Child Sex (male)	34 (63.0%)
Child's age at assessment	10.7 ± 0.6
WISC-IV IQ	71.7 ± 12.3
Maternal education (yr)	8.7 ± 2.9
Maternal marital status (married)	29 (53.7%)
Maternal Peabody Picture Vocabulary Test (PPVT) IQ[a]	61.6 ± 18.5
Maternal Raven score[b]	29.7 ± 10.9
Absolute alcohol consumed per day at conception (oz) (*n* = 35)[c]	1.2 ± 0.9
Absolute alcohol consumed per day across pregnancy (oz) (n = 39)[c]	0.8 ± 0.7
Absolute alcohol consumed per occasion across pregnancy (oz) (n = 39)[c]	3.5 ± 2.0
Drinking days per week across pregnancy (*n* = 39)[c]	1.5 ± 1.1
FASD Diagnosis	
Fetal alcohol syndrome	5 (9.3%)
Partial FAS	15 (27.8%)
Heavily exposed nonsyndromal	17 (31.5%)
Controls	17 (31.5%)
Cigarettes smoked per day during pregnancy (*n* = 42)[c]	8.5 ± 6.9
Marijuana use during pregnancy (occasions/month) (*n* = 6)[c]	1.3 ± 1.3

Values are mean ± standard deviation or number (%).
[a]Missing for 5 participants.
[b]Missing for 3 participants
[c]Consumers only.

The low IQ scores reflect the highly disadvantaged backgrounds of the children in this population (Jacobson et al., 2008). Due to the small number of children with FAS, the FAS and PFAS groups were combined in the data analysis. There were no significant between-group differences in spectral SNR ($F(2,53) = 0.02$, $p = 0.98$) or FWHM ($F(2,53) = 0.22$, $p = 0.80$). Prenatal alcohol exposure was very high, averaging 7.6 standard drinks/occasion for the FAS/PFAS group and 6.6 for the nonsyndromal HE group. All but two of the 17 control mothers abstained from drinking during pregnancy; one drank two drinks on three occasions; the other, one drink on six occasions.

4.3.2 ^{1}H MRS Findings

Figure 4.2 shows the improvement to our prospectively motion-corrected data after pre-processing (Hess et al., 2011a). For the example shown in Figure 4.2a, moderate motion during the scan resulted in relatively poor SNR (Fig. 4.2b) despite prospective motion and shim correction, which was substantially improved after pre-processing (Fig. 4.2c).

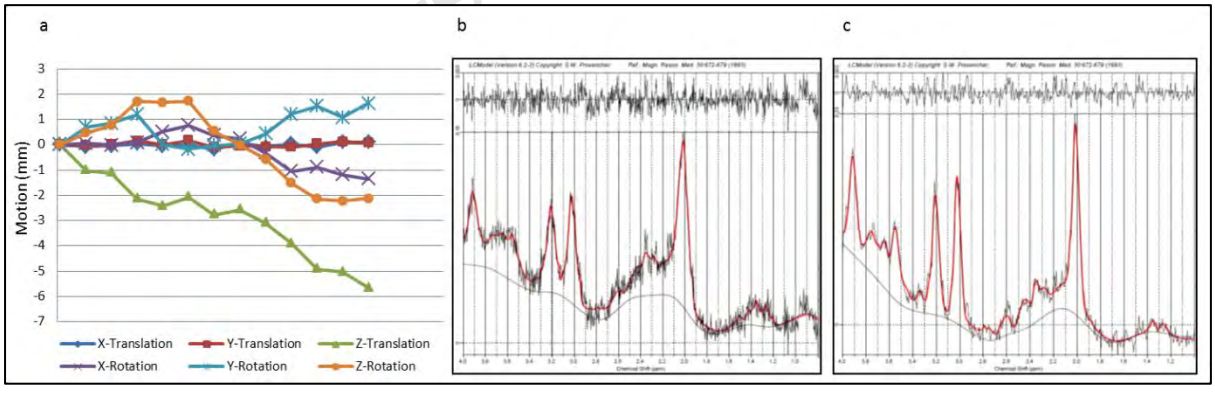

Fig. 4.2: Spectrum for a single subject: (a) Translational and rotational motion (mm) during the scan as determined by the volumetric navigator. (b) LCModel output without offline frequency and phase correction prior to averaging (Hess et al., 2011b) [full-width at half maximum (FWHM) = 10.2 Hz, signal-to-noise ratio (SNR) = 9]. (c) LCModel output with offline frequency and phase correction prior to averaging (FWHM = 7.7 Hz, SNR = 13).

Absolute metabolite concentrations are summarized in Table 4.2. Choline levels in the deep nuclei were similar to those seen in neocortical white matter and hippocampus in the Astley et al. (2009) study, where the median exposure group average was 1.4 mM; NAA and creatine levels in the deep nuclei were somewhat lower (7.7 mM and 5.5 mM, respectively). Virtually none of the correlations between the nine control variables and the six metabolites were significant at $p < 0.20$; the sole exceptions were a positive correlation between maternal smoking during pregnancy and Glx ($r = 0.24$, $p < 0.10$) and lower levels of Ins in the boys ($r = -0.24$, $p < 0.10$).

Table 4.2: Absolute metabolite levels

Metabolite	Levels (mM)
N-Acetylaspartate (NAA)	5.2 ± 0.5
Glycerophosphocholine + Phosphocholine (Cho)	1.2 ± 0.2
Creatine + Phosphocreatine (tCr)	4.7 ± 0.6
Glutamate (Glu)	5.0 ± 1.2
Glutamate + Glutamine (Glx)	6.0 ± 1.4
Myo-Inositol (Ins)	3.7 ± 0.8

Values are means ± standard deviation

Table 4.3 shows the results of the multiple regression analyses, both before and after controlling for potential confounders. As hypothesized, higher levels of maternal alcohol consumption at conception were associated with lower NAA levels (Fig. 4.3).

Table 4.3: Relation of prenatal alcohol exposure to absolute metabolite concentrations in the deep cerebellar nuclei

Metabolite	*N*	AA/day at time of conception		AA/day across pregnancy	
		r	*β*	*r*	*β*
N-Acetylaspartate (NAA)	49	-0.33*	-0.33*	-0.26†	-0.26†
Glycerophosphocholine + Phosphocholine (Cho)	54	-0.23†	-0.23†	-0.37**	-0.37**
Creatine + Phosphocreatine (tCr)	51	0.01	0.01	-0.10	-0.10
Glutamate (Glu)	54	0.21†	0.21†	0.23†	0.23†
Glutamate + Glutamine (Glx)[a]	54	0.35**	0.32*	0.38**	0.35**
Myo-Inositol (Ins)[b]	51	-0.16	-0.13	-0.14	-0.13

AA = absolute alcohol; *r* represents the simple correlation between alcohol exposure and the metabolite; *β* is the standardized regression coefficient, after adjustment for the potential confounding variables listed below. *N*s vary in the regression analyses due to missing cases for certain of the control variables.
[a]Control variables: smoking during pregnancy
[b]Control variables: child gender
$^{\dagger}p < 0.10$, $^{*}p < 0.05$, $^{**}p < 0.01$

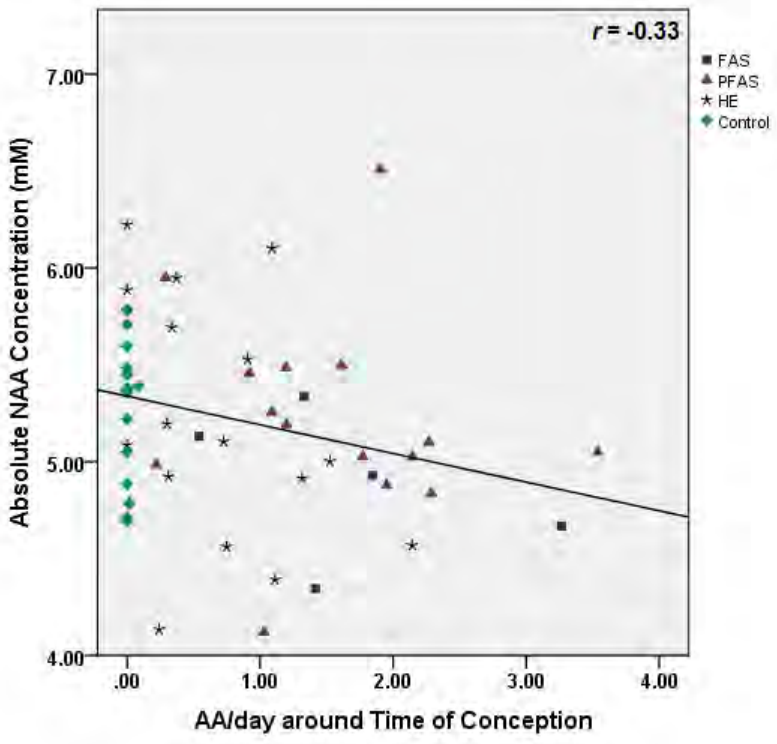

Figure 4.3: Relation of prenatal alcohol exposure at conception to N-acetylaspartate (NAA) levels in the deep cerebellar nuclei

Following the Hochberg (Hochberg, 1988) procedure to correct for multiple comparisons, the threshold for statistical significance for the three other associations with *p*-values < 0.05 was adjusted by dividing 0.05 by 3, generating a critical *p*-value of 0.017. Using this cut-off, higher levels of alcohol consumption during pregnancy were significantly related to lower Cho levels (Fig. 4.4), and both measures of alcohol consumption were related to higher levels of Glx (Fig. 4.5). By contrast to the continuous measures of prenatal alcohol exposure, diagnostic group was not related to the levels of any of the metabolites (all *p*'s > 0.20). However, as predicted, NAA was significantly lower in the FAS group than in the controls, (t (20) = -2.30, $p < 0.03$).

Partial correlation analysis was used to determine the degree to which the effects of maternal drinking during pregnancy on Cho and Glx might be attributable to poorer neuronal integrity, as measured by NAA. After controlling for NAA, the relation of AA/day during pregnancy to Cho remained significant (partial $r = -0.35$, $p < 0.01$), as did the relation of AA/day at conception and during pregnancy to Glx (partial *r*'s = 0.34 and 0.38, respectively, both *p*'s < 0.01), indicating that the effects of prenatal alcohol exposure on the levels of these metabolites are mediated by independent mechanisms. The effect of alcohol consumption during pregnancy on Glx was also not attributable to its effect on Cho (partial $r = 0.35$, $p = 0.01$).

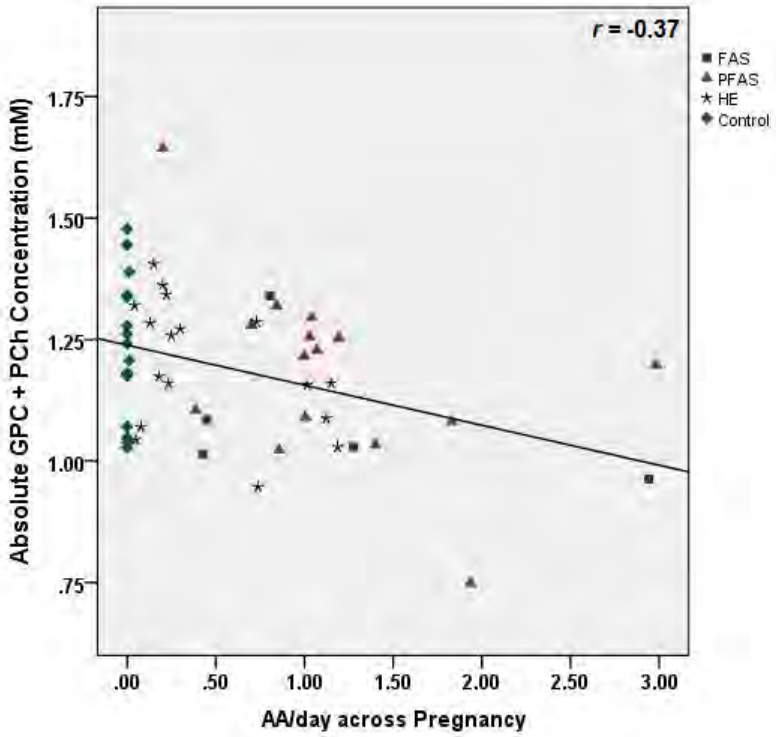

Figure 4.4: Relation of prenatal alcohol exposure during pregnancy to glycerophosphocholine plus phosphocholine (Cho) levels in the deep cerebellar nuclei

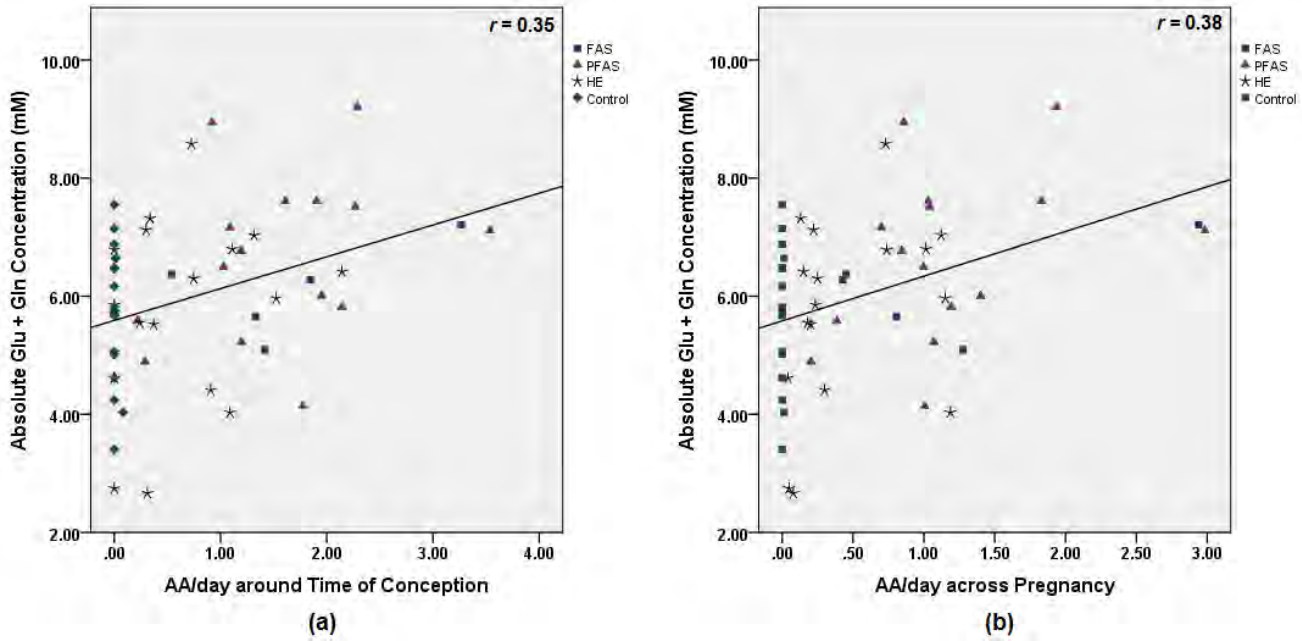

Figure 4.5: Relation of (a) prenatal alcohol exposure at conception and (b) prenatal alcohol exposure during pregnancy to glutamate plus glutamine (Glx) levels in the deep cerebellar nuclei

With regard to the relation of these metabolites with child outcome, none of the metabolites were significantly related to IQ scores or eyeblink conditioning performance for the sample as a whole (all *p*'s > 0.10). In the control group, however, higher levels of NAA were related to delay eyebink conditioning at both 5 years ($r = 0.72$ $p < 0.01$) and 9 years ($r = 0.54$, $p < 0.05$). By contrast, NAA was unrelated to eyeblink conditioning in the exposed children at either age (*r*'s = -0.16 and -0.02 at 5 and 9 years, respectively, both *p*'s > 0.20).

4.4 Discussion

This study is the first to use *in vivo* ^{1}H MRS to examine effects of prenatal alcohol exposure on the neurochemistry of the deep cerebellar nuclei. Prenatal alcohol was associated with lower levels of NAA, which is indicative of poorer neuronal integrity and consistent with findings of decreased numbers of neurons found in this region in heavily exposed laboratory rats (Green et al., 2002b). As predicted, NAA levels were also lower in the FAS group when compared with the controls. NAA concentrations increase rapidly during early brain development, particularly in the cerebellum, thalamus and gray matter, areas where formation of dendritic arborizations and synaptic connections occur at a high rate during childhood (Van der Knaap et al., 1992; Pouwels et al., 1999). The lower levels of NAA seen in the children with prenatal alcohol exposure may, therefore, reflect impairment in the early developmental formation of dendritic arborizations and synaptic connections (Pouwels et al., 1999; Stanley et al., 2007). NAA is also an important osmolyte in the brain, participates in oligodendrocyte myelin formation, and plays a role in neuroimmune reactions and intercellular signalling (Baslow, 2003). Decreased NAA levels are seen in neurodegenerative disorders, such as Alzheimer's disease (Schott et al., 2010) and disorders characterized by a lack of progressive cortical development, such as early onset schizophrenia (Stanley et al., 2007).

One strength of this study is the detailed drinking histories obtained prospectively during pregnancy using timeline follow-back interviews (Jacobson et al., 2002), which enabled us to assess metabolite levels as a function of continuous measures of prenatal alcohol exposure. As in several previous studies (Woods et al., 2013; Meintjes et al., 2013), the continuous measures were more sensitive than fetal alcohol diagnosis. Our finding that lower NAA levels in the deep nuclei were related to poorer eyeblink conditioning but not to overall IQ in the control children is consistent with the critical role of this region in cerebellar-mediated learning. The lack of association of NAA with eyeblink performance in the exposed children suggests that the effect of fetal alcohol exposure on this elemental form of learning may not be mediated by poorer neuronal integrity but rather by impairment in other aspects of the eyeblink conditioning cerebellar-brain stem circuit.

In this study, prenatal alcohol exposure was assessed both at time of conception and averaged across pregnancy. The effect on NAA was significant for exposure at conception but fell short of significance for exposure across pregnancy; conversely, the effects on Cho and Glu were significant only for the across pregnancy measure. Because these two exposure measures were highly correlated ($r = 0.89$) and the effects of both measures were similar in magnitude, we do not believe that these findings reflect differences in timing of exposure but are instead likely the product of fluctuations associated with small sample size.

Only a few studies have used *in vivo* ^{1}H MRS to examine neurochemical effects of prenatal alcohol exposure, and only one of these (Astley et al., 2009) adjusted for tissue fractions in the voxel. One primate study (Astley et al., 1995) reported an increased ratio of Cho to tCr with increasing prenatal alcohol exposure in a VOI that included the thalamus, basal ganglia, and adjacent white matter. However, failure to adjust for tissue fractions wasproblematic in this primate study due to the large voxel size, which included both white and grey matter. Another study (Cortese et al., 2006) that found increased NAA levels in the caudate nuclei in children with FASD compared with non-exposed controls, both when reported as a ratio relative to tCr and absolute levels, was limited by small sample size ($n = 13$). Fagerlund et al. (2006) performed multi-voxel *in vivo* ^{1}H MRS in a large portion of

the cerebrum and the cerebellum and found decreased NAA/Cho and NAA/tCr ratios in voxels from the cerebral cortex, white matter, thalamus and cerebellum. Although the authors viewed the absolute signals with caution, as no adjustment was made for tissue fractions, the absolute metabolite levels suggested that the findings of lower NAA/Cho and NAA/tCr ratios were driven by higher levels of Cho and tCr. The voxels sampled in the cerebellum were not isolated to specific structures but included segments from different cerebellar regions. Also, the sample size for this study was small, consisting of 10 subjects each in the exposure and control groups.

In the only prior study that adjusted for tissue fractions in the voxel, *in vivo* ^{1}H MRS was used to assess the metabolites in a fronto-parietal white matter and a hippocampal/basal nuclear region (Astley et al., 2009). Adjustment for tissue fractions was performed by segmentation of the MR image, and absolute metabolite concentrations were calculated by means of water scaling using LCModel. This study found significantly lower levels of Cho in fronto-parietal white matter of children prenatally exposed to alcohol. Lower Cho was also seen in the hippocampal/basal nuclear region of children with FASD compared to healthy controls, but this difference fell short of statistical significance. Thus, the principal consistent finding that emerges from the two larger studies that adjusted for tissue fractions of GM, WM, and CSF is an inverse relation between prenatal alcohol exposure and Cho.

Given that Cho comprises phosphocholine (PCh) and glycerophosphocholine (GPC), which are precursors and breakdown products, respectively, of membrane phospholipids, the observed inverse relation with prenatal alcohol exposure suggests decreased membrane phospholipid content in the deep cerebellar nuclei. It will be of interest to see whether this effect of fetal alcohol exposure, which was seen in two very different brain regions—fronto-parietal white matter previously (Astley et al., 2009) and deep cerebellar nuclei in this study—will be evident in other brain regions in future studies. The finding that the correlations of prenatal alcohol exposure with Cho remain significant even after controlling for NAA indicates that the effect of prenatal alcohol exposure on Cho is independent of its effect on neuronal integrity indicated by the reduction in NAA.

Glu, the primary excitatory neurotransmitter in the brain, plays a critical role in learning. During excitatory action Glu is released at the pre-synaptic terminal, taken up by the surrounding glia, converted to Gln, transported back to the pre-synaptic terminal and converted to Glu, completing the Glu-Gln cycling process. The finding that prenatal alcohol exposure was significantly related to increased Glx but not to Glu *per se* suggests a disruption in the Glu-Gln cycling during excitatory neurotransmission in the deep cerebellar nuclei. This effect was independent of the effects of prenatal alcohol on both NAA and Cho. Although Glx was not measured in the previous *in vivo* ^{1}H MRS studies of FASD, glutamatergic transmission is known to be affected in adult alcoholism, as alcohol has an inhibitory effect on NMDA receptors, which play a critical role in glutamatergic neurotransmission (Tsai et al., 1998). The glutamatergic system attempts to compensate for this inhibition by up-regulation of NMDA receptors. Once chronic alcohol exposure ends, as would be experienced by a new-born prenatally exposed to alcohol, increased glutamatergic excitability and, ultimately, glutamatergic excitotoxicity remains.

4.5 Conclusion

In conclusion, the hypothesis that prenatal alcohol exposure would be associated with a reduction in NAA levels in the deep cerebellar nuclei was confirmed in this study, consistent with evidence from animal studies of alcohol exposure-related impairment in neuronal integrity in this region. We also found evidence of an alcohol-related disruption in choline metabolism that could influence learning by adversely affecting synaptogenesis and/or expansion and maintenance of dendritic arborization. The observed alcohol-related alterations in Glx suggest disruption of the excitatory neurotransmission of glutamatergic neurons. It is possible that prenatal alcohol exposure will be found to be associated with similar alterations of these metabolites in other regions, thereby providing information regarding aspects of cellular function at the neurochemical level that may mediate prenatal alcohol effects on a range of neurobehavioral endpoints.

Acknowledgements

This research was funded by grants from the National Institute on Alcohol Abuse and Alcoholism (NIAAA): R01 AA016781 and an administrative supplement to R01 AA09524 (S. Jacobson, PI); U01 AA014790 (S. Jacobson, PI); R21AA017410 (E. Meintjes and A. van der Kouwe, PIs); and U24 AA014815 (K. Jones, PI) in conjunction with the NIAAA Collaborative Initiative on Fetal Alcohol Spectrum Disorders (CIFASD). This research was also supported by a grant from the NIH Office of Research on Minority Health, the South African Research Chairs Initiative of the Department of Science and Technology and National Research Foundation of South Africa, Focus Area Grant FA2005040800024 from the South African National Research Foundation (E. Meintjes, PI), and seed money grants from the University of Cape Town, the President of Wayne State University, and the Joseph Young, Sr., Fund from the State of Michigan. We thank Bruce Spottiswoode, Ph.D., the CUBIC radiographers Marie-Louise de Villiers and Nailah Maroof, and our UCT and WSU research staff Maggie September, Mariska Pienaar, Nicolette Hamman, and Neil Dodge. We also thank the dysmorphologists, H. Eugene Hoyme, Luther K. Robinson, and Nathanial Khaole, who conducted the dysmorphology examinations of the children for the FASD diagnosis. We greatly appreciate the participation of the mothers and children in the longitudinal study.

The authors declare no competing financial interests.

Chapter Five

Neural Correlates of Cerebellar-mediated Timing during Finger Tapping in Children with Fetal Alcohol Spectrum Disorders

Lindie du Plessis[1,2], Joseph L. Jacobson[2,3,4], Sandra W. Jacobson[2,3,4,] Christopher D. Molteno[3], Ernesta M. Meintjes[1,2], Frances C. Robertson[1,2]

Abstract

Classical eyeblink conditioning (EBC) is an elemental form of learning that is among the most sensitive indicators of fetal alcohol spectrum disorders. The cerebellum plays a key role in maintaining timed movements with millisecond accuracy, which is required for EBC. Functional MRI (fMRI) was used to identify cerebellar regions that mediate timing in healthy controls and the degree to which these areas are also recruited in children with prenatal alcohol exposure.

fMRI data were acquired during an auditory rhythmic/non-rhythmic finger tapping task. We present results for 17 children with fetal alcohol syndrome (FAS) or partial FAS, 17 heavily exposed (HE) nonsyndromal children and 16 non- or minimally-exposed controls.

Controls showed greater cerebellar activation in right Crus I, vermis IV-V, vermis VI and right lobule VI during rhythmic than non-rhythmic tapping. Although alcohol-exposed and

[1] MRC/UCT Medical Imaging Research Unit, University of Cape Town, UCT
[2] Department of Human Biology, UCT
[3] Department of Psychiatry and Mental Health, UCT
[4] Department of Psychiatry and Behavioral Neurosciences, Wayne State University School of Medicine

control children performed equally well on this simple task both before and after applying exclusionary criteria, the alcohol-exposed children showed smaller activation increases during rhythmic tapping in right Crus I than the control children and the most severely affected children with either FAS or PFAS showed smaller increases in vermis IV-V. Higher levels of maternal alcohol intake per drinking occasion during pregnancy were associated with reduced activation increases during rhythmic tapping in all four regions associated with rhythmic tapping in controls.

The four cerebellar areas activated by the controls more during rhythmic than non-rhythmic tapping have been implicated in the production of timed responses in several previous studies using diverse methodologies. These data provide evidence linking binge-like drinking during pregnancy to poorer function in specific cerebellar regions involved in timing and somatosensory processing needed for complex tasks requiring precise timing, such as EBC.

5.1 Introduction

Fetal alcohol spectrum disorders (FASD) are characterized by a broad range of physical and behavioural impairments, including poorer learning and memory (Burden et al., 2005; Jacobson et al., 1993; Mattson et al., 2011) and lower IQ (Jacobson et al., 2004; Mattson et al., 1997). Fetal alcohol syndrome (FAS), the most severe FASD, is characterized by a distinctive craniofacial dysmorphology, including a flat philtrum, thin upper lip and small palpebral fissures, smaller head circumference and growth retardation (Hoyme et al., 2005). A partial FAS (PFAS) diagnosis requires the presence of at least two of the facial features as well as either small head circumference, retarded growth, or neurobehavioral deficits and confirmation that the mother drank during pregnancy. Heavily exposed (HE) nonsyndromal children may also exhibit neurobehavioral and attention deficits but are more difficult to identify because they lack the characteristic facial features (Hoyme et al., 2005).

In the 5-year follow-up assessment of the Cape Town Longitudinal Cohort, we found a remarkably striking deficit in eyeblink conditioning performance in children with prenatal alcohol exposure (Jacobson et al., 2008), findings subsequently confirmed in a school-aged cohort (Jacobson et al., 2011). None of the children in the longitudinal Cape Town sample with full FAS met criteria for delay conditioning at the end of three training sessions at five years, compared to 75% of the healthy controls. Only 33.3% of the children with PFAS and 37.9% of the HE nonsyndromal children met criteria for conditioning. Eyeblink conditioning is a nonverbal elemental learning paradigm, in which a conditioned stimulus (CS), typically a pure tone, is presented 500ms before a brief air puff to the eye (unconditioned stimulus (US)) that elicits a reflexive blink. After repeated pairings, the tone comes to elicit a conditioned eyeblink response just prior to the puff, as the subject is able to use the CS to anticipate the timing of the onset of the air puff. The cerebellar-brain stem neural pathways that mediate eyeblink conditioning have been studied extensively in animal models (Christian and Thompson, 2003; Lavond and Steinmetz, 1989).

Successful conditioning relies on a well-functioning cerebellar-mediated internal timing mechanism in order to produce responses with millisecond accuracy. Alcohol-related eyeblink conditioning deficits have also been demonstrated in rodents and sheep (Goodlett et al., 2000; Stanton and Goodlett, 1998) and in another human study (Coffin et al., 2005).

The cerebellum has been identified as playing a key role in producing and maintaining timed movements with millisecond accuracy (Ivry and Keele, 1989; Ivry et al., 1988; Spencer et al., 2003; Tesche and Karhu, 2000). Ivry and Keele (1989) used a paced/unpaced finger tapping task during which subjects were required to maintain a rhythm after a pacing metronome terminated to compare performance among patients with Parkinson's disease, cerebellar-, cortical- and peripheral neuropathy, and healthy controls. Patients with cerebellar lesions performed worst of all, with a 50% increase in the standard deviation (SD) of the inter-tapping interval (ITI) compared to controls. Subsequently, it was demonstrated that poor maintenance of rhythm in patients with lateral cerebellar lesions was attributable to deficits in the internal timing mechanism (Wing et al., 1984), whereas in

patients with medial cerebellar lesions it was attributable to impaired motor response (Ivry et al., 1988). In a separate finger flexion/extension study, it was confirmed that cerebellar patients showed greater temporal variability during rhythmic discrete movements, but no timing deficits during continuous finger movement (Spencer et al., 2003).

Key areas identified as being involved in timed movements in adults using functional MRI (fMRI) include superior vermis and cerebellar lobules V/VI, all of which show greater activation during discrete finger flexion/extension compared to continuous movements (Spencer et al. 2007). Bengtsson et al. (2005) performed a conjunction analysis to localise brain regions involved in timing, independent of the effector used. Six tasks were performed by the subjects, including sequential bilateral finger tapping, bilateral isochronous finger tapping, and sequential and isochronous silent speech paced by auditory stimuli. fMRI results showed increased ipsilateral activation in vermis V/VI and lateral lobule VI during timed activity.

Neuroimaging studies have indicated that children often activate different or more extensive neural circuitry when performing simple tasks, compared with adults (Davis et al., 2009; Konrad et al., 2005; Meintjes et al., 2010). Similarly, children have been shown to activate more cerebellar regions than adults during unpaced rhythmic finger tapping, including right lobule VIIb and IX, bilateral Crus II and vermis VI, VIIb, VIII and Crus II (De Guio et al., 2012).

We were interested in examining whether the impaired eyeblink conditioning performance observed in children with FASD may, in part, be attributed to a deficit in the internal timing mechanism in these children and whether children prenatally exposed to alcohol recruit areas involved in the maintenance of timed responses with millisecond accuracy to the same extent as controls. We used fMRI in children prenatally exposed to alcohol and healthy non- or minimally-exposed controls during a finger tapping task, which interleaves blocks of rhythmic and non-rhythmic tapping in response to an auditory cue, to examine differences in cerebellar activations related to timing in these children. We assumed that significant differences in activation between rhythmic and non-rhythmic conditions will

be seen between the children prenatally exposed to alcohol and the control children in areas involved in the maintenance of timed responses in control children.

5.2 Materials and Methods

5.2.1 Participants

Pregnant women from the Cape Coloured (mixed ancestry) community in Cape Town, South Africa, were recruited between 1999 and 2002 at their first visit to an antenatal clinic (Jacobson et al., 2008). The incidence of FASD in this population is among the highest reported in the world (May et al., 2000; 2007).

The Cape Coloured population, comprised of descendants of white European settlers, Malaysian slaves, Khoi-San aboriginals, and black Africans, historically constituted the large majority of workers in the wine-producing region of the Western Cape. The high prevalence of FAS in this community is attributable to very heavy maternal drinking during pregnancy (Croxford and Viljoen, 1999; Jacobson et al., 2006; 2008), due to poor psychosocial circumstances and residual impact of the now-outlawed *dop* system, in which farm labourers were paid, in part, with wine.

All pregnant women who reported consuming at least 14 standard drinks/week or engaging in binge drinking (≥ 5 drinks/occasion) during pregnancy were invited to participate in the study. In addition, pregnant women who abstained or drank minimally during pregnancy (< 7 drinks/week and no binge drinking) were invited to participate as controls. Women younger than 18 years of age, as well as women with diabetes, epilepsy, or cardiac problems requiring treatment, and religiously observant Muslim women, whose religious practices prohibit alcohol consumption, were excluded from the study. Infant exclusionary criteria were major chromosomal anomalies, neural tube defects, multiple births, and seizures.

Maternal alcohol consumption was assessed using a timeline follow-back approach (Jacobson et al., 2002). At recruitment the mother was interviewed regarding the incidence

and amount of her drinking on a day-by-day basis during a typical 2-week period at time of conception. She was also asked whether her drinking had changed since conception; if so, when the change occurred and how much she drank on a day-by-day basis during the preceding 2-week period. This procedure was repeated in mid-pregnancy and again at one month postpartum to provide information about drinking during the latter part of pregnancy. Volume was recorded for each type of beverage consumed each day, converted to absolute alcohol (AA) using multipliers proposed by Bowman et al. (1975), and averaged to provide three summary measures of alcohol consumption at conception and during pregnancy: average ounces of AA consumed/day, AA/drinking day (dose/occasion) and frequency (days/week). The number of cigarettes smoked on a daily basis, as well as the frequency of marijuana and other drug use were also recorded.

Each child was examined for growth and FAS dysmorphology by two U.S.-based expert dysmorphologists following the revised Institute of Medicine criteria during a 6-day clinic in 2005 (Hoyme et al., 2005; Jacobson et al., 2008). Four children who did not attend the clinic (1 FAS, 2 HE and 1 control) were examined by a Cape Town-based dysmorphologist with expertise in FAS diagnosis. There was substantial agreement among the dysmorphologists on the assessment of all dysmorphic features, including the three principal fetal alcohol-related characteristics—philtrum and vermilion measured using the *Lip-Philtrum Guide* (Astley and Clarren, 2001) and palpebral fissure length (median $r = 0.78$). Each of the alcohol-exposed children was assigned to one of the following diagnostic groups at a case conference: FAS, PFAS, or nonsyndromal HE.

IQ data were collected from the children on the *Wechsler Intelligence Scale for Children-IV* (WISC-IV) at 10 years at our Child Development Research Laboratory at UCT (Diwadkar et al., 2013; Jacobson et al., 2011). In the 5-yr follow-up of the children from our longitudinal cohort, we administered the *Junior South African Individual Scales* (JSAIS; Madge et al., 1981), which is available in Afrikaans and English and has been normed for South African children. IQ scores from the *JSAIS* were strongly correlated with the WISC-IV

scores, $r = 0.73$, $p < 0.001$, confirming the validity of our translation of the WISC-IV for use with this population (Jacobson et al., 2011).

Mothers and children were transported to the Cape Universities Brain Imaging Centre (CUBIC) for neuroimaging. 82 (10 FAS, 19 PFAS, 29 HE, 24 controls; 47 boys) right-handed children were scanned on the 3T Allegra (Siemens, Erlangen, Germany) MRI scanner at CUBIC between January 2009 and December 2011 (mean age ± SD = 10.7 ± 0.6 years, age range 9.5 to 12.0). We acquired high-resolution structural images and functional MRI data during rhythmic and non-rhythmic finger tapping.

5.2.2 Experimental Task

The experimental tasks were programmed using E-Prime software (Psychology Software Tools, Inc., Pittsburgh, USA) and were presented through a waveguide in-line with the bore of the magnet in the rear wall of the scanner room using a data projector and a rear projection screen mounted at the end of the magnet bore. Responses were recorded using a Lumitouch response system (Photon Control Inc., Burnaby, Canada). The child was able to talk to the examiner using an intercom that is built into the scanner and could stop the scan at any time by squeezing a ball held in his/her left hand. All children were accompanied into the scanner room by a research nurse/assistant who stayed with them throughout the scan.

All children practiced the task before the scan to ensure that they understood the instructions and could perform the task. Children also lay down in a mock scanner prior to the scan to listen to a recording of the scanner noises, which helped to reduce anxiety.

The experimental task was designed to distinguish between brain regions activated during rhythmic tapping compared to non-rhythmic tapping. This task, which was adapted from the design (Fig.5.1) used by Lutz et al. (2000), employed an auditory rather than visual stimulus. Each block comprises two different active conditions (rhythmic and non-rhythmic

finger tapping) interleaved with rest blocks. The children are instructed to press a button with their right index finger every time they hear a tone.

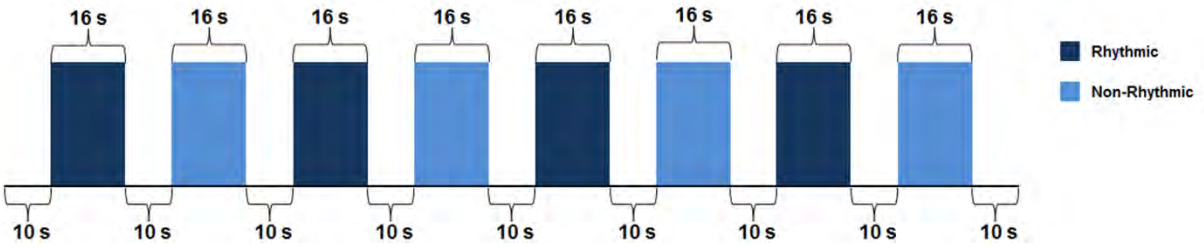

Figure 5.1: Timing diagram of the rhythmic/non-rhythmic finger tapping task

The first block is preceded by a rest block of 8 s, during which four dummy scans are acquired and an instruction to get ready is displayed. During the rhythmic blocks, tones are equally spaced (SD = 0 ms) with an inter-stimulus interval (ISI) of 736 ms. The non-rhythmic blocks comprise tones at irregular intervals (mean ISI = 736 ms, SD = 256 ms). Both the rhythmic- and non-rhythmic blocks last for 16 s and are interleaved with 10 s of rest between active blocks. Each set of blocks (rhythmic, rest, non-rhythmic, rest) is repeated four times. The principal performance measure is rhythmicity of tapping, determined by averaging for each condition the SDs of the inter-tap intervals (ITIs) within each block of that condition.

5.2.3 fMRI Imaging Protocol

High-resolution T_1-weighted structural MR images were acquired using a 3D echo planar imaging (EPI) navigated multi-echo MPRAGE sequence that had been optimized for morphometric analyses using FreeSurfer (version 5.1.0, http://surfer.nmr.mgh.harvard.edu) software (Tisdall et al., 2009; Van der Kouwe et al., 2008). Imaging parameters were: FOV

256 x 256 mm^2; 128 sagittal slices, TR 2530 ms; TE 1.53/3.21/4.89/6.57 ms; TI 1100 ms; flip angle 7°; voxel size 1.3 x 1.0 x 1.3 mm^3. The 3D EPI navigator provided real-time motion tracking and correction, which served to substantially reduce the presence of any motion artifacts in structural imaging data, despite significant subject motion.

A T_2*-weighted gradient echo, EPI sequence was used to acquire 114 functional volumes that are sensitive to BOLD contrast (TR 2000 ms, TE 30 ms, 34 interleaved slices, 3 mm slice thickness, gap 1.5 mm, FOV 200 x 200 mm^2, in-plane resolution 3.125 x 3.125 mm^2) while the children performed the task.

All procedures were performed according to protocols that had been approved by the Human Investigation Committee of Wayne State University and the Faculty of Health Sciences Human Research Ethics Committee at the University of Cape Town. All parents/guardians provided informed written consent; all children provided oral assent.

5.2.4 Data Analyses

The following criteria were used to ensure that only data from blocks in which the child was fully engaged in the task were included in the fMRI data analysis. In the rhythmic tapping condition, only blocks with SDs less than 150 ms, mean ITIs between 500 and 1000 ms, and 6 or fewer missed taps were included in the analyses. ITIs during the rhythmic blocks that exceeded 1200 ms were assumed to occur due to one or more missed taps. In such instances, for the purposes of computing SD, additional taps were inserted with an ITI as close to 736 ms as possible to ensure that missed taps were interpolated with the appropriate rhythm. Inserted taps were counted as “missed” in determining whether to include the block in the analysis. Non-rhythmic tapping blocks were included in the analysis only if their SDs were greater than 170 ms and if the difference between the number of tones presented and the number of button presses did not exceed nine. Blocks that did not meet inclusion criteria were labelled as ‘bad’ blocks and treated as separate predictors in the general linear model (GLM).

Only children who met criteria for two or more blocks in each condition were included in the study as only these children were considered to be fully engaged in the task.

fMRI data analyses were performed in Brain Voyager QX (Brain Innovation, Maastricht, The Netherlands). The first four dummy scans were excluded from all analyses. Pre-processing included motion correction relative to the first volume that was acquired during the functional scan, linear scan time correction, temporal filtering with a high pass filter of 3 cycles / point, and linear trend removal. Scans with motion exceeding 3 mm translation or 3^{o} rotation within a functional run were excluded from all further analyses. Whole-brain group analyses were performed with a random effects analysis of variance using the GLM with predictor time courses for the successful rhythmic and non-rhythmic tapping blocks convolved by the standard hemodynamic response function. The six motion correction parameters were *z*-transformed and added as predictors of no interest together with the predictors for the excluded ('bad') rhythmic and non-rhythmic tapping blocks.

Beta maps were created for each subject for the contrast comparing activation during rhythmic and non-rhythmic finger tapping. The beta maps were exported in Analyze format for second level analyses using the spatially unbiased atlas template (SUIT) toolbox in SPM5 (Statistical Parametric Mapping) to obtain more detailed information on activation patterns in the cerebellum (Diedrichsen et al., 2009). This atlas, which is based on the structural data of 20 healthy individuals, has been shown to significantly improve the alignment of individual fissures in the cerebellum when compared to normalization to the MNI whole-brain template.

Each subject's cerebellum was initially isolated in the structural images by calculating the probability of each voxel belonging to the cerebellum or brain stem. The isolation maps were then used to transform each subject's cerebellum to the SUIT template in the subsequent step, which normalized the data. Manual correction was applied using MRICRON (Rorden and Brett, 2000) for each subject to eliminate contamination from the visual cortex. The functional data for the cerebella were then resliced according to the

isolated and normalized structural data for each subject to render the data in the SUIT atlas space.

5.2.5 Statistical Analyses

A one-sample *t*-test was used to identify clusters where percent signal change values comparing rhythmic and non-rhythmic tapping were significantly different from zero in the control children. Cluster size correction with a cluster defining threshold of 0.05 on the normalised group images was applied to reduce the risk of multiple comparisons and a minimum cluster size of 193 mm^3 was found to be statistically significant.

In order to determine whether normalising the children's cerebella to an adult template would lead to excessively small effective regions of interest (ROIs), cerebellar volumes generated by FreeSurfer (version 5.1.0, http://surfer.nmr.mgh.harvard.edu) were compared to values reported in adult studies (Luft et al., 1999, Woodruff-Pak et al., 2001). Woodruff-Pak and colleagues (2001) calculated cerebellar volumes ranging from 122.73 to 142.37 ml in eight young adults (age 21 to 35 years) and Luft and colleagues (1999) found a range of 99.86 to 170.6 ml in 48 adults (age 19.8 to 73.1 years). The children included in our functional study had an average cerebellar volume of 130.85 ± 13.03 ml (range 107.18 to 170.11 ml), which is within the limits of the aforementioned studies. The overall effect of normalisation to an adult template was, therefore, deemed negligible.

ROIs were defined with radius 3 mm, centered on the peak coordinates, in these regions. Due to the large cluster sizes in the vermal lobules, percent signal changes were extracted around the centre of mass instead of the peak voxels in these two clusters. Mean percent signal change values were extracted in these ROIs for each child and exported to SPSS (version 20; IBM, New York, USA) to examine differences in activation in these regions as a function of diagnosis as well as associations with the extent of prenatal alcohol exposure.

Differences between diagnostic groups in each ROI were examined using analysis of variance. Eight control variables were considered as potential confounders: child's sex, age at assessment, postnatal lead exposure, IQ and cerebellar volume; maternal education, smoking (cigarettes/day) during pregnancy and age at delivery. Pearson correlations were used to examine the relations of the mean percent signal change values in the ROIs to each of the potential confounders. All control variables related to a given outcome at $p < 0.10$ were considered as possible confounders. These variables were entered into an analysis of covariance (ANCOVA) to determine whether group differences in the ROIs remained significant after controlling for these measures.

Correlations between extent of prenatal alcohol exposure and activation were also examined in SPSS. Although the control group's continuous measures were essentially all zero, the data for these children were included in the correlation analyses to avoid artificially truncating the range of exposure. Hierarchical multiple regression analyses were used to control for confounding. The alcohol measure was entered in the first step of each analysis for each outcome. All control variables related to the outcome at $p < 0.10$ were entered in the second step to determine if the effect of the continuous alcohol measure on activation patterns continued to be significant after statistical adjustment for potential confounders.

5.3 Results

5.3.1 Sample Characteristics

After applying exclusion criteria, we report data for 50 (30 male, 20 female) right-handed children (mean age 10.7 ± 0.6 yr), including 7 children with full FAS, 10 with PFAS, 17 nonsyndromal HE children, and 16 non- or minimally-exposed controls. The data for 8 children were excluded due to excessive motion (1 PFAS, 2 HE, 5 controls), as were data from 24 children who did not meet performance criteria (3 FAS, 8 PFAS, 10 HE, 3 controls). Due to the smaller number of children with FAS, the FAS and PFAS groups were combined in the data analysis. Table 5.1 summarizes the demographic information for these children.

The children in the HE group were slightly older than children in the other two groups. The low IQ scores of all of the children reflect the highly disadvantaged backgrounds and poor education of the children in this community; nevertheless, as expected, the lowest scores were seen in the FAS/PFAS group. The mothers of the children in the FAS/PFAS group were also older and had completed fewer years of formal education. Prenatal alcohol exposure was very high, averaging 8.2 standard drinks/occasion for the FAS/PFAS group and 5.4 for the nonsyndromal HE group across pregnancy. All but 1 of the 16 control mothers abstained from drinking during pregnancy; that mother drank 2 drinks on 3 occasions. No group differences were found for maternal smoking during pregnancy or lead exposure.

Table 5.1: Sample characteristics (*N* = 50)

	FAS/PFAS	HE	Controls	*F* or χ^2
N	17	17	16	NA
Child's age at assessment (yr)[a]	10.5 ± 0.6	11.0 ± 0.7	10.6 ± 0.4	4.04*
Sex (M/F)	11/6	11/6	8/8	0.98
WISC-IV IQ[b]	67.2 ± 11.6	77.7 ± 8.9	73.8 ± 11.3	4.17*
Child's Cerebellar Volume (ml)[c]	124.4 ± 10.5	136.2 ±	130.9 ± 9.3	4.95*
Maternal age at delivery (yr)[d]	30.2 ± 7.8	24.8 ± 5.1	25.5 ± 3.2	4.37*
Maternal education (yr)[e,f]	7.4 ± 3.4	9.3 ± 2.4	10.4 ± 1.4	5.02*
AA/day across pregnancy (oz)	1.1 ± 0.9	0.4 ± 0.4	0.0 ± 0.0	16.16**
AA/occasion across pregnancy (oz)	4.1 ± 1.9	2.7 ± 1.6	0.1 ± 0.3	32.14**
Frequency of drinking across pregnancy	1.8 ± 1.0	0.9 ± 0.8	0.0 ± 0.0	22.51**
Cigarettes smoked per day during	7.1 ± 5.2	6.3 ± 5.2	3.7 ± 6.8	0.56
Lead exposure (µg/dℓ)	11.6 ± 6.8	9.8 ± 3.0	8.8 ± 4.0	1.38

Values are means ± SD
FAS = fetal alcohol syndrome, PFAS = partial FAS, HE = heavily exposed non-syndromal
[a]FAS/PFAS < HE ($p = 0.02$), HE > control ($p = 0.02$)
[b]FAS/PFAS < HE ($p = 0.01$), FAS/PFAS < control ($p = 0.09$)
[c]FAS/PFAS < HE ($p < 0.01$), FAS/PFAS < control ($p = 0.09$)
[d]FAS/PFAS > HE ($p = 0.01$), FAS/PFAS > control ($p = 0.03$)
[e]FAS/PFAS < HE ($p = 0.04$), FAS/PFAS < control ($p < 0.01$)
[f] Maternal education missing for mother of 1 child with FAS
*$p < 0.05$, **$p < 0.01$

In accordance with previous findings (Mattson et al., 1994; Archibald et al., 2001), significant differences in cerebellar volumes were seen between the diagnostic groups and *post-hoc* analyses showed that this result was driven by the significantly reduced cerebellar volume of the most heavily exposed children compared to both the HE and control groups.

5.3.2 Behavioural Data

Both before and after exclusions, the groups didn't differ on performance during rhythmic or non-rhythmic tapping. Table 5.2 shows a summary of these values for the 50 children included in the fMRI study. For the rhythmic tapping, the SD after correcting for missed taps is shown. Since this study focuses on effects of prenatal alcohol exposure on functional activation, the behavioural results were used only to identify children who were able to perform adequately on the task, as evidenced from the absence of group differences in Table 5.2.

Table 5.2: Behavioural performance by diagnostic group (*N* = 50)

		FAS/PFAS *N* = 17	HE *N* = 17	CTL *N* = 16	*F*	*p*
Rhythmic tapping	**SD**	91.12 ±7.47	92.02 ± 29.90	81.56 ± 31.20	0.45	0.64
	Number of Missed Taps	2.32 ± 1.56	2.89 ± 1.67	2.16 ± 1.86	0.83	0.45
Non-rhythmic tapping	**SD**	351.60 ± 151.39	334.62 ± 131.65	328.83 ± 113.40	0.54	0.59
	Difference between taps and stimuli presented	2.72 ± 4.22	1.58 ± 3.24	1.81 ± 2.95	1.97	0.14

Values are means ± SD
FAS = fetal alcohol syndrome, PFAS = partial FAS, HE = heavily exposed non-syndromal
$^{*}p < 0.05$, $^{**}p < 0.01$

5.3.3 fMRI Data

Four regions in the cerebellum showed greater activation during rhythmic tapping compared to non-rhythmic tapping in the control children (Table 5.3 and Fig. 5.2).

Table 5.3: Cerebellar regions showing significantly greater activation during rhythmic finger tapping compared to non-rhythmic finger tapping in control children

	MNI Peak Coordinates				
Brain Region	**x**	**y**	**z**	***t*-statistic**	**Cluster size (mm^3)**
Right Crus I	50	-59	-36	5.18	194
Vermis IV-V	2	-59	-2	4.40	1151
Vermis VI	4	-79	-24	4.19	796
Right Lobule VI	12	-62	-17	3.55	219

Minimum cluster size 193 mm^3
Nomenclature as proposed by Schmahmann et al. (2000)

Table 5.4 and Fig. 5.3 summarize mean percent signal change values in ROIs defined in these regions for each group. A significant group difference was detected in right Crus I. *Post hoc* analyses showed that the activation in right Crus I was significantly higher in control children than in both the FAS/PFAS ($p < 0.01$) and HE ($p = 0.01$) groups, with no difference between the FAS/PFAS and HE groups ($p > 0.20$). A group difference falling short of statistical significance ($F = 2.68$, $p = 0.08$) was seen in vermis IV-V, due to lower activation in the FAS/PFAS group compared with the controls (*post hoc* $p = 0.05$).

Figure 5.2: (a) Right anterolateral, (b) superior coronal and (c) left anterolateral views of right Crus I, vermi IV-VI and right lobule VI regions showing greater activation in control children during rhythmic tapping compared to non-rhythmic tapping. Functional data are shown in the Spatially Unbiased Cerebellar Atlas Template space (MNI coordinates).

Table 5.4: Comparison by diagnostic group of differences in brain activation between rhythmic and non-rhythmic finger tapping in four cerebellar ROIs that are activated more during rhythmic tapping than non-rhythmic tapping in control children.

Brain Region	FAS/PFAS *N* = 17	HE *N* = 17	CTL *N* = 16	*F*	*p*
Right Crus I[a]	-0.05 ± 0.39	0.03 ± 0.70	0.73 ± 0.98	5.59**	0.01
Vermis IV-V[b,c]	0.10 ± 0.53	0.57 ± 0.65	0.60 ± 0.88	2.68†	0.08
Vermis VI[c]	0.12 ± 0.43	0.22 ± 0.53	0.21 ± 0.26	0.28	0.76
Right Lobule VI	0.12 ± 0.33	0.19 ± 0.51	0.29 ± 0.29	0.79	0.46

Nomenclature as proposed by Schmahmann et al. (2000)
Values are means ± SD
FAS = fetal alcohol syndrome, PFAS = partial FAS, HE = heavily exposed non-syndromal
$^{\dagger}p < 0.1$, $^{*}p < 0.05$, $^{**}p < 0.01$
[a]FAS/PFAS < control ($p < 0.01$), HE < control ($p = 0.01$)
[b]FAS/PFAS < HE ($p = 0.06$), FAS/PFAS < control ($p = 0.05$)
[c]Percent signal change around centre of mass

Pearson correlation analyses identified two potential confounding variables. Girls showed greater activations in right Crus I ($r = 0.32$, $p < 0.05$), while maternal smoking during pregnancy was associated with lower activations in vermis IV-V ($r = -0.26$, $p < 0.10$). The group difference in right Crus I remained significant ($F = 5.47$, $p = 0.01$) after adjustment for sex, and the effect on vermis IV-V was not reduced after adjustment for maternal smoking ($F = 2.63$, $p = 0.06$). None of the control variables were related to activations in vermis VI or right lobule VI.

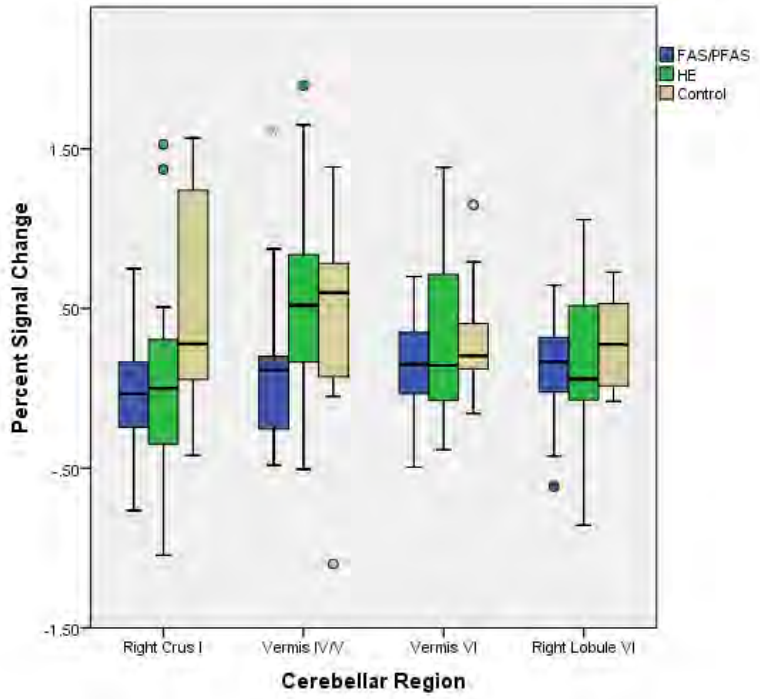

Figure 5.3: Comparison of changes in activation between diagnostic groups for the contrast comparing rhythmic to non-rhythmic finger tapping in regions significantly activated in non- or minimally exposed controls

Relations of extent of prenatal alcohol exposure to differences in activation between rhythmic and non-rhythmic finger tapping in the four cerebellar ROI's are summarized in Table 5.5. Greater prenatal alcohol exposure was associated with smaller differences in brain activation between rhythmic and non-rhythmic finger tapping in right Crus I. The strongest association was with frequency of drinking across pregnancy (Fig. 5.4). In right lobule VI, greater absolute alcohol consumed per occasion, both around conception and across pregnancy, was associated with smaller differences in activation between rhythmic and non-rhythmic tapping (see Fig. 5.5). Multiple regression analyses showed that the relation in right Crus I remained significant after controlling for sex. Greater alcohol consumption per drinking occasion around conception and during pregnancy was also associated with lower percentage signal change in both vermal regions. Multiple regression analysis showed that the effect of drinking per occasion across pregnancy on activation in vermis IV-V continued to be significant after adjustment for maternal smoking.

Table 5.5: Relation of prenatal alcohol exposure to activation in regions with significant differences in activation comparing rhythmic and non-rhythmic finger tapping in control children

	AA/day at time of conception		AA/occasion around time of conception		Frequency of drinking around time of conception (days/week)		AA/day across pregnancy		AA/occasion averaged across pregnancy		Frequency of drinking across pregnancy (days/week)	
	r	***β***	***r***	***β***	***r***	***β***	***r***	***β***	***r***	***β***	***r***	***β***
Right Crus I[a]	-0.32*	-0.28*	-0.18	-0.16	-0.40**	-0.35**	-0.36**	-0.32*	-0.30*	-0.28*	-0.46**	-0.41**
Vermis IV-V[b,c]	-0.23	-0.17	-0.31*	-0.26†	-0.23	-0.18	-0.20	-0.13	-0.35*	-0.28*	-0.18	-0.11
Vermis VI[c]	-0.04	-0.04	-0.29*	-0.29*	0.63	0.63	-0.04	-0.04	-0.25†	-0.25†	-0.02	-0.02
Right Lobule VI	-0.25†	-0.25†	-0.42**	-0.42**	-0.09	-0.09	-0.26†	-0.26†	-0.37**	-0.37**	-0.15	-0.15

Nomenclature as proposed by Schmahmann et al. (2000)
[a]Controlling for sex in the multiple regression analysis
[b]Controlling for maternal smoking
[c]Percent signal change around centre of mass
r is the simple Pearson correlation between alcohol exposure and percent signal change values; *β* is the standardized regression coefficient after adjustment for the potential confounding variables.
$^{\dagger}p < 0.10$, $^{*}p < 0.05$, $^{**}p < 0.01$.

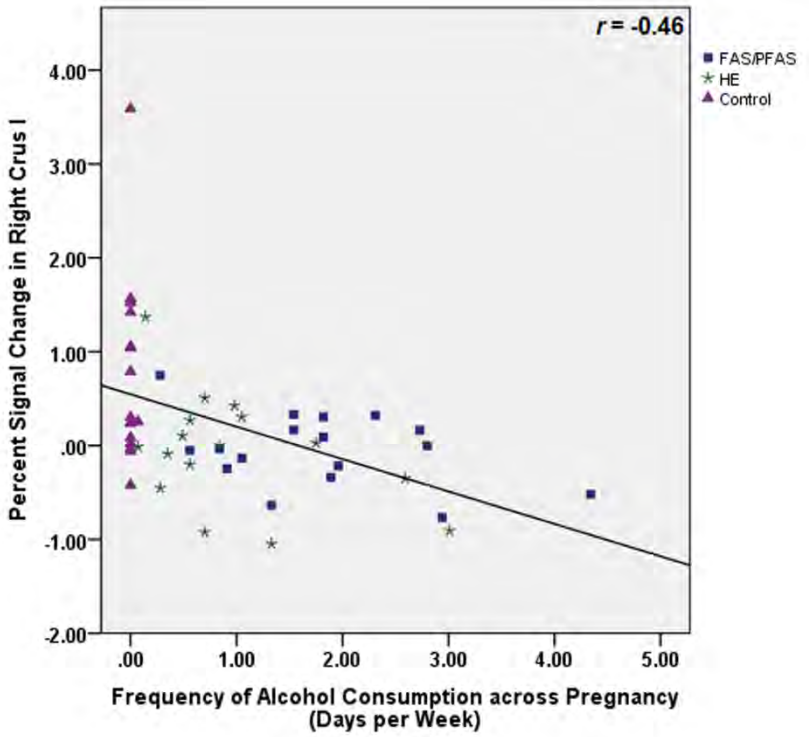

Figure 5.4: Correlation of frequency of alcohol exposure across pregnancy with activation in right Crus I

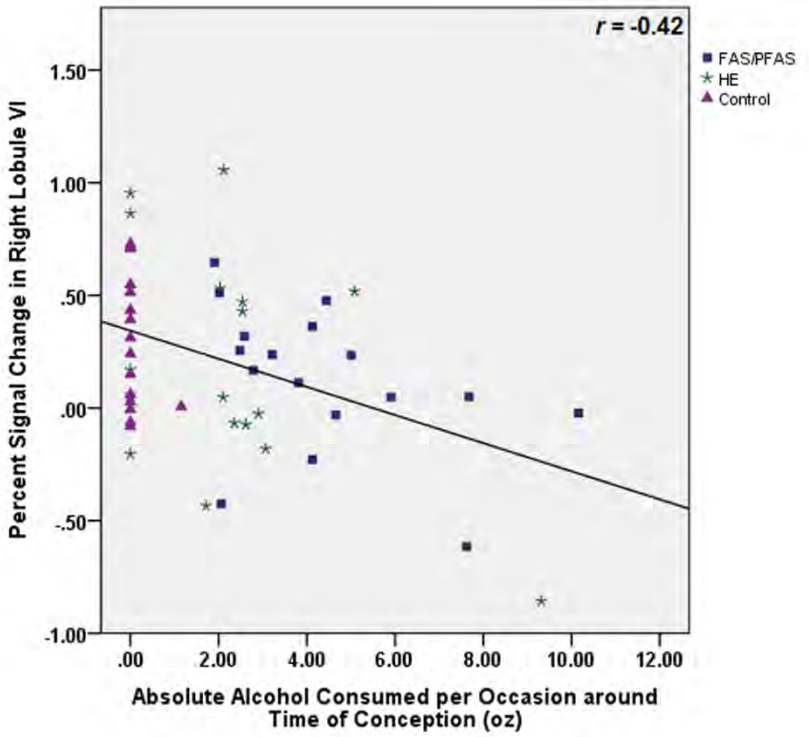

Figure 5.5: Correlation of dosage dependent alcohol exposure around time of conception and activation in right lobule VI

5.4 Discussion

This study used fMRI to investigate differences in the neural circuitry involved in performing timed movements in children prenatally exposed to alcohol compared with healthy controls. The controls showed increased activations during rhythmic tapping compared to non-rhythmic tapping in four cerebellar regions that have been implicated in the production of timed movements in previous studies with adults (Gerwig et al., 2003; Grodd et al., 2001; Schlerf et al., 2006; Spencer et al., 2007). Our continuous measure of maternal alcohol intake per occasion during pregnancy was associated with reduced differences in activation between rhythmic and non-rhythmic tapping in all four regions. When the children were compared by diagnostic group, both the FAS/PFAS and nonsyndromal HE groups showed significantly less of an increase in brain activation during rhythmic tapping in right Crus I compared with controls, while only the children with FAS or PFAS showed significantly smaller differences in activation between rhythmic and non-rhythmic tapping in vermis IV-V than the controls.

Vermis V and VI have been previously implicated in timing in a study in which these regions showed greater activation during discrete rhythmic finger extension/flexion than during continuous finger movements (Spencer et al., 2007). This finding, with the addition of the involvement of hemispheric lobule VI, was corroborated by the aforementioned study by Bengtsson and colleagues (2005). In a recent study of paced/unpaced finger tapping in children, both these regions also showed increased activation during unpaced tapping compared with rest (De Guio et al., 2012).

In a study of adults using a procedure very similar to our task, Lutz et al. (2000) also found differences in activation in vermis VI, as well as in the right cerebellar nuclei, when comparing rhythmic vs. non-rhythmic finger tapping. However, in contrast to the findings in the previous studies (Bengtsson et al., 2005; Spencer et al., 2007), as well as our own, Lutz et al. (2000) found more activity during non-rhythmic than rhythmic finger tapping in these regions. Schlerf et al. (2006) administered four timing conditions to adults in a rhythmic/non-

rhythmic finger tapping task—one regular and three irregular that ranged from low to high ISI variability. Activation was generally higher in the anterior lobe and lateral lobule VI for the regular and most highly variable conditions, compared to the low and moderate variability conditions, indicating increased activation for processing both regular and highly irregular temporal patterns. When considered together, the Lutz et al. (2000) and Schlerf et al. (2006) studies suggest that the increased activation during the irregular tapping condition in vermis VI and lateral lobule VI may reflect greater effort to predict the timing of the onset of the next stimulus when the timing is irregular. We did not see this increase during highly irregular tapping in the children in our study.

It is noteworthy that lateral lobule VI has been shown to be of major importance in eyeblink conditioning in numerous animal studies (Miller et al., 2003; Steinmetz, 2000; Yeo and Hesslow, 1998), as well as fMRI studies in humans (Dimitrova et al., 2002; Ramnani et al., 2000), including a recent study from our cohort (Cheng et al., 2014). In the present study we found that the differences in activation between rhythmic and non-rhythmic tapping in ipsilateral lobule VI were most strongly related to alcohol consumed per drinking occasion, an exposure measure that predicted lower activations in all four regions identified in the control group. This finding suggests that cerebellar timing is more sensitive to heavy episodic binge-like drinking than sustained moderate drinking around the time of conception and throughout pregnancy.

By contrast to vermis VI and lateral lobule VI, which have been most directly implicated in cerebellar-mediated timing, activations in vermis IV-V have been associated with the execution of intentional movements (Grodd et al., 2001) as well as somatosensory processing of motor response (Allen et al., 1997; Desmond et al., 1997; Nitschke et al., 1996). The greater response in vermis IV-V during rhythmic compared to non-rhythmic tapping by the control children in our study may be attributable to greater somatosensory demands in the rhythmic condition. Our finding that heavier maternal drinking during pregnancy is associated with lower activation in this region is consistent with a previous report that this region is smaller in alcohol-exposed children (Sowell et al., 1996). These data

also suggest that the impaired eyeblink conditioning observed in children with FASD may involve both deficits in timing and impaired somatosensory function.

Although activation in ipsilateral Crus I has not been implicated in timing during finger tapping tasks in either adults (Jueptner et al., 1995; Lutz et al., 2000) or children (De Guio et al., 2012), it has been shown to play a role during both reflexive eyeblinks (Dimitrova et al., 2002) and eyeblink conditioning (Cheng et al., 2014; Gerwig et al., 2003; Ramnani et al., 2000).

5.5 Conclusion

Eyeblink conditioning is an elemental form of learning that is highly sensitive to prenatal alcohol exposure and requires precise millisecond timing. In this study, we used an fMRI finger tapping paradigm to examine effects of alcohol exposure on motor responses requiring millisecond accuracy. Increased maternal alcohol intake per drinking occasion during pregnancy was associated with lower activation increases during rhythmic compared with non-rhythmic tapping in several cerebellar regions that have been implicated in millisecond timing in studies with adults. In addition, in comparisons by fetal alcohol diagnostic group, children in the FAS/PFAS group, which is particularly affected in eyeblink conditioning, showed lower activation particularly in vermis IV-V. This region has been implicated in the execution of intentional movements and somatosensory processing of motor responses. In summary, these data provide evidence linking binge-like drinking during pregnancy to poorer function in specific cerebellar regions involved in timing and somatosensory processing. These findings show that several cerebellar regions are adversely affected by prenatal alcohol exposure. Although the full extent of this damage cannot be covered by a single finger tapping study, the results could indicate that damage caused by prenatal alcohol exposure also adversely affects cerebellar regions responsible for successful performance in the EBC task.

Acknowledgements

This research was supported by the following grants from the National Institute on Alcohol Abuse and Alcoholism: R01 AA016781 and an administrative supplement to R01 AA09524 (S. Jacobson, PI); U01 AA014790 (S. Jacobson, PI); R21AA017410 (E. Meintjes and A. van der Kouwe, PIs); and U24 AA014815 (K. Jones, PI) in conjunction with the Collaborative Initiative on Fetal Alcohol Spectrum Disorders. This research was also supported by a grant from the NIH Office of Research on Minority Health (S. Jacobson, PI), the South African Research Chairs Initiative of the Department of Science and Technology and National Research Foundation of South Africa, Focus Area Grant FA2005040800024 from the South African National Research Foundation (E. Meintjes, PI), and seed money grants from the University of Cape Town, the President of Wayne State University (WSU), and the Joseph Young, Sr, Fund from the State of Michigan. We thank Richard Ivry (PhD) and John Schlerf (PhD), University of California, Berkeley, for consultation regarding the task. We thank the CUBIC radiographers Marie-Louise de Villiers and Nailah Maroof and our UCT and WSU research staff Nicolette Hamman, Mariska Pienaar, Maggie September, Emma Makin, Renee Sun and Neil Dodge. We also greatly appreciate the participation of the mothers and children in the longitudinal study.

The authors declare no competing financial interests.

Chapter Six

The Effects of Prenatal Alcohol Exposure on Cerebellar Function during a Finger Tapping Task Requiring Millisecond Timing in Pre-adolescent Children: An fMRI Study

Lindie du Plessis[1,2], Joseph L. Jacobson[2,3,4], Frances C. Robertson[1,2], Sandra W. Jacobson[2,3,4,] Christopher D. Molteno[3], Ernesta M. Meintjes[1,2]

Abstract

Children prenatally exposed to alcohol have been reported to be impaired in classical eyeblink conditioning (EBC). We were interested in examining whether the observed EBC deficit may be due to effects of prenatal alcohol exposure on mechanisms involved in timing requiring millisecond precision. The cerebellum is known to mediate timed movements with millisecond accuracy. We used functional MRI (fMRI) to examine differences in activation patterns in the cerebellum between children with fetal alcohol spectrum disorders (FASD) and controls during a paced/unpaced finger tapping task that required maintaining a rhythm with millisecond precision after termination of an auditory 2 Hz pacing metronome.

fMRI data were analysed for 5 children with fetal alcohol syndrome (FAS), 9 children with partial FAS (PFAS), 22 heavily exposed nonsyndromal (HE) children and 16 non- or minimally exposed controls.

[1] MRC/UCT Medical Imaging Research Unit, University of Cape Town, UCT
[2] Department of Human Biology, UCT
[3] Department of Psychiatry and Mental Health, UCT
[4] Department of Psychiatry and Behavioral Neurosciences, Wayne State University School of Medicine

We identified four cerebellar regions associated with task performance in controls – right lobule VIIIa and b, left lobule VIIIa and right lobule VI. However, we were unable to reliably assign activation to either motor or clock due to several limitations in calculating the Wing-Kristofferson (1973) estimates.

All four these regions have consistently been implicated in motor control, with additional evidence of a timing component in lobule VI (Stoodley and Schmahmann, 2009; Grodd et al., 2001; Spencer et al., 2007; Bengtsson et al., 2005).

In all these regions except right lobule VIIIa, higher levels of prenatal alcohol exposure, especially dosage dependent measures, were associated with smaller activation increases during unpaced tapping.

The specific region identified in right lobule VI has been implicated in previous studies of EBC (Blaxton et al., 1996; Cheng et al., 2014) and our findings relating alcohol exposure to activation in this region could form an integral part of the impaired EBC performance seen in children with FASD.

6.1 Introduction

Fetal alcohol spectrum disorder (FASD) is the most widely encountered preventable form of mental retardation worldwide and is caused by maternal drinking during pregnancy. In the United States the incidence of FASD is 1 - 3 per 1000 live births, but it is estimated to be 18 to 141 times greater in the Cape Coloured (mixed ancestry) population in the Western Cape Province of South Africa (May et al., 2000; 2007), which is among the highest reported incidences in the world. The Western Cape is known for its vineyards and wine production, and a large portion of the Cape Coloured community traditionally worked on these wine farms, many of whom were paid, in part, with wine – a remuneration method called the *dop* system. Socioeconomic deprivation combined with the easy access to alcohol led to excessive maternal drinking and therefore a high prevalence of FASD (Croxford and Viljoen, 1999). Although the *dop* system has been declared illegal, heavy alcohol consumption

persists in both the urban and rural Cape Coloured communities (Jacobson et al., 2006; 2008).

FASD includes a range of conditions, of which fetal alcohol syndrome (FAS) is the most severe. FAS is characterized by a distinctive craniofacial dysmorphology, including a flat philtrum, thin upper lip and small palpebral fissures (Jones and Smith, 1973). Affected children also have smaller head circumference and growth retardation. A partial FAS (PFAS) diagnosis requires the presence of two of the three facial features as well as either small head circumference, signs of growth retardation, or neurobehavioral deficits. Children with alcohol-related neurodevelopmental disorder (ARND) exhibit neurobehavioral deficits without the characteristic facial features.

The earliest autopsy studies in humans reporting damaging effects of heavy prenatal alcohol exposure identified errors in cell migration, agenesis or thinning of the corpus callosum, and anomalies in the cerebellum and brain stem (Jones and Smith, 1973; Clarren, 1977; Clarren et al., 1978). Comprehensive morphometric analyses of the 4 major cortical lobes, cerebellum, and principal subcortical regions found a significant deficit in total brain volume, with proportionately greater reductions particularly in the cerebellum, parietal lobe, and caudate nucleus, including a 15% reduction in cerebellar volume in individuals with FAS (Archibald et al., 2001; Chen et al., 2012).

The function of the cerebellum has traditionally been linked to motor control, but from more recent studies it has emerged that this brain structure is also involved in several other functions including language, spatial processing, working memory, and event planning, which includes event timing (Desmond and Fiez, 1998; Luna et al., 2002; Ivry and Keele, 1989).

Many of the behavioural deficits seen in individuals with FASD, including spatial recognition, motor learning, and fine motor control, are mediated, in part, by the cerebellum (Guerri, 1998). In the 5-year follow-up of the Cape Town Longitudinal Cohort, we reported a

remarkably striking deficit in eyeblink conditioning (EBC) in children with prenatal alcohol exposure. EBC is a nonverbal elemental learning paradigm in which a conditioned stimulus (CS), typically a pure tone, is paired with a brief air puff to the eye (unconditioned stimulus, US) that elicits a reflexive blink. After repeated pairings, the tone comes to elicit a conditioned eyeblink response (CR). Successful EBC relies on producing and maintaining timed movements with millisecond accuracy, which is known to be mediated, at least in part, by the cerebellum. As such, one possible explanation for the impaired EBC response may be an alcohol-related timing deficit.

The cerebellar-mediated internal timing mechanism has been widely studied (Spencer et al., 2007; Bengtsson et al., 2005; Oullier et al., 2005; Penhune et al., 1998; Diedrichsen et al., 2007) using, amongst others, the paced/unpaced finger tapping task, in which subjects first tap to a steady pacing metronome and then maintain the same tapping speed after the metronome ceases. This task and variations of it have been widely used in studies of motor control and the internal timing mechanism (see meta-analysis by Witt et al., 2008).

A common difficulty encountered in these studies requiring self-paced motor tasks is the ability to distinguish between the contribution of the actual clock component and the extent to which motor control affects timing variability. This issue was addressed by Wing and Kristofferson (1973) who proposed a model that discriminates between the clock and motor components by analysis of the inter-tapping intervals (ITIs) during self-paced motor tasks requiring millisecond accuracy. This model has received wide support and has been used in numerous studies to evaluate the respective contributions of these two components to timing variability.

An initial lesion study compared performance of motor production and perception of timing in groups with different neurological disorders, including patients with Parkinson's disease, patients with cortical lesions, patients with cerebellar lesions, an elderly control

group, and a college-aged control group during a paced/unpaced finger tapping task (Ivry and Keele, 1989). Application of the Wing-Kristofferson (1973) model in this study indicated that cerebellar patients showed higher variability compared to other groups, which was largely attributed to internal timing deficits. In a follow-up study in patients with focal cerebellar lesions (Ivry et al., 1988) using the same paced/unpaced tapping task, patients with lateral lesions, ipsilateral to the hand performing the task, showed greater clock variability while patients with medial lesions, ipsilateral to the hand performing the task, had higher motor delay contributions, suggesting that timing is mediated by the lateral cerebellum, while the implementation and execution of motor responses relies on medial cerebellar function.

fMRI studies frequently depend on previously defined functional topographic maps to link activity to certain functions. From the initial theory that the cerebellum was mainly responsible for motor control, functional studies have extensively studied the cerebellar circuitry involved in motor function and the general consensus is that two homunculi in the cerebellum are responsible for motor control – the anterior lobe and parts of lobule VI, as well as lobule VIIIa/b in the posterior lobe (Nitschke et al., 1996; Grodd et al., 2001, Stoodley and Schmahmann, 2009).

In the evaluation of cerebellar functional topography, Stoodley and Schmahmann (2009) performed an activation likelihood estimate (ALE) analysis of previous neuroimaging articles that studied activation patterns associated with different types of tasks. These included motor, somatosensory, spatial, language, working memory, executive function, as well as limbic tasks. Their results indicate that activation in overlapping cerebellar regions is seen between distinct tasks. For instance, right lobule VI is implicated in motor, language, working memory and limbic tasks. This suggests that the functional topography of the cerebellum does not adhere to distinct anatomical regions. Therefore, caution should be used when interpreting functional data by using previously defined maps as this practice can lead to incorrect deductions about the functional association of the activation.

As an alternative to using the Wing-Kristofferson (1973) model, fMRI task design can be formulated to minimise the contribution of motor effects. Bengtsson et al. (2005) performed a conjunction analysis to localise brain regions involved in timing, independent of the effector used. Six tasks were performed by the subjects, including sequential bilateral finger tapping, bilateral isochronous finger tapping, and sequential and isochronous silent speech paced by auditory stimuli. This study associated activation in ipsilateral vermis V/VI and lateral lobule VI with timing.

An fMRI study by Spencer et al. (2007) investigated differences in brain activation between discrete and continuous finger flexion/extension and found that the superior vermis (V/VI) showed increased activation only during discrete movements. It was therefore considered that more demands are placed on this region due to event timing compared to continuous movements. In contrast, lateral lobule VI was activated during both conditions and was linked to sensorimotor demands.

The discrepancy in findings related to lobule VI suggests that brain activation of this region is complex and supports various different domains.

Although cerebellar-mediated timing has been widely studied in adults, not many studies have included children (Lundy-Ekman et al., 1991; Simmonds et al., 2007). A recent study by De Guio et al. (2012) demonstrated that, as in other neuroimaging studies (Davis et al., 2009; Meintjes et al., 2010; Konrad et al., 2005), children activated more extensive neural circuitry than adults during unpaced rhythmic finger tapping in a paced/unpaced task identical to the one used in this study. In this study, the contrast comparing unpaced finger tapping to rest was examined and therefore both timing and motor components emerged. For the children, the results showed a large cluster ipsilateral to the hand performing the task, which spanned from lobules IV to VI and included portions of vermis VI. This activation was associated with the first motor homunculus. A second large cluster in the posterior lobule, consisting of midline structures ranging from lobule VII to IX also emerged. Both

these clusters were located towards the medial portions of the cerebellum. Additional clusters with significant changes in activation were seen more laterally in bilateral Crus II, right lobule VIIb and left lobule VIIIa. Functional differences between the groups indicated that children activated the superior vermis (vermis VI) to a much greater extent than adults and in accordance with the findings of Spencer et al. (2007) the authors attributed this activation to timing.

In the present study, we wanted to examine whether the striking EBC deficit observed in children with prenatal alcohol exposure may be due to effects of alcohol on brain function in regions responsible for movements requiring millisecond timing. fMRI data were acquired during an auditory paced/unpaced finger tapping task to study alcohol related differences in cerebellar activations between children with FAS, PFAS, non-dysmorphic heavily exposed children (HE), and non- or minimally-exposed control children. We compared unpaced finger tapping to rest, which enabled us to analyse differences in activation associated with both internal timing and motor control.

6.2 Materials and Methods

6.2.1 Participants

Pregnant women from the Cape Coloured community were recruited between 1999 and 2002 at their first visit to an antenatal clinic in Cape Town, South Africa, where heavy alcohol consumption is prevalent (Jacobson et al., 2008). All pregnant women who reported consuming at least 14 drinks/week or engaging in binge drinking (≥ 5 drinks/occasion) during pregnancy were invited to participate in the study. In addition, pregnant women who abstained or drank minimally during pregnancy (< 7 drinks/week and no binge drinking) were invited to participate as control subjects. None of the control mothers drank more than one drink per occasion more than once per month during pregnancy.

Timeline follow-back interviews were conducted with each mother at recruitment, during a follow-up antenatal visit, and at 1 month postpartum to determine the amount of alcohol consumed both around time of conception and across pregnancy (Jacobson et al., 2008). Volume was recorded for each type of beverage consumed each day, converted to absolute alcohol (AA) using multipliers proposed by Bowman et al. (1975), and averaged to provide three summary measures – AA/day, AA consumed per drinking occasion, and the number of drinking days per week. All three these measures were obtained for the time around conception and across pregnancy. Number of cigarettes smoked on a daily basis and frequency of marijuana and other drug use were also recorded.

Each child was examined for growth and FAS dysmorphology by two U.S.-based dysmorphologists following the revised Institute of Medicine criteria (Hoyme et al., 2005) during a 6-day clinic in 2005 (Jacobson et al., 2008). A few children who did not attend the clinic were assessed by a Cape Town-based dysmorphologist with expertise in FAS diagnosis. There was substantial agreement among the examiners on the assessment of all dysmorphic features, including the three principal fetal alcohol-related characteristics—palpebral fissure length, and philtrum and vermilion measured using the *Lip-Philtrum Guide* (Astley and Clarren, 2001) (median $r = 0.78$). Each of the heavily exposed children was assigned to one of the following diagnostic groups at a case conference: FAS, PFAS, or HE nonsyndromal.

81 (9 FAS, 18 PFAS, 30 HE, 24 controls; 47 boys) right-handed children received MRI scanning on the 3T Allegra (Siemens, Erlangen, Germany) MRI scanner at the Cape Universities Brain Imaging Centre (CUBIC) between January 2009 and December 2011, mean age 10.0 ± 1.0 years. We acquired high-resolution structural images and fMRI data during an auditory paced/unpaced rhythmic finger tapping task.

6.2.2 Experimental Task

The experimental task was programmed using E-Prime software (Psychology Software Tools, Inc., Pittsburgh, USA) and was presented through a waveguide in-line with the bore of the magnet in the rear wall of the scanner room using a data projector and a rear projection screen mounted at the end of the bore of the magnet. Responses were recorded using a Lumitouch response system (Photon Control Inc., Burnaby, Canada). The child was able to talk to the examiner using an intercom that is built into the scanner and could stop the scan at any time by squeezing a ball held in his/her left hand. All children were accompanied into the scanner by a research nurse/assistant who stayed with them throughout the scan, facilitating the high rate of successful scans.

All children practiced the tasks before the scan in order to ensure that they understood the instructions and could perform the task. Children also had the opportunity to lie in a mock scanner prior to the scan and listen to a recording of the scanner noises, which helped to reduce anxiety.

The design of the task was similar to that used in previous studies (Rivkin et al., 2003; De Guio et al., 2012; O'Boyle et al., 1996) and was aimed at identifying cerebellar brain regions involved in self-paced rhythmic finger tapping.

The task started automatically on receipt of a trigger from the scanner after the acquisition of 4 dummy scans. The first paced block is preceded by a rest block of 4 s during which an instruction to get ready is displayed. Children were instructed to press the button using their right index finger every time they hear a beep and to continue tapping at that speed when the tones stop until the word "stop" appears on the screen. Paced blocks have a 6 s duration during which the children hear 12 tones, inter-stimulus interval (ISI) 500 ms. The paced block is followed by 16 s of unpaced tapping by the child and a 16 s rest block. Paced, unpaced and rest blocks are repeated 6 times (Fig. 6.1) during the task. Each child repeated the task twice in the scanner.

Figure 6.1: Timing diagram of the paced/unpaced finger tapping task

6.2.3 fMRI Imaging Protocol

Structural scans were acquired using two different protocols. For 57 of the children, a magnetization-prepared rapid gradient echo (MPRAGE) structural image was acquired in a sagittal orientation with the following parameters: TR = 2300 ms, TE = 3.93 ms, TI = 1100 ms, 160 slices, flip angle 12°, voxel size = 1.3 x 1.0 x 1.0 mm^3, scan time = 6:03 minutes. For 24 children who were scanned later, high-resolution T_1-weighted structural MR images were acquired using a 3D EPI-navigated (Tisdall et al., 2009) multi-echo MPRAGE (Van der Kouwe et al., 2008) sequence that had been optimized for morphometric analyses using Freesurfer software (version 5.1.0, http://surfer.nmr.mgh.harvard.edu). Imaging parameters were: FOV 256 x 256 mm^2; 128 sagittal slices, TR 2530 ms; TE 1.53/3.21/4.89/6.57 ms; TI 1100 ms; flip angle 7°; voxel size 1.3 x 1.0 x 1.3 mm^3. The 3D EPI navigator provided real-time motion tracking and correction, which served to substantially reduce the presence of any motion artifacts in the structural imaging data, despite frequent significant subject motion.

A T_2*-weighted gradient echo, echo planar imaging (EPI) sequence was used to acquire 120 functional volumes (240 s) that are sensitive to BOLD contrast (TR = 2000 ms, TE = 30 ms, 34 interleaved slices, 3 mm thick, gap 1.5 mm, 200 mm x 200 mm field of view,

in-plane resolution 3.125 x 3.125 mm^2) while the children performed the paced/unpaced task.

All procedures were performed according to protocols that had been approved by the Human Investigation Committee of Wayne State University and the Faculty of Health Sciences Human Research Ethics Committee at the University of Cape Town. All parents/guardians provided informed written consent; all children provided oral assent.

6.2.4 Behavioural Data Analyses

The behavioural data recorded during scanning were analysed by applying the Wing-Kristofferson (1973) model to distinguish the degree to which variability in ITIs were due to motor delay or clock variability - two processes assumed to operate independently. According to the model, any ITI is the sum of the internal clock response and a motor delay and is presented by:

$$I_j = C_j + MD_j - MD_{j-1}, \quad \text{(Eq. 6.1)}$$

where I_j is the ITI for any interval j, C_j is the interval between consecutive clock pulses, and MD_j – MD_{j-1} is the difference between motor delays from the initiation and termination of the ITI.

Wing and Kristofferson (1973) showed that the variance of the ITI is equal to the sum of the clock variance and twice the motor variance and is given by

$$\sigma_{ITI} = \sigma_{clock} + 2\sigma_{motor}. \quad \text{(Eq. 6.2)}$$

The overall ITI variability for each block is calculated directly from the behavioural data, while the motor delay is determined by means of the lag 1 autocovariance of the ITI, which is the autocovariance of the ITI's shifted by one position. From these, the clock estimate can then be calculated.

In our data, individual ITIs that differed by more than 50% from the correct ITI (i.e. ITI < 250 ms or ITI > 750 ms) were excluded. Blocks with no excluded ITIs constitute 'perfect' blocks. Since the implementation of the Wing and Kristofferson (1973) model by Ivry and Keele (1989) required at least six 'perfect' blocks, we present data both for (i) all blocks from the whole sample, and (ii) for only 'perfect' blocks in children who had six or more such blocks. The average ITI and ITI variability measures were computed for each block. The motor delay for each block was computed using the lag 1 autocovariance of the ITI, and the clock estimate computed using equation 6.2. In blocks violating the Wing-Kristofferson (1973) criterion that the lag 1 autocovariance should be between -0.5 and 0, it was assumed that all variance was due to the clock estimate and the motor delay was set to 0. This was done according to the method proposed by Ivry and Keele (1989).

The mean ITI, mean overall ITI variability, as well as the motor- and clock estimates were finally averaged over all blocks to render single values for each subject.

6.2.5 Functional Data Analyses

In order to decide which data to include in the fMRI analyses, it was important to decide which subjects were fully engaged in the task and were able to maintain the rhythm successfully during unpaced blocks.

ITIs during the unpaced blocks greater than 800 ms were assumed to occur due to one (or more) missed tap(s). For such instances, additional taps were inserted with an ITI as close to 500 ms as possible, ensuring that missed taps were performed rhythmically. Inserted taps were counted as missed taps. Unpaced blocks were deemed unusable if the mean ITI - corrected for missed taps - was less than 400 ms or greater than 600 ms, or if the standard deviation (SD) of the mean corrected ITI was greater than 65 ms. Unpaced blocks were also excluded if a child had 5 or more missed taps. Such blocks were labelled as 'bad' blocks. Only children who met criteria for more than seven of the twelve unpaced tapping

blocks administered (i.e. have fewer than 5 'bad' blocks) were included in the functional analyses, as only these children were considered to have learnt and maintained the rhythm.

fMRI data analyses for these children were performed in Brain Voyager QX (Brain Innovation, Maastricht, The Netherlands). The first four dummy scans were excluded from all analyses. Pre-processing included motion correction relative to the first volume that is acquired during the functional scan, linear scan time correction, temporal filtering with a high pass filter of 3 cycles / point, and linear trend removal. Scans with motion exceeding 3 mm translation or 3^{o} rotation within a functional run were excluded from all further analyses. The 6 motion correction parameters were z-transformed and then added as predictors of no interest during the analysis. Beta maps were created for each subject for the contrast comparing activation during unpaced finger tapping with rest. The beta maps were exported into Analyze format for second level analysis in SPM5 (Statistical Parametric Mapping).

In order to obtain more detailed information on activation patterns in the cerebellum, second level analyses were performed using the spatially unbiased atlas template (SUIT) toolbox (Diedrichsen et al., 2009). This atlas is based on the structural data of 20 healthy adults and has been shown to significantly improve the alignment of individual fissures when compared to normalization to the MNI whole-brain template.

The cerebellum was isolated by calculating the probability for each voxel of belonging to the cerebellum or brain stem. The isolation maps were then used to transform each subject's cerebellum to the SUIT template in the subsequent step which normalized the data. Manual correction was applied using MRICRON (Rorden and Brett, 2000) for each subject to eliminate contamination from the visual cortex. The beta maps for the cerebella were then resliced according to the isolated and normalized structural data for each subject to render the data in the SUIT atlas space.

To examine whether normalising the children's cerebella to an adult template would lead to excessively small effective ROI's, cerebellar volumes of the children generated by FreeSurfer (version 5.1.0, http://surfer.nmr.mgh.harvard.edu) were compared to values

reported in adult studies. Woodruff-Pak and colleagues (2001) calculated cerebellar volumes ranging from 122.73 to 142.37 ml in eight young adults (age 21 to 35 years) and Luft and colleagues (1999) found a range of 99.86 to 170.6 ml in 48 adults (age 19.8 to 73.1 years). The children included in the fMRI study had an average cerebellar volume of 130.01 ± 11.18 ml (range 107.18 to 153.11 ml), which is within the limits of the aforementioned studies. The overall effect of normalisation to an adult template was, therefore, deemed negligible.

Regression analyses were performed in SPM5 to identify regions where activation during unpaced tapping in the control children significantly correlated with the Wing-Kristofferson (1973) estimates. Cluster size correction indicated that clusters larger than 13 mm^3 in the regression analyses were significant at a corrected $p < 0.05$.

Percent signal change values in these VOI's, averaged over spheres with radius 3 mm centred on the peak values, were extracted for all children included in the fMRI analyses and exported to SPSS (version 20; IBM, New York, USA) for further analysis.

6.2.6 Statistical Analyses

For the behavioural analysis including the full cohort, the outcomes from the Wing-Kristofferson (1973) analysis (mean ITI, total ITI variability, clock estimate and motor delay) were examined for diagnostic group differences as well as possible correlations with measures of the extent of prenatal alcohol exposure. SPSS (version 20; IBM, New York, USA) was used to perform ANOVA's and Pearson correlations; *p*-values < 0.05 were deemed statistically significant.

Five control variables were considered as potential confounders: child's gender and age at the time of assessment, maternal smoking (cigarettes/day) and marijuana use (days/month) during pregnancy, as well as age at delivery.

To determine whether the effect of the continuous alcohol measures on behavioural outcomes continued to be significant after statistical adjustment for potential confounders, hierarchical multiple regression analyses were used to test for confounding. The alcohol

exposure measure was entered in the first step of each analysis of each outcome. All control variables related weakly ($p < 0.1$) to the outcome were entered in the second. In the analysis of group differences, ANCOVA's were used to control for possible confounders.

Percent signal change values during unpaced tapping compared to rest obtained from the functional analyses were examined for associations with continuous measures of prenatal alcohol exposure both at conception and throughout pregnancy using Pearson correlation. Using the same multiple regression procedure described previously for the behavioural analyses, we controlled for potential confounding influences of child sex, child age, maternal smoking and drug use during pregnancy, and mother's age at delivery.

6.3 Results

6.3.1 Sample Characteristics

The sample characteristics of the 81 children scanned are shown in Table 6.1.

As would be expected, highly significant differences are seen between diagnostic groups in the level of alcohol exposure. Notably, mothers of the alcohol exposed children in this sample exhibit a binge-like pattern of drinking with drinking concentrated over one to three days per week. On average, the mothers of the most severely affected children with FAS drank 9.6 drinks per occasion across pregnancy, compared to 7.0 drinks per occasion by mothers of children with PFAS, and 6.2 drinks per occasion by mothers of HE children. None of the control mothers drank more than 1 drink per occasion more than once per month during pregnancy.

The low IQ scores reflect the highly disadvantaged backgrounds of the children in this population, with significantly lower scores among the children with FAS and PFAS (Jacobson et al., 2008).

Table 6.1: Sample characteristics

Demographic	FAS	PFAS	HE	Control	*F* or χ^2
N	9	18	30	24	NA
Gender (% male)	5 (55.6%)	10 (55.6%)	18 (60.0%)	13 (54.2%)	-0.14
Child's age at assessment[a] (yr)	9.80±1.16	9.42±0.34	10.51±1.12	9.92±0.80	5.73**
WISC-IV IQ[b,c]	66.28±12.90	65.00±9.61	76.16±10.67	74.54±11.26	5.21**
Maternal Age at Delivery[d] (yr)	32.57±7.29	26.61±6.20	25.19±4.98	25.64±3.91	4.78**
AA/day at conception (oz)	2.71±3.44	1.21±0.73	0.69±0.61	0.00±0.02	11.47**
AA/occasion (oz) at time of conception	5.70±2.78	3.76±2.34	2.73±2.11	0.06±0.24	23.92**
Frequency of drinking at time of conception (days per week)	2.83±1.94	2.29±1.34	1.44±1.12	0.04±0.12	20.47**
AA/day across pregnancy (oz)	1.77±2.24	0.87±0.53	0.49±0.46	0.00±0.00	11.29**
AA/occasion (oz) across pregnancy	4.83±1.83	3.54±1.96	3.11±2.35	0.07±0.26	22.37**
Frequency of drinking across pregnancy (days per week)	2.09±1.82	1.74±0.97	1.08±0.87	0.01±0.03	17.58**
Cigarettes smoked per day during pregnancy	7.69±5.71	7.61±6.13	6.21±5.84	4.25±6.85	1.27
Marijuana use during pregnancy (occasions/month)	0.00±0.00	0.22±0.75	0.02±0.06	0.11±0.55	0.87
Cerebellar Volume (ml)[e]	121.79±10.87	131.87±18.69	132.61±10.69	131.27±10.84	1.70

FAS – fetal alcohol syndrome; PFAS – partial FAS; HE – heavily exposed, non-dysmorphic
[a] Post-hoc analyses: FAS < HE ($p = 0.044$); PFAS < HE ($p < 0.001$); PFAS < control ($p = 0.085$); HE > control ($p = 0.020$)
[b] WISC-IV = Wechsler Intelligence Scale for Children—Fourth Edition
[c] Post-hoc analyses: FAS < HE ($p = 0.019$); FAS < control ($p = 0.056$); PFAS < HE ($p = 0.001$); PFAS < control ($p = 0.006$)
[d] Post-hoc analyses: FAS > PFAS ($p = 0.007$); FAS > HE ($p < 0.001$); FAS > control ($p = 0.001$);
[e] Post-hoc analyses: FAS < PFAS ($p = 0.060$); FAS < HE ($p = 0.031$); FAS < control ($p = 0.065$)
[†] $p < 0.10$, * $p < 0.05$, ** $p < 0.01$.

Although the overall ANOVA comparing cerebellar volumes between the four diagnostic groups did not reach statistical significance ($F = 1.70$, $p = 0.17$), *post hoc* analyses indicated that cerebellar volumes tended to be smaller in the most heavily exposed FAS children - a result that has been noted in previous studies (Mattson et al., 1994; Archibald et al., 2001). Although the overall effect of normalisation to the adult template is deemed insignificant, these group differences suggest that cerebellar volume should be included as a potential confounder in the analyses.

6.3.2 Behavioural Results

Analysis of our behavioural data makes the inclusion of the Wing-Kristofferson (1973) estimates in this study questionable and results should be interpreted with caution. Of all the tapping blocks completed by the full cohort, 44.8% violated the model by having positive lag 1 autocorrelations. For all these blocks we implemented the method proposed by Ivry and Keele (1989), which assumes that all variance is due to the clock estimate and set the motor delay equal to zero. This assumption may significantly bias our results as it affected almost half of the unpaced tapping blocks in this study. Table 6.2 presents the behavioural results based on all tapping blocks completed for the entire sample.

Only 52 children (6 FAS, 5 PFAS, 22 HE, 19 controls) fulfilled the criterion of having at least six 'perfect' blocks where none of the ITIs deviated by more than 50% from the correct ITI. In table 6.3 we present the results only for those children based only on inclusion of the perfect blocks. FAS and PFAS children were combined for this analysis due to their small sample size.

Table 6.2: Wing-Kristofferson (1973) behavioural outcomes based on inclusion of all blocks in all children (*N* = 81)

Estimate	FAS	PFAS	HE	Control	*F*	*p*
N	9	18	30	24	NA	NA
Total number of blocks completed	108	216	360	288	NA	NA
Total Number of Perfect Blocks (%)[a]	61 (56.5%)	92 (42.6%)	227 (63.1%)	156 (54.2%)	46.58	0.06
Average Number of Perfect Blocks per subject[b]	6.8±3.1	5.1±2.9	7.6±3.2	6.5±2.0	2.85	0.04
Mean ITI (ms)[c]	519.7±21.5	477.6±43.8	490.4±38.7	489.0±49.1	2.04	0.12
Total ITI Variability (ms)	47.4±11.0	53.2±11.9	51.4±17.9	52.1±9.9	0.36	0.78
Motor Estimate (ms)	14.0±5.1	9.7±5.8	13.1±8.9	13.2±6.9	1.11	0.35
Clock Estimate (ms)	38.5±10.4	46.5±12.6	42.1±13.1	43.2±7.2	1.14	0.34

[a]Chi Square Test
[b]Post-hoc analyses: PFAS < HE ($p = 0.01$)
[c]Post-hoc analyses: FAS > PFAS ($p = 0.02$), FAS > HE ($p = 0.07$), FAS > control ($p = 0.06$)

Table 6.3: Wing-Kristofferson (1973) behavioural outcomes only for children with six or more perfect blocks based only on inclusion of the perfect blocks (*N* = 52)

Estimate	FAS/PFAS	HE	Control	*F*	*p*
N	11	22	19	NA	NA
Total Number of Perfect Blocks	117	201	147	NA	NA
Average Number of Perfect Blocks per subject[a]	6.07±3.00	9.09±2.07	6.88±1.82	8.60	0.00
Number of Perfect Blocks with Positive Lag 1 Autocovariance (%)[b]	44 (37.6%)	90 (44.8%)	53 (36.1%)	6.34	0.00
Mean ITI (ms)	493.06±57.45	496.41±33.04	493.52±42.54	0.03	0.97
Total ITI Variability (ms)	45.05±9.84	44.30±13.05	50.65±9.56	1.79	0.18
Motor Estimate (ms)	9.81±4.58	10.92±9.33	15.22±8.81	1.94	0.16
Clock Estimate (ms)	39.59±9.70	36.24±7.68	39.74±7.02	1.20	0.31

[a]Post-hoc analyses: FAS/PFAS < HE ($p < 0.001$), HE > control ($p = 0.005$)
[b]Post-hoc analyses: FAS/PFAS < HE ($p = 0.002$)

Contrary to our expectation, we did not observe poorer performance in the alcohol exposed children on the unpaced tapping task in any of the Wing-Kristofferson (1973) measures. We also did not find any significant associations between any of these performance measures and the continuous measures of alcohol exposure. Despite the absence of alcohol-related effects on any of the performance measures assessed, it is noteworthy that only 40.7% of children with FAS or PFAS had 6 or more perfect blocks, compared to 73.3% of HE children and 79.2% of controls, suggesting that the most severely affected children did struggle more to maintain concentration and perform well throughout the task.

Table 6.4 presents relations between performance measures (based on inclusion of all blocks in all children) and potential confounders. These correlations reveal that increased age is significantly associated with improved performance in terms of the overall ITI variability, motor delay and the clock estimate. Results were essentially unchanged when using the behavioural measures based on inclusion of only perfect blocks in children with 6 or more such blocks.

Table 6.4: Relationships between behavioural performance measures and potential confounders (*N* = 81)

Demographic	Mean ITI (ms)	Total ITI Variability	Motor Estimate	Clock Estimate
Gender	0.155	0.028	0.160	-0.084
Child's age at assessment (yr)	0.082	-0.346**	-0.230*	-0.258*
WISC-IV IQ[a]	0.155	-0.048	0.112	-0.143
Maternal Age at Conception (yr)	0.050	0.012	0.016	0.026
Cigarettes smoked per day during pregnancy	0.069	0.008	0.096	-0.049
Marijuana use during pregnancy (occasions/month)	0.059	-0.053	-0.136	-0.007
Cerebellar Volume (ml)	-0.169	0.129	0.026	0.122

[a] WISC-IV = Wechsler Intelligence Scale for Children—Fourth Edition
*$p < 0.05$, **$p < 0.01$

Re-evaluating the relationships between the behavioural measures and the continuous alcohol exposure measures after controlling for the strong effect of age on performance still yielded no significant correlations.

Behavioural Results for the Children Included in the fMRI Analyses (N = 52)

For the functional analyses, the data for 21 subjects (2 FAS, 7 PFAS, 7 HE, 5 controls) were excluded as they did not meet criteria with regards to the number of blocks completed successfully, while data for 6 more children (1 FAS, 2 PFAS, 1 HE, 2 controls) were excluded due to excessive motion during the scan. In addition, 2 children (1 FAS, 1 control) were excluded for being extreme outliers (calculated as > 2 standard deviations above or below the mean) based on percent signal change values.

After applying exclusion criteria, we report data for 52 (29 male, 23 female) right-handed children (mean age 10.2 ± 1.0 yr), including 5 children with full FAS, 9 children with PFAS, 22 nonsyndromal HE children and 16 non- or minimally exposed controls (Table 6.5). Due to the small sample size of the most heavily exposed children meeting criteria for inclusion, the FAS and PFAS groups were combined for subsequent analyses.

It should be noted that only 41 of the 52 children included in the fMRI analysis had six or more 'perfect' blocks (4 FAS, 2 PFAS, 21 HE, 14 controls)

A comparison of the sample characteristics between the children included and the children excluded from the study reveals that the included children are significantly older than the excluded children ($t = 0.97$, $p = 0.004$). This supports the correlations seen between task performance and age in the entire group (Table 6.4), which indicates that better task performance is related to increased age in the children.

Table 6.5: Sample characteristics of children whose data were included in the fMRI analysis (*N* = 52)

Demographic	FAS/PFAS	HE	Control	*F*
N	14	22	16	NA
Gender (% male)	7 (50.0%)	13 (59.1%)	9 (56.3%)	0.134
Child's age at assessment[a] (yr)	9.46±0.65	10.96±0.97	9.96±0.78	15.04**
WISC-IV IQ[b,c]	68.43±7.84	76.41±12.22	71.31±10.81	2.54†
Maternal Age at Delivery (yr)	28.82±8.07	24.84±5.40	25.14±3.76	2.24
AA/day at conception (oz)	1.31±0.75	0.78±0.63	0.01±0.02	20.38**
AA/occasion (oz) at time of conception	4.49±3.03	3.03±2.18	0.07±0.29	21.77**
Frequency (drinking days per week) at time of conception	2.06±1.31	1.59±1.11	0.03±0.13	17.91**
AA/day across pregnancy (oz)	0.85±0.55	0.55±0.48	0.00±0.00	15.71**
AA/occasion (oz) across pregnancy	4.09±2.06	3.36±2.62	0.07±0.29	17.77**
Frequency (drinking days per week) across pregnancy	1.42±0.80	1.18±0.87	0.00±0.02	18.41**
Cigarettes smoked per day during pregnancy[d]	8.25±6.12	6.39±6.34	2.81±5.01	3.36*
Marijuana use during pregnancy (occasions/month)	0.28±0.84	0.02±0.07	0.17±0.68	0.96
Cerebellar Volume (ml)[e]	122.06±114.40	131.80±10.47	134.49±8.59	6.14**

[a] Post-hoc analyses: FAS/PFAS < HE ($p < 0.001$); HE > control ($p = 0.001$)
[b] WISC-IV = Wechsler Intelligence Scale for Children—Fourth Edition
[c] Post-hoc analyses: FAS/PFAS < HE ($p = 0.035$)
[d] Post-hoc analyses: FAS/PFAS > control ($p = 0.015$)
[e] Post-hoc analyses: FAS/PFAS < HE ($p = 0.007$); FAS/PFAS < control ($p = 0.002$)
†$p < 0.10$, *$p < 0.05$, **$p < 0.01$.

For the subsequent fMRI analysis, we focus on the three Wing-Kristofferson (1973) estimates that provide a measure of timing variability.

In table 6.6 is presented a summary of the behavioural data for the subset of children included in the fMRI study. The table presents also values after controlling for the effect of age on performance. (Relations of all three the behavioural measures were significantly correlated with age: overall ITI variability: r = -0.41, p = 0.003; motor delay: r = -0.31, p = 0.026; clock estimate: r = -0.30, p = 0.026).

Table 6.6: Wing-Kristofferson (1973) behavioural outcomes based on all blocks for children included in the fMRI study

Behavioural Parameter	FAS/PFAS N = 14	HE N = 22	Control N = 16	*F*	*p*
Total ITI Variability[a] (ms)	50.37±12.36	44.5±9.1	51.2±8.2	2.62†	0.08
Motor Delay (ms)	17.93±8.15	14.2±6.2	17.8±5.7	1.94	0.15
Clock Estimate (ms)	42.48±10.79	39.2±8.2	44.1±7.0	1.53	0.23
Total ITI Variability Corrected for Age (ms)	47.39±2.81	47.24±2.30	50.10±2.39	0.47	0.63
Motor Delay Corrected for Age (ms)	16.33±1.93	15.66±1.59	17.24±1.65	0.23	0.80
Clock Estimate Corrected for Age (ms)	40.54±2.54	41.01±2.08	43.34±2.17	0.49	0.61

[a] Post-hoc analyses: FAS/PFAS > HE (p = 0.089), HE < control (p = 0.044)
†p < 0.1. *p < 0.05, **p < 0.01

Table 6.6 clearly shows how strongly the behavioural performance was influenced by age. Prior to controlling for age, the older HE children showed the lowest variability in terms of all three Wing-Kristofferson (1973) measures, albeit below conventional levels of significance. After controlling for age differences, groups do not differ in any of the performance measures. Using only perfect blocks did not alter the results and still resulted in no group differences after controlling for age.

Correlations between the behavioural performance and continuous alcohol exposure measures were not significant, both before and after controlling for age.

6.3.3 Functional Results

Four distinct cerebellar regions were identified in the control children where the change in activation during unpaced tapping compared to rest is correlated with the behavioural outcomes from the Wing-Kristofferson (1973) analysis (Table 6.7 and Fig. 6.2). Activations in these regions were therefore assumed to be involved in performing rhythmic tapping with millisecond accuracy.

Table 6.7: Regions identified in regression analysis between activation and behavioural measures in control children (*N* = 16)

Region[a]	Coordinates (x y z)[b]	Cluster size (mm^3)[c]	Overall ITI Variability	Motor Delay	Clock Estimate
Right VIIIa[d]	16 -64 -58	14	-0.53*	-0.23	-0.56*
Left VIIIa[d]	-34 -58 -60	24	-0.77**	-0.56*	-0.65**
Right VIIIb[d]	26 -52 -50	28	-0.82**	-0.43†	-0.78**
Right VI[e]	26 -66 -26	22	0.59*	0.60*	0.39

[a]Nomenclature as proposed by Schmahmann et al. (2000)
[b]Montreal Neurological Institute (MNI) coordinates
[c]Minimum cluster size of 13mm^3 for $p_{corrected} < 0.05$
[d]Cluster identified in regression analysis with overall ITI variability; a cluster in a similar location was identified in regression analysis with the clock estimate
[e]Cluster identified in regression analysis with overall ITI variability; a cluster in a similar location was identified in regression analysis with the motor delay
$^{\dagger}p_{corrected} < 0.1$, $*p_{corrected} < 0.05$, $**p_{corrected} < 0.01$

All the regions identified in the regression analysis with overall ITI variability, were also identified in either the regression analysis with motor delay or the clock estimate, with only small differences in peak coordinates.

Increased activation bilaterally in lobule VIII was associated with decreased variability in ITI (i.e. better performance), a result that seemed to be largely driven by decreased variability in the clock estimate. Although two clusters are located in right lobule VIII, their peaks are distinct and are located in lobules VIIIa and VIIIb, respectively.

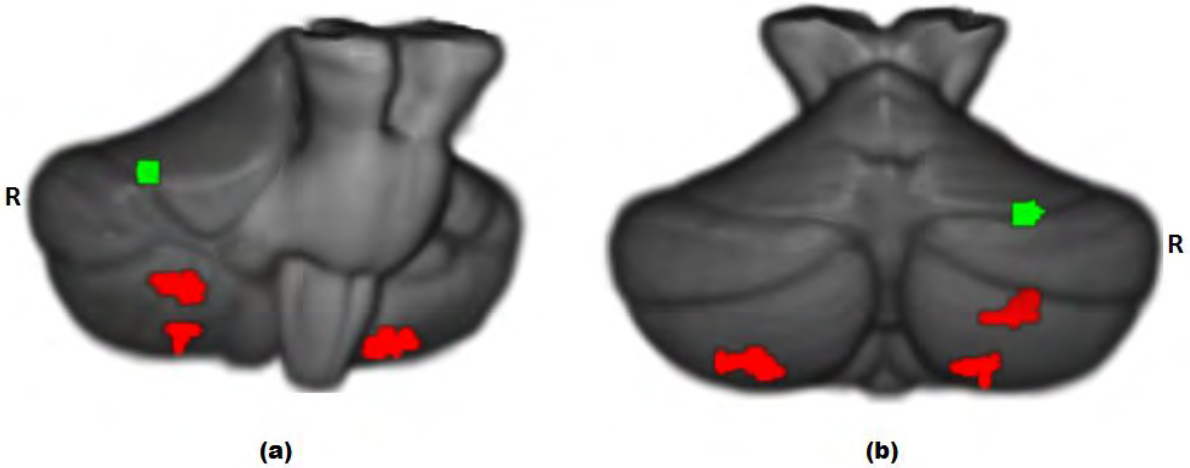

Figure 6.2: (a) Right anterolateral and (b) posterior views of the cerebellar regions showing correlations associated with the calculated Wing-Kristofferson (1973) clock estimate (red) and motor delay (green) for the contrast comparing unpaced finger tapping to rest. Functional data are shown in the Spatially Unbiased Cerebellar Atlas Template space (MNI coordinates)

In contrast, increased activation in right lobule VI was related to poorer performance, arguably largely due to increased motor delay.

Upon extracting measures of percent signal change during unpaced tapping in these four regions for all children included in the fMRI analyses, several of these correlations remain. Table 6.8 shows for all 52 children the relationships between activation in these four regions and performance measures, as well as the standard regression coefficient after adjustment for maternal smoking and child's age, which emerged as possible confounders ($p < 0.1$).

Table 6.8: Relations for all children included in the fMRI analysis between activation and performance measures in the four regions where performance was related to brain activation in the control children

Region[a]	Coordinates (x y z)[b]	Cluster size (mm^3)[c]	Overall ITI Variability		Motor Delay		Clock Estimate	
			r	*β*	*r*	*β*	*r*	*β*
Right VIIIa[d]	16 -64 -58	14	-0.22	-0.25†	0.10	0.09	-0.34*	-0.37*
Left VIIIa	-34 -58 -60	24	-0.25†	-0.25†	-0.14	-0.14	-0.26†	-0.26†
Right VIIIb[e]	26 -52 -50	28	-0.20	-0.07	-0.05	0.08	-0.20	-0.12
Right VI[d]	26 -66 -26	22	0.32*	0.30*	0.42**	0.41**	0.13	0.10

r is the simple Pearson correlation between alcohol exposure and percent signal change values; *β* is the standardized regression coefficient after adjustment for the potential confounding variables.
[a]Nomenclature as proposed by Schmahmann et al. (2000)
[b]Montreal Neurological Institute (MNI) coordinates
[c]Minimum cluster size of 13 mm^3 for $p_{corrected} < 0.05$
[d]Controlling for maternal smoking
[e]Controlling for child's age and maternal smoking
$^{\dagger}p_{corrected} < 0.1$, $*p_{corrected} < 0.05$, $**p_{corrected} < 0.01$

The weaker relations between brain activation and performance after inclusion of the alcohol affected children could indicate that alcohol exposure alters brain activation in these identified regions. In three of the four cerebellar regions identified as playing a role in performing timed movements in control children (namely left VIIIa, right VIIIb, and right VI) brain activation was related to extent of prenatal alcohol exposure (Table 6.9), despite the absence of differences in behavioural performance between diagnostic groups and the absence of associations between behavioural performance and the degree of prenatal alcohol exposure in this subgroup of children. The strongest associations were found with dose per occasion around the time of conception – effects that largely remained significant after controlling for the potential confounding influences of maternal smoking and child's age.

Table 6.9: Correlations between brain activation during unpaced tapping in four regions related to timing performance in control children and measures of extent of prenatal alcohol exposure

Region[a]	AA/day at time of conception (oz)		AA/occasion at time of conception (oz)		Drinking Days per week at time of conception		AA/day across pregnancy (oz)		AA/occasion across pregnancy (oz)		Drinking Days per week across pregnancy	
	r	***β***	***r***	***β***	***r***	***β***	***r***	***β***	***r***	***β***	***r***	***β***
Right VIIIa[b]	-0.13	-0.03	-0.01	0.13	-0.05	0.02	-0.09	0.11	0.06	0.17	-0.02	0.14
Left VIIIa	**-0.34***	**-0.34***	**-0.45****	**-0.45****	-0.15	-0.15	**-0.30***	**-0.30***	**-0.33***	**-0.33***	-0.20	-0.20
Right VIIIb[c]	**-0.39****	**-0.35***	**-0.36****	**-0.33***	-0.21	-0.21	-0.25†	-0.19	**-0.30***	**-0.32***	-0.12	-0.05
Right VI[b]	-0.17	-0.17	**-0.30***	**-0.30***	0.00	0.00	-0.17	-0.17	**-0.25†**	**-0.25†**	-0.07	0.07

r is the simple Pearson correlation between alcohol exposure and percent signal change values; *β* is the standardized regression coefficient after adjustment for the potential confounding variables.
[a]Nomenclature as proposed by Schmahmann et al. (2000)
[b]Controlling for maternal smoking
[c]Controlling for child's age and maternal smoking
†$p_{corrected} < 0.1$, *$p_{corrected} < 0.05$, **$p_{corrected} < 0.01$

In all three regions, higher doses per occasion were associated with smaller differences in activation between unpaced tapping and rest. Activation in none of these regions differed between diagnostic groups.

Although the control group's continuous alcohol exposure measures were essentially all zero, the data for these children were included in the correlation analyses to avoid artificially truncating the range of exposures.

6.4 Discussion

The Wing-Kristofferson (1973) model has received wide support in previous studies of timing. In our study we attempted to identify cerebellar regions employed during paced/unpaced finger tapping in healthy control children by directly inserting the Wing-Kristofferson (1973) estimates in a voxelwise regression analysis of the fMRI data. The regions identified in this regression analysis were then used to study differences in functional activity in alcohol exposed children in these regions.

However, we had to adapt the calculation of the Wing-Kristofferson (1973) estimates which makes it necessary to interpret our findings related to the behavioural outcomes with caution. The previous studies required six 'perfect' blocks i.e. no ITIs deviating with more than 50% from the standard. If we applied these criteria, fMRI data for only 6 of the original 27 FAS/PFAS children would remain, which would defy the study of FASD.

We analysed the behavioural data for three different subgroups – the full cohort (*N* = 81) including all blocks, the group of children performing six or more 'perfect' blocks (*N* = 52) based on these 'perfect' blocks, as well as the children meeting the requirements for inclusion into the fMRI analysis (*N* = 52 of whom 41 had six or more 'perfect' blocks).

No significant alcohol related differences were seen in the behavioural data in any of these groups, although the low number of children with FAS/PFAS able to perform six or more perfect blocks suggests a deficit related to performing timed movements with millisecond accuracy. A single trend showing the best performance in overall ITI variability by the HE children in the group included in the fMRI study was negated by controlling for the significantly higher age of these children.

The absence of alcohol related differences in behavioural performance is contradictory to our expectations. Even comparing the Wing-Kristofferson (1973) measures in children performing six or more 'perfect' blocks did not render insightful results regarding alcohol exposure. However, as shown in table 6.3, a large proportion of the 'perfect' blocks violated the Wing-Kristofferson (1973) model by having positive lag 1 autocovariance. As outlined in the methods section, we set the motor delay in these blocks to zero and attributed all variability to the clock estimate. In the previous studies incorporating this method, the number of blocks violating criteria was considerably less than encountered in our study. Ivry and Keele (1989) found that 12.8% of tapping blocks in their control group violated the Wing-Kristofferson (1973) model compared to 26.0% of cerebellar patients. In the subjects studied by Greene and Williams (1993), only 2.2% of the blocks had positive lag 1 autocovariance. We found that 40.2% of the perfect blocks violated the criteria and therefore it is a very bold assumption to assign all variance due to the clock estimate in such a large part of the data.

This assumption necessitates caution in interpretation of our behavioural data and could be the reason that no alcohol related differences are seen. Alternatively, the young age of the children could mean that timing precision is not fully developed in any of the children, which makes it difficult to detect alcohol related differences. The strong age related effects on performance in the timing control of repetitive movements has previously been seen (Greene and Williams, 1993). In that study, the Wing-Kristofferson (1973) measures indicated that the highest variability during unpaced finger tapping was seen in the youngest

group (age 6 -7 years). Variability decreased with increasing age up until peak performance in a group ranging from 21 to 30 years. As the age of subjects increased beyond this point, variability increased as well.

Using the behavioural estimates, we identified four distinct regions where activation in the control children was correlated with these performance measures. All regions identified in the regression analysis with overall ITI variability, also emerged when the regression was done with either the motor delay or clock variability. However, the uncertainty created by our altered calculation of these performance measures means that assigning activation specifically to the clock estimate or motor delay in any of these regions should be done with caution.

The control children showed significantly correlated changes in activation related to the Wing-Kristofferson (1973) behavioural measures in four cerebellar regions – right lobule VIIIa and VIIIb, left lobule VIIIa, as well as right lobule VI.

In the three clusters in lobule VIII decreased activation is associated with higher overall ITI variability in the control children. This same relationship is seen with the clock estimate; however, the limitations in our calculation of the Wing-Kristofferson (1973) measures preclude us from assigning this specific pattern to timing.

Lobule VIII has consistently been implicated in motor control (Stoodley and Schmahmann, 2009; 2010; Stoodley et al., 2012), suggesting that the increased variability associated with smaller changes in activation in these lobules is most likely attributable to a motor effect. Activation in this lobule is, however, generally ipsilateral to the effector used and therefore interpretation of the significant cluster in the left hemisphere is not that obvious. De Guio et al. (2012) showed that, in addition to right lobule VIIIa, children activated left lobule VIIIa more than adults in a paced/unpaced finger tapping study. We therefore attribute the inclusion of the activation seen in contralateral lobule VIII to the children requiring more extensive neural circuitry in this task.

Including the alcohol exposed children into these correlations greatly reduces the significance of the correlations between changes in activation and the behavioural performance measures. This finding suggests that altered functional activity is seen in these regions in the children prenatally exposed to alcohol.

Indeed, we did find significant inverse correlations between alcohol exposure and activation in both right lobule VIIIb and left lobule VIIIa. In left lobule VIIIa strong inverse correlations are seen between activation and the average amount of alcohol consumed per day and dosage dependent alcohol consumption, both around time of conception and across pregnancy. Right lobule VIIIb similarly shows correlations with both measures around time of conception and dosage dependent alcohol consumption across pregnancy. Our findings therefore suggest that impaired performance in this task in the most severely affected children as evidenced by the small number who met inclusion criteria may, at least in part, be related to the adverse effects of alcohol on these cerebellar regions in bilateral lobules VIII.

A strong positive correlation between changes in activation in right lobule VI and task performance in the control children was also seen. Once again, these correlations become less significant when including the full cohort. This correlation was attributable to the motor delay if the inclusion of the other Wing-Kristofferson (1973) estimates were to be reliable. However, once again, this finding is interpreted with caution.

As mentioned previously, contradictory evidence of whether hemispheric lobule VI is involved in timing or motor function is seen in previous studies of self-paced motor tasks (Spencer et al., 2007; Bengtsson et al., 2005). The questionability of the calculation of the Wing-Kristofferson (1973) estimates in our study also doesn't allow us to attribute the variability to motor or clock variance.

As the main motivation for our study was to examine whether altered function in brain regions involved in performing timed movements with millisecond precision may explain, in

part, the impaired EBC seen in children prenatally exposed to alcohol, we refer back to previous studies investigating cerebellar activation in this paradigm (Molchan et al., 1994; Knuttinen et al., 2002; Blaxton et al., 1996; Miller et al., 2003; Schreurs et al., 1997; Cheng et al., 2008). In spite of the contradictory findings regarding the activation in hemispheric lobule VI ipsilateral to the eye receiving the US in these studies, these articles unanimously indicate the learning dependent involvement of this cerebellar region.

Several of these studies indicate that parts of ipsilateral lobule VI is deactivated during EBC and this is attributed to depressed Purkinje cell firing in order to disinhibit neuronal functioning in the interpositus nucleus for production of the required motor output (Molchan et al., 1994; Blaxton et al., 1996; Miller et al., 2003; Schreurs et al., 1997).

More relevant to our study, two studies identified increased activation during EBC in ipsilateral lobule VI with coordinates very similar to the region we identified in this paced/unpaced finger tapping study. Blaxton et al. (1996) used positron emission tomography (PET) to measure regional cerebral blood flow (rCBF) during EBC. They identified five regions in the bilateral cerebellum where learning associated increases in rCBF were observed and one region in the right hemisphere where deactivation was seen. One cluster showing increased activation was seen ipsilateral to the eye that received the air puff at $x = 20$, $y = -65$, $z = -25$ (Talairach coordinates were converted to MNI units by means of GingerALE, version 2.3, Research Imaging Institute, UTHSCSA). Similarly, Cheng et al. (2008) also identified this region ($x = -25$, $y = -62$, $z = -24$) as having increased ipsilateral activation during EBC and established that this region is activated during both delay and trace conditioning.

These regions are in very close proximity to the area we identified ($x = 26$, $y = -66$, $z = -26$) and the identification of this region in the paced/unpaced finger tapping task supports the assumption that this task could be used as a proxy for EBC.

Once again, the limitations in the determination of the Wing-Kristofferson (1973) estimates do not allow reliable assignment of activation in this region to either motor or clock estimates during this task. However, from the aforementioned studies, we know that this particular region in lobule VI is involved in EBC irrespective of the specific aspect of the involvement.

Furthermore, our results indicate that increased dosage dependent alcohol consumption, especially around the time of conception, leads to smaller increases in activation in this region during self-paced finger tapping compared to rest. This alcohol related effect on functioning in this area could therefore, at least partially, account for the impaired EBC performance seen in children with FASD.

6.5 Conclusion

We used fMRI during a paced/unpaced finger tapping task to evaluate the ability of children prenatally exposed to alcohol to perform a motor response with millisecond accuracy similar to that required for successful EBC.

As we analysed the fMRI data for the contrast comparing unpaced finger tapping to rest, we attempted to discriminate between the motor and clock components of the task by implementation of the Wing-Kristofferson (1973) model. However, a large portion of our data violated the model and bold assumptions were made, which necessitates caution when interpreting these results.

The behavioural data showed that overall differences in task performance were associated with age. Although none of the behavioural measures were associated with alcohol, a large proportion of the most severely affected children with FAS/PFAS were unable to perform the task well enough for inclusion in the Wing-Kristofferson (1973) or fMRI analyses, suggesting an alcohol-related deficit.

Four regions where functional activation was associated with overall ITI variability in the control children were identified in the regression analyses. Three significant clusters in bilateral lobule VIII and one in right lobule VI emerged.

In spite of the limitations of our behavioural data, higher levels of alcohol exposure were associated with decreased activation increases in right lobule VIIIb, left lobule VIIIa, and right lobule VI during the paced/unpaced finger tapping task. Although we cannot attribute these effects to timing or motor components, the correlations seen between activation and prenatal alcohol exposure indicate altered functioning of these regions in children with FASD. Notably, activation in the specific region of right lobule VI identified in this study has previously been linked to EBC. The altered functioning of this region in children prenatally exposed to alcohol may therefore be involved, in part, in the impaired EBC performance seen in these children.

Acknowledgements

This research was supported by the following grants from the National Institute on Alcohol Abuse and Alcoholism: R01 AA016781 and an administrative supplement to R01 AA09524 (S. Jacobson, PI); U01 AA014790 (S. Jacobson, PI); R21AA017410 (E. Meintjes and A. van der Kouwe, PIs); and U24 AA014815 (K. Jones, PI) in conjunction with the Collaborative Initiative on Fetal Alcohol Spectrum Disorders. This research was also supported by a grant from the NIH Office of Research on Minority Health, the South African Research Chairs Initiative of the Department of Science and Technology and National Research Foundation of South Africa, Focus Area Grant FA2005040800024 from the South African National Research Foundation (E. Meintjes, PI), and seed money grants from the University of Cape Town, the President of Wayne State University, and the Joseph Young, Sr, Fund from the State of Michigan. We thank Bruce Spottiswoode, Ph.D., the CUBIC radiographers Marie-Louise de Villiers and Nailah Maroof, and our UCT and WSU research

staff Nicolette Hamman, Mariska Pienaar, Maggie September, Emma Makin, Renee Sun and Neil Dodge. We also greatly appreciate the participation of the mothers and children in the longitudinal study.

The authors declare no competing financial interests.

Chapter Seven

Discussion and Conclusion

The main purpose of this study was to examine the integrity of two components of the cerebellar-brainstem circuit critical to eyeblink conditioning (EBC) in children prenatally exposed to alcohol in order to assess whether deficits in these regions may explain, or at least contribute to, the striking EBC deficit that has been reported in this population. We used MR spectroscopy (MRS) and functional MRI (fMRI) to assess neurometabolism in the cerebellar deep nuclei and brain activity in the cerebellar cortex, respectively, in a group of children with different FASD diagnoses and varying levels of prenatal alcohol exposure, as well as non- or minimally exposed controls. Due to the challenges associated with performing EBC during fMRI acquisition, activation of the cerebellar cortex involved in maintaining timed movements with millisecond accuracy, such as required for a successful EBC response, was targeted instead. We hypothesized that alcohol exposure would lead to altered metabolism, specifically decreased levels of NAA, in the cerebellar deep nuclei and altered activation of the cerebellar cortex during timed movements requiring millisecond precision. Finally, we wished to examine the extent to which the above measures - metabolite levels in the deep nuclei and brain activation in the cerebellar cortex - were associated with EBC performance in order to ascertain the extent to which alterations in these two regions play a role in the observed EBC deficit or whether other parts of the circuit are responsible. We hypothesized that metabolite levels in the deep nuclei and brain activation in the cerebellar cortex would be associated with EBC performance.

MRS of the Cerebellar Deep Nuclei

The critical involvement of the cerebellar deep nuclei in EBC, specifically the interpositus nucleus, was outlined in chapter two. In our study of the metabolic composition of these nuclei we hypothesized that decreased NAA levels would be seen in the children prenatally exposed to alcohol, since NAA has widely been linked to the functional integrity of neurons and could mitigate the ability of these children to reach conditioning.

As hypothesized, increasing alcohol exposure around the time of conception was associated with lower levels of NAA in the deep nuclei. This is in line with previous studies showing decreased NAA levels in several pathologies (Schott et al., 2010; Adalsteinsson et al., 2000; Winsberg et al., 2000; Grossman et al., 1992; Hugg et al., 1993), as well as Green et al.'s (2006) animal study showing decreased neuronal density in the deep nuclei, which was also associated with decreased EBC performance.

However, in our study higher levels of NAA were related to delay eyeblink conditioning performance at both 5 and 9 years *only* in the control children and *not* in the alcohol-exposed children suggesting that the observed deficit in EBC performance in alcohol-exposed children is not due to compromised neuronal integrity in the deep cerebellar nuclei, but due to damage to some other element of the cerebellar-brainstem circuit.

Our MRS findings could be indicative of abnormalities outside the neurons themselves. As the voxel placement in our study included white matter as well as grey matter, metabolite levels across the synapses between the Purkinje cells and the neurons in the deep nuclei would be included. In a review article, Guerri et al. (2001) suggested that prenatal alcohol exposure affects glia to a greater extent than the neurons themselves. Glia are vital to the maintenance and homeostasis of neuronal cells (Fields and Stevens-Graham, 2002; Haydon, 2001) and alterations in these cells directly affect neuronal functioning.

Myelin sheaths surrounding neuronal axons create an insulated environment for optimal conductivity and therefore neurotransmission. Oligodendrocytes are responsible for this myelination and previous studies have shown that prenatal alcohol exposure adversely

affects these glia and delays the expression of the myelin basic protein (Chiappelli et al., 1991). Choline is a vital component in the formation of cell membranes and these myelin sheaths (Burgerstein, 2001). Our finding of reduced choline levels with increasing alcohol exposure therefore suggests that the integrity of the cell membranes and myelin sheaths may be compromised by the adverse effects of prenatal alcohol exposure in oligodendroglia.

In line with the hypothesis that damage to glia from prenatal alcohol exposure are, to a great extent, responsible for neurodevelopmental issues, we turn our attention to astroglia.

Astrocytes have also been found to play a big role in neurotransmission (Haydon, 2001; Haydon and Carmignoto, 2006). Astrocytes regulate potassium ions in the extracellular fluid, which is crucial for the production of proper nerve impulses, and also absorb the released neurotransmitters, glutamate (Glu) and GABA, and transform them into glutamine (Gln). As outlined in chapter two, the level of excitatory and inhibitory neurotransmitters at the synapses to the neurons of the interpositus nucleus must be balanced in order to maintain a specified level of excitation in this structure for optimal EBC learning and performance. Our finding that the FASD children have increased Glx (Glu+Gln) levels associated with increasing exposure indicates that this delicate neurotransmitter balance is disturbed by prenatal alcohol exposure. The increased activity of the interpositus nucleus that would be associated with increased levels of glutamate would impede the acquisition and retention of conditioned responses (CR's) in the alcohol-exposed children. Increased levels of Glx in the synapses could be due to glial cell damage or alternatively it could be the same mechanism as observed in alcoholics after alcohol consumption has stopped (Tsai et al., 1998). In either case, the increased Glx levels could be sufficient in disrupting the EBC response in the FASD children due to the overactive nuclear cells in the interpositus nucleus. Goodlett et al. (2001) corroborated the finding of altered neurotransmission in FASD.

Goodlett et al. (2001) also suggested that spontaneous apoptosis through oxidative stress could lead to damage to, amongst others, cell membranes. This phenomenon was seen in another MRS study of FASD and interpreted as decreased membrane integrity

(Astley et al., 2009). The inverse correlation between alcohol exposure across pregnancy and Cho levels seen in this study supports Goodlett et al.'s (2001) statement as Cho represents precursor and breakdown products of cell membranes.

Our finding of decreased NAA with increased alcohol exposure could therefore be indicative of improper support systems for the neurons caused by damage to the glia, which, in turn, will alter neuronal functioning. Altogether, our MRS findings suggest that prenatal alcohol exposure alters the children's synaptic plasticity at the interpositus nucleus. The absence of a relation between neurometabolite levels and EBC performance in the alcohol-exposed children suggests, however, that this part of the cerebellar-brainstem circuit is not primarily responsible for the impaired EBC response.

fMRI of the Cerebellar Cortex

In this study, we focused on assessing brain activity in children prenatally exposed to alcohol in cerebellar regions involved in performing timed movements with millisecond accuracy. This approach was based on the assumption that the brain regions activated to perform precisely timed movements in the rhythmic/non-rhythmic and paced/unpaced finger tapping tasks used in this study would be similar to the regions required to achieve millisecond precision for a successful EBC response.

Neither of the rhythmic finger tapping studies indicated significant differences in performance between the diagnostic groups. This was contrary to our expectations, since we hypothesized that a timing deficit caused by prenatal alcohol exposure may be responsible for the impaired EBC performance in the children with FASD. However, lack of differences in task performance between diagnostic groups on the simple tasks typically administered in the scanner has been reported in previous studies of FASD (Meintjes et al., 2010; Diwadkar et al., 2013). Despite similar performance by children in all diagnostic groups during a simple maths (Meintjes et al., 2010) and 1-back (Diwadkar et al., 2013) task in these studies, children with prenatal alcohol exposure recruited different and more

extensive brain regions to successfully complete the tasks. These studies suggests that alcohol exposed children do not recruit the brain circuitry specialised for these tasks and need to exert more effort to achieve the same performance than the control children. It is therefore possible that the alcohol exposed children in our studies recruited different cerebellar regions to reach the same level of performance in these tasks. However, this aspect was not investigated in our study as only the extent to which the alcohol-exposed children activated the cerebellar regions employed by the control children was examined.

It has previously been shown that performance in tasks requiring timed motor responses are related to age (Greene and Williams, 1993) – a finding consistent with the results of our paced/unpaced finger tapping results. The lack of differences in the behavioural data could therefore be due to the fact that this skill is not fully developed in any of the children, including the non- or minimally exposed controls, which would make alcohol related differences difficult to identify.

In our fMRI analyses, we first identified regions activated significantly more by control children during rhythmic finger tapping compared to non-rhythmic finger tapping or that were activated to a greater extent with improved ability to maintain rhythm during unpaced tapping. We then examined whether alcohol-exposed children activated these same regions to a greater or lesser extent.

By contrast to the rhythmic/non-rhythmic task where activation of motor components should be similar during the two tapping conditions and as such accounted for by considering the rhythmic versus non-rhythmic contrast, a limitation of the unpaced versus rest contrast considered in the paced/unpaced tapping task is that it is not possible to assign activation specifically to timing or motor components. In the latter, the activation during 'learning' of the temporal task was not directly taken into account and activations reflect only the cerebellar regions recruited to maintain the 'learnt' temporal motor response.

Referring to previously defined topographic functional maps to distinguish between different cerebellar functions, such as motor or clock performance, should be done with caution as these generally refer to the gross anatomical scale (cerebellar lobules) without

breaking down regions within these anatomical volumes. As mentioned in Chapter 2, functional activity in the distinct cerebellar lobules is not restricted to particular mechanisms. Allocating activation in a subsection of a lobule is therefore questionable as voxel-by-voxel functioning in the cerebellum has not been established.

Results in control children reveal striking differences in activated regions between the two finger tapping tasks. With the exception of right Crus I, activation in the rhythmic/non-rhythmic task is situated more medially than activation clusters during the paced/unpaced finger tapping task, with the largest activations for the former in vermis IV-VI and smaller activations in right lobule VI and Crus I. A previous study of motor reactions in time with regular pacing stimuli indicated that responses start occurring prior to the actual receiving of the stimulus, suggesting that movement becomes generated internally instead of in response to the stimulus (Aschersleben and Prinz, 1995). Using a task similar to our own, Lutz et al. (2000) determined that more extensive neural circuitry is required for production of responses to random stimuli.

By contrast, activations during unpaced tapping were associated with the ability to maintain rhythm bilaterally in lobule VIII and in right lobule VI. While the activations in right lobule VI for the two tasks do not overlap (coordinates (12,-62,-17) and (26,-66,-26) in the rhythmic/non-rhythmic and paced/unpaced tasks, respectively), they are close. In view of the very different mechanisms and contrasts studied in these tasks, the differences between the activation patterns are not surprising.

The lesion study performed by Ivry et al. (1988) implementing the Wing-Kristofferson (1973) estimates suggested that medial portions of the cerebellum are implicated in motor control, while the clock estimate is mediated by lateral cerebellar regions.

The results from our study, however, do not support these findings. The design and contrast used in the rhythmic/non-rhythmic study should eliminate contributions from motor control as both the rhythmic and non-rhythmic tapping requires the same motion response, suggesting that the activations found in the three medial regions in this task are related to

processes other than motor control. It is, however, not possible to assign these activations to timing *per se* as the cerebellum has been implicated in many processes.

We were unable to definitively assign activation during the paced/unpaced finger tapping task to either motor control or clock as the results from our Wing-Kristofferson (1973) analysis cannot be deemed reliable. However, lobule VIII has consistently been implicated in motor control and since no changes in activation were seen in the primary motor homunculus, we attribute activation in these lobules to the motor component of the task (Stoodley and Schmahmann, 2009; Grodd et al., 2001).

As mentioned in Chapter 5, activation in lobule VI has been attributed to both motor control and timing (Stoodley and Schmahmann, 2009; Grodd et al., 2001; Bengtsson et al., 2005), which makes it difficult to interpret activation of this lobule in the paced/unpaced finger tapping task. However, the close proximity of the clusters in right lobule VI identified in both our functional studies could be indicative of a central component, although it cannot be attributed to a distinct function as voxel-by-voxel function of the cerebellum has not been established.

With regards the effects of prenatal alcohol exposure on brain activation in these two tasks, group differences in activation were only evident in the rhythmic/non-rhythmic finger tapping task – in right Crus I and vermis IV-V. The results show significantly smaller differences in activation between rhythmic and non-rhythmic tapping in all alcohol exposed children in right Crus I and in the most severely affected FAS/PFAS children in vermis IV-V.

As would be expected, the more sensitive continuous alcohol exposure measures showed significant correlations with activation in seven of the eight regions identified in the two fMRI tasks combined – only in right VIIIa was there no association of activation with extent of alcohol exposure. This result is consistent with previous studies that have demonstrated that extent of prenatal alcohol exposure is often more sensitive to detect damaging effects of alcohol exposure than diagnostic groups (for example, Taylor et al., in press; Meintjes et al., 2014).

In order to extrapolate our findings to the impaired EBC performance seen in children with FASD, we turn to previous studies of this paradigm. Hemispheric lobule VI has consistently been implicated to be involved in the acquisition and retention of EBC responses (Yeo and Hardiman, 1992; Gerwig et al., 2003; Molchan et al., 1994; Blaxton et al., 1995; Cheng et al., 2008; Miller et al., 2003). Significant clusters of activation in ipsilateral lobule VI emerged in both the paced/unpaced and rhythmic/non-rhythmic finger tapping. More significantly, we found that activation in these clusters is related to prenatal alcohol exposure indicating that the functioning in sections of this lobule is affected in children with FASD. We did, however, not find any significant correlations between activations in this region and the EBC performance measures.

In addition to hemispheric lobule VI, Crus I has also been shown previously to be involved in EBC (Schreurs et al., 1997; Blaxton et al., 1996; Yeo and Hardiman, 1992). Once again, we found differences in activation related to prenatal alcohol exposure but no association with EBC performance.

Thus, in spite of the limitations in our study and the lack of significant differences in behavioural measures, we were able to determine that two cerebellar regions consistently implicated in EBC are affected by prenatal alcohol exposure. While this altered activation could play a role in the impaired EBC performance of the alcohol exposed children, they were still able to perform the finger tapping tasks with precision similar to the control children and activation in neither of these regions was related to EBC performance. We are therefore not able to attribute the deficient EBC performance directly to altered activation in these regions.

Although right lobule VIIIb, left lobule VIIIa, vermis IV/V and vermis VI have not previously been implicated in EBC, we also found significant effects of exposure in these four regions, which highlights the extensive damaging effects of prenatal alcohol exposure in these children.

Conclusion

In summary, our studies have shown that two core components of EBC, metabolism in the cerebellar deep nuclei and function in the cerebellar cortex, are affected by prenatal alcohol exposure. It has been suggested that converging inputs to the cerebellar cortex from the CS and US lead to Purkinje cell depression in order to stop inhibition of the deep nuclei.

The main findings of the MRS study indicated that increased prenatal alcohol exposure was associated with lower levels of both NAA and choline-containing metabolites, and with higher levels of glutamate plus glutamine (Glx). These findings reflect impairment in neuronal integrity in this region, as well as possible damage to the supporting glial cells. These alcohol related effects would lead to impaired functioning to this structure which has been found to be crucial to the acquisition and retention of EBC responses.

In addition to this, our functional studies indicated alcohol related effects on activation in two regions – ipsilateral hemispheric lobule VI and Crus I – consistently implicated in EBC performance. Although we cannot directly extrapolate our findings to EBC, our results do indicate that prenatal alcohol exposure causes extensive damage to cerebellar cortex.

One major limitation of our study is our inability to assign activation of the cerebellar regions identified to either motor or clock variance in the paced/unpaced finger tapping task, since we could not reliably calculate the Wing-Kristofferson (1973) estimates. We can therefore not directly relate our results to an alcohol-related effect on internal timing so that we can neither confirm nor refute the hypothesis that impaired EBC performance is due to an internal timing deficit.

Ideally, it should be ensured that each subject performs at least six ‘perfect’ blocks while performing the paced/unpaced finger tapping task so that the Wing-Kristofferson (1973) model can be applied more reliably. It would also be most informative if this was done at age 20 to 30 which has been said to be the age where optimal performance in this task is seen according to Greene and Williams (1993). The strong age-related effect we saw

in performance should then be eliminated and the true effect of prenatal alcohol exposure could be studied.

References

Adalsteinsson, E., et al., *Longitudinal decline of the neuronal marker N-acetyl aspartate in Alzheimer's disease.* The Lancet, 2000. 355(9216):1696-1697

Aguirre, G.K. et al., *The variability of human, BOLD hemodynamic responses.* NeuroImage, 1998. 8(4):360-369

Aksenov, D., et al., *GABA neurotransmission in the cerebellar interposed nuclei: involvement in classically conditioned eyeblinks and neuronal activity.* Journal of Neurophysiology, 2004. 91(2):719-727.

Aksenov, D.P., et al., *Glutamate neurotransmission in the cerebellar interposed nuclei: involvement in classically conditioned eyeblinks and neuronal activity.* Journal of Neurophysiology, 2005. 93(1):44-52.

Allen, G., et al., *Attentional activation of the cerebellum independent of motor involvement*. Science, 1997. 275:1940-1943.

Amaro, E. and Barker, G.J., *Study design in fMRI: Basic principles.* Brain and Cognition, 2006. 60:220-232

Aoki, S., et al., *Normal deposition of brain iron in childhood and adolescence: MR imaging at 1.5 T*. Radiology, 1989. 172:381-385.

Archibald, S.L., et al., *Brain dysmorphology in individuals with severe prenatal alcohol exposure.* Developmental Medicine and Child Neurology, 2001. 43(3):148-154.

Aschersleben, G. and Prinz, W., *Synchronizing actions with events: The role of sensory information.* Perception & Psychophysics, 1995. 57(3):305-317

Ashburner, J., *SPM: a history*. NeuroImage, 2012. 62:791-800

Astley, S.J. and Clarren, S.K., *Measuring the facial phenotype of individuals with prenatal alcohol exposure: correlations with brain dysfunction.* Alcohol and Alcoholism, 2001. 36(2):147-159.

Astley, S.F., et al., *Magnetic resonance imaging in ethanol exposed Macaca nemestrina*. Neurotoxicology and Teratology, 1995. 17:523-530.

Astley, S.J., et al., *Magnetic resonance spectroscopy outcomes from a comprehensive magnetic resonance study of children with fetal alcohol syndrome.* Magnetic Resonance Imaging, 2009. 27:760-778.

Baslow, M.H., *N-Acetyl aspartate in the vertebrate brain: Metabolism and function.* Neurochemical Research, 2003. 28:941-953.

Bengtsson, S.L., et al., *Effector-independent voluntary timing: behavioural and neuroimaging evidence.* European Journal of Neuroscience, 2005. 22(12):3255-3265.

Berntson, G.G., et al., *Evidence for higher functions of the cerebellum: eating and grooming elicited by cerebellar stimulation in cats.* Proceedings of the National Academy of Sciences, 1973. 70(9):2497-2499.

Blaxton, T.A., et al*., Functional mapping of human learning: a positron emission tomography activation study of eyeblink conditioning*. Journal of Neuroscience, 1996. 16(12):4032-4040

Bloch, F., et al., *The nuclear induction experiment*. Physical Review, 1946. 70(7&8): 474-485

Bowman, R.S., et al., *Measurement and interpretation of drinking behavior: I. On measuring patterns of alcohol consumption: II. Relationships between drinking behavior and social adjustment in a sample of problem drinkers*. Journal of Studies on Alcohol and Drugs, 1975. 36:1154-1172.

Braitenbach, V., *Is the cerebellar cortex a biological clock in the millisecond range?* Progress in Brain Research, 1967. 25:334-336

Buonomano, D.V. and Karmarkar, U.R., *Book review: How do we tell time?* Neuroscientist, 2002. 8:42-51

Buonomano, D.V and Laje, R., *Population clocks: motor timing with neural dynamics.* Trends in Cognitive Sciences, 2010. *14*(12):520-527

Burden, M.J., et al., *Relation of prenatal alcohol exposure to cognitive processing speed and efficiency in childhood*. Alcoholism: Clinical and Experimental Research, 2005. 29:1473-1483.

Burgerstein, L., *Burgerstein's handbook of nutrition: Micronutrients in the prevention and therapy of disease* (2001). Thieme, 2001

Buxton, R.B., et al., *Modeling the hemodynamic response to brain activation*. NeuroImage, 2004. 23(S1):S220-S233

Calhoun, F. and Warren, K., *Fetal alcohol syndrome: historical perspectives*. Neuroscience & Biobehavioral Reviews, 2007. 31:168-171.

Chen, X., et al., *Understanding specific effects of prenatal alcohol exposure on brain structure in young adults*. Human Brain Mapping, 2012. 33:1663-1676

Cheng, D.T., et al., *Neural substrates underlying human delay and trace eyeblink conditioning*. Proceedings of the National Academy of Sciences, 2008. 105(28):8108-8113

Cheng, D.T., et al., *Functional MRI of cerebellar activity during eyeblink classical conditioning in children and adults*. Human Brain Mapping, 2014. 35(4):1390-1403

Choi, J.S. and Moore, J.W., *Cerebellar neuronal activity expresses the complex topography of conditioned eyeblink responses.* Behavioral Neuroscience, 2003. 117(6):1211.

Chiappelli, F. et al., *Fetal alcohol delays the developmental expression of myelin basic protein and transferrin in rat primary oligodendrtocyte cultures*. International Journal of Developmental Neuroscience, 1991. 9(1):67-75

Christian, K.M. and Thompson, R.F., *Neural substrates of eyeblink conditioning: acquisition and retention.* Learning & Memory, 2003. 10(6):427-455.

Clarren, S.K., *Central nervous system malformations in two offspring of alcoholic women.* Birth Defects – Original Article Series, 1977. 13(3D):151.

Clarren, S.K., et al., *Brain malformations related to prenatal exposure to alcohol*. Journal of Pediatrics, 1978. 92:64-67

Coffin, J.M., et al., *Impaired cerebellar learning in children with prenatal alcohol exposure: a comparative study of eyeblink conditioning in children with ADHD and dyslexia*. Cortex, 2005. 41:389-398.

Cortese, B.M., et al., *Magnetic resonance and spectroscopic imaging in prenatal alcohol-exposed children: preliminary findings in the caudate nucleus.* Neurotoxicology and Teratology, 2006. 28:597-606.

Croxford, J. and Viljoen, D., *Alcohol consumption by pregnant women in the Western Cape.* South African Medical Journal, 1999. 89(9):962-965.

Daniel, H., et al., *Cellular mechanisms of cerebellar LTD.* Trends in Neurosciences, 1998. 21(9):401-407.

Davis, N., et al., *The neural correlates of calculation ability in children: an fMRI study.* Magnetic Resonance Imaging, 2009. 27(9):1187-1197.

De Guio, F., et al., *Functional magnetic resonance imaging study comparing rhythmic finger tapping in children and adults.* Pediatric Neurology, 2012. 46(2):94-100.

De Graaf, R.A., *In vivo NMR spectroscopy: principles and techniques*. 2008: John Wiley & Sons

Delgado-García, J. and Gruart, A., *The role of interpositus nucleus in eyelid conditioned responses.* The Cerebellum, 2002. 1(4):289-308.

Desmond, J.E., et al., *Lobular patterns of cerebellar activation in verbal working-memory and finger-tapping tasks as revealed by functional MRI.* Journal of Neuroscience, 1997. 17(24):9675-9685.

Desmond, J.E. and Fiez, J.A., *Neuroimaging studies of the cerebellum: language, learning and memory.* Trends in Cognitive Sciences, 1998. 2(9):355-362.

Diedrichsen, J., et al., *Dissociating timing and coordination as functions of the cerebellum.* Journal of Neuroscience, 2007. 27(23):6291-6301.

Diedrichsen, J., et al., *A probabilistic MR atlas of the human cerebellum.* Neuroimage, 2009. 46(1):39-46.

Dikranian, K., et al., *Ethanol-induced neuroapoptosis in the developing rodent cerebellum and related brain stem structures*. Developmental Brain Research, 2005. 155:1-13.

Dimitrova, A., et al., *Eyeblink-related areas in human cerebellum as shown by fMRI*. Human Brain Mapping, 2002. 17:100-115.

Dimitrova, A., et al., *Probabilistic 3D MRI atlas of the human cerebellar dentate/interposed nuclei*. Neuroimage, 2006. 30:12-25.

Diwadkar, V., et al., *Differences in cortico-striatal-cerebellar activations during working memory in syndromal and non-syndromal children with prenatal alcohol exposure.* Human Brain Mapping, 2013. 34:1931-1945.

Dunty, W.C., et al., *Selective Vulnerability of Embryonic Cell Populations to Ethanol-Induced Apoptosis: Implications for Alcohol-Related Birth Defects and Neurodevelopmental Disorder.* Alcoholism: Clinical and Experimental Research, 2001. 25:1523-1535.

Eccles, J.C., *The cerebellum as a neuronal machine.* 1967.

Ekerot, C.F. and Kano, M., *Stimulation parameters influencing climbing fibre induced long-term depression of parallel fibre synapses.* Neuroscience Research, 1989. 6(3):264-268.

Ernst, T., et al., *Absolute quantitation of water and metabolites in the human brain. I. Compartments and water*. Journal of Magnetic Resonance, Series B, 1993. 102:1-8.

Fagerlund, A., et al., *Brain metabolic alterations in adolescents and young adults with fetal alcohol spectrum disorders*. Alcoholism: Clinical and Experimental Research, 2006. 30:2097-2104.

Ferrier, D., *Functions of the cerebellum.* 1886.

Fields, R.D. and Stevens-Graham, B., *New insights into neuron-glia communication.* Science, 2002. 298(5593):556-562.

Forman, S.D., et al., *Improved assessment of significant activation in functional magnetic resonance imaging (fMRI): use of a cluster-size threshold*. Magnetic Resonance in Medicine, 1995. 33(5)636-647

Freeman, J.H. and Nicholson, D.A., *Developmental changes in eye-blink conditioniing and neuronal activity in the cerebellar interpositus nucleus*. The Journal of Neuroscience, 2000. 20:813-819.

Gasparovic, C., et al., *Use of tissue water as a concentration reference for proton spectroscopic imaging.* Magnetic Resonance in Medicine, 2006. 55:1219-1226.

Gerwig, M., et al., *Comparison of eyeblink conditioning in patients with superior and posterior inferior cerebellar lesions*. Brain, 2003. 126:71-94.

Gerwig, M., et al., *The involvement of the human cerebellum in eyeblink conditioning*. The Cerebellum, 2007. 6:38-57.

Glickstein, M., et al., *Cerebellum: history.* Neuroscience, 2009. 162(3):549-559.

Goebel, R., et al., *Analysis of functional image analysis contest (FIAC) data with Brainvoyager QX: From single-subject to cortically aligned group general linear model analysis and self-organizing group independent component analysis.* Human Brain Mapping, 2006. 27:392-401

Goodlett, C.R., et al., *Alcohol-induced damage to the developing brain: functional approaches using classical eyeblink conditioning.* Eyeblink Classical Conditioning: Volume 2: Springer US, 2000. 135-153.

Goodlett, C.R. and Horn, K.H., *Mechanisms of alcohol-induced damage to the developing nervous system.* Alcohol research and Health, 2001. 25(3):175-184.

Green, J.T. and Woodruff-Pak, D.S., *Eyeblink classical conditioning: Hippocampal formation is for neutral stimulus associations as cerebellum is for association–response.* Psychological Bulletin, 2000. 126(1):138.

Green, J.T., et al., *Eyeblink classical conditioning and interpositus nucleus activity are disrupted in adult rats exposed to ethanol as neonates*. Learning & Memory, 2002a. 9:304-320.

Green, J.T., et al., *Neonatal ethanol produces cerebellar deep nuclear cell loss and correlated disruption of eyeblink conditioning in adult rats.* Brain Research, 2002b. 956:302-311.

Green, J.T., et al., *The effects of moderate neonatal ethanol exposure on eyeblink conditioning and deep cerebellar nuclei neuron numbers in the rat.* Alcohol, 2006. 39(3):135-150.

Greene, L.S. and Williams, H.G., *Age-related differences in timing control of repetitive movement: application of the Wing-Kristofferson model*. Research Quarterly for Exercise and Sport, 1993. 64(1):32-38

Grodd, W., et al., *Sensorimotor mapping of the human cerebellum: fMRI evidence of somatotopic organization.* Human Brain Mapping, 2001. 13(2):55-73.

Grossman, R., et al., *MR proton spectroscopy in multiple sclerosis.* American journal of neuroradiology, 1992. 13(6):1535-1543.

Guerri, C., *Neuroanatomical and neurophysiological mechanisms involved in central nervous system dysfunctions induced by prenatal alcohol exposure.* Alcoholism: Clinical and Experimental Research, 1998. 22(2):304-312.

Guerri, C., et al., *Glia and fetal alcohol syndrome.* Neurotoxicology, 2001. 22(5):593-599.

Habas, C., et al., *Distinct cerebellar contributions to intrinsic connectivity networks.* Journal of Neuroscience, 2009. 29(26):8586-8594.

Hamre, K.M. and West, J.R.*, The effects of the timing of ethanol exposure during the brain growth spurt on the number of cerebellar Purkinje and granule cell nuclear profiles.* Alcoholism: Clinical and Experimental Research, 1993. 17:610-622.

Hashemi, R.H., et al., *MRI: the basics*. Lippincott Williams & Wilkins, 2012.

Haydon, P.G., *GLIA: listening and talking to the synapse.* Nature Reviews Neuroscience, 2001. 2(3):185-193.

Haydon, P.G. and Carmignoto, G., *Astrocyte control of synaptic transmission and neurovascular coupling.* Physiological reviews, 2006. 86(3):1009-1031.

Hess, A.T., et al., *Real-time motion and B0 corrected singel voxel spectroscopy using volumetric navigators*. Magnetic Resonance in Medicine, 2011a. 66:314-323.

Hess, A.T., et al., *Water-independent frequency- and phase-corrected spectroscopic averaging using cross-correlation and singular value decomposition*, in Proceedings of the International Society for Magnetic Resonance in Medicine, ISMRM 19th Scientific Meeting, Montréal, Canada, May 2011b. ISSN# 1545-4428, 148.

Hesslow, G., *Inhibition of classically conditioned eyeblink responses by stimulation of the cerebellar cortex in the decerebrate cat.* Journal of Physiology, 1994. 476(2):245-256.

Herbert, J.S., et al., *The ontogeny of human learning in delay, long-delay, and trace eyeblink conditioning.* Behavioral Neuroscience, 2003. 117:1196.

Hirano, T., *Depression and potentiation of the synaptic transmission between a granule cell and a Purkinje cell in rat cerebellar culture.* Neuroscience Letters, 1990. 119(2):141-144.

Hochberg, Y., *A sharper Bonferroni procedure for multiple tests of significance*. Biometrika, 1988. 75:800-802.

Hoyme, H.E., et al*., A practical clinical approach to diagnosis of fetal alcohol spectrum disorders: clarification of the 1996 institute of medicine criteria*. Pediatrics, 2005. 115:39-47.

Hugg, J.W., et al., *Neuron loss localizes human temporal lobe epilepsy by in vivo proton magnetic resonance spectroscopic imaging.* Annals of neurology, 1993. 34(6):788-794.

Ito, M., *Cerebellar circuitry as a neuronal machine.* Progress in Neurobiology, 2006. 78(3):272-303.

Itō, M., *Cerebellum: The Brain for an Implicit Self*. 2012: FT Press.

Ivry, R.B., et al., *Dissociation of the lateral and medial cerebellum in movement timing and movement execution.* Experimental Brain Research, 1988. 73(1):167-180.

Ivry, R.B. and Keele, S.W., *Timing functions of the cerebellum.* Journal of Cognitive Neuroscience, 1989. 1(2):136-152.

Ivry, R.B., *Cerebellar involvement in the explicit representation of temporal information*. Annals of the New York Academy of Sciences, 1993. 682(1):214-230

Ivry, R.B. et al., *The cerebellum and event timing*. Annals of the New York Academy of Sciences, 2002. 978:302-317

Ivry, R.B. and Schlerf, J.E., *Dedicated and intrinsic models of time perception*. Trends in Cogitive Sciences, 2008. 12(7): 273-280

Jacobson, S.W., et al., *Prenatal alcohol exposure and infant information processing ability*. Child Development, 1993. 64:1706-1721.

Jacobson, S.W., et al., *Validity of maternal report of alcohol, cocaine, and smoking during pregnancy in relation to infant neurobehavioral outcome*. Pediatrics, 2002. 109:815-825.

Jacobson, S.W., et al., *Maternal age, alcohol abuse history, and quality of parenting as moderators of the effects of prenatal alcohol exposure on 7.5-year intellectual function.* Alcoholism: Clinical and Experimental Research, 2004. 28:1732-1745.

Jacobson, J.L., et al., *Prospective examination of the incidence of heavy drinking during pregnancy among Cape Coloured South African Women.* Alcoholism: Clinical and Experimental Research, 2006. 30:233A.

Jacobson, S.W., et al., *Impaired eyeblink conditioning in children with fetal alcohol syndrome.* Alcoholism: Clinical and Experimental Research, 2008. 32(2):365-372.

Jacobson, S.W., et al., *Impaired Delay and Trace Eyeblink Conditioning in School-Age Children With Fetal Alcohol Syndrome.* Alcoholism: Clinical and Experimental Research, 2011. 35:250-264.

Jezzard, P. and Smith, M.P., *Functional MRI. An Introduction to Methods*. 2009: Oxford University Press.

Jones, K.L et al., *Pattern of malformation in offspring of chronic alcoholic mothers.* Lancet, 1973. 1:1267-1271

Jones, K.L. and Smith, D.W., *Recognition of the fetal alcohol syndrome in early infancy.* Lancet, 1973. 2:999-1001.

Jueptner, M., et al., *Localization of a cerebellar timing process using PET.* Neurology, 1995. 45:1540-1545.

Karachot, L., et al., *Stimulus parameters for induction of long-term depression in in vitro rat Purkinje cells.* Neuroscience Research, 1994. 21(2):161-168.

Keele, S.W., et al., *Do perception and motor production share common timing mechanisms: A correlational analysis.* Acta Psychologica, 1985. 60(2):173-191

Kim, J.J. and Thompson, R.E., *Cerebellar circuits and synaptic mechanisms involved in classical eyeblink conditioning.* Trends in Neurosciences, 1997. 20(4):177-181.

Kleim, J.A., et al., *Synapse formation is associated with memory storage in the cerebellum.* Proceedings of the National Academy of Sciences, 2002. 99(20):13228-13231.

Knuttinen, M.G., et al., *Electromyography as a recording system for eyeblink conditioning with functional magnetic resonance imaging*. Neuroimage, 2002. 17:977-987

Konrad, K., et al., *Development of attentional networks: an fMRI study with children and adults.* Neuroimage, 2005. 28(2):429-439.

Kreis, R., et al., *Development of the human brain: in vivo quantification of metabolite and water content with proton magnetic resonance spectroscopy*. Magnetic Resonance in Medicine, 1993. 30:424-437.

Kwong, K.K., et al., *Dynamic magnetic resonance imaging of human brain activity during primary sensory stimulation*. Proceedings of the National Academy of Sciences of the United States of America, 1992. 89(12):5675-5679

Lavond, D.G. and Steinmetz, J.E., *Acquisition of classical conditioning without cerebellar cortex*. Behavioural Brain Research, 1989. 33:113-164.

Leiner, H.C., et al., *Cognitive and language functions of the human cerebellum.* Trends in Neurosciences, 1993. 16(11):444-447.

Leiner, H.C., et al., *The underestimated cerebellum.* Human Brain Mapping, 1994. 2(4):244-254.

Lemoine, P., et al., *Les enfants de parents alcooliques: Anomalies observées a propos de 127 cas*. Ouest Medical, 1968. 21

Lindquist, D.H., et al., *Cerebellum and Eyeblink Conditioning*, in *Handbook of the Cerebellum and Cerebellar Disorders*. 2013, Springer. 1175-1190.

Luft, A.R., et al., *Patterns of age-related shrinkage in cerebellum and brainstem observed in vivo using three-dimensional MRI volumetry*. Cerebral Cortex, 1999. 9(7):712-721

Luna, B., et al., *Neocortical system abnormalities in autism An fMRI study of spatial working memory.* Neurology, 2002. 59(6):834-840.

Lundy-Ekman, L., et al., *Timing and force control deficits in clumsy children.* Journal of Cognitive Neuroscience, 1991. 3(4):367-376.

Lutz, K., et al., *Tapping movements according to regular and irregular visual timing signals investigated with fMRI.* Neuroreport, 2000. 11(6):1301-1306.

Madge, E.M., et al., *Junior South African Individual Scales*. Pretoria: Human Sciences Research Council, 1981.

Mattson, S.N. et al., *A decrease in the size of the basal ganglia following prenatal alcohol exposure: a preliminary report*. Neurotoxicology and Teratology, 1994. 16(3)283-289

Mattson, S.N. et al., *Heavy prenatal alcohol exposure with or without physical features of fetal alcohol syndrome leads to IQ deficits*. Journal of Pediatrics, 1997. 131:718-721.

Mattson, S.N. et al., *Fetal alcohol spectrum disorders: neuropsychological and behavioral features*. Neuropsychology Review, 2011. 21:81-101.

Mauk, M.D., *Roles of cerebellar cortex and nuclei in motor learning: contradictions or clues?* Neuron, 1997. 18(3):343-346.

Mauk, M.D., et al., *Cerebellar function: Coordination, learning or timing?* Current Biology, 2000. 10:R522-R525

Mauk, M.D and Buonomano, D.V., *The neural basis of temporal processing*. Annual Review of Neuroscience, 2004. 27:307-340

May, P.A., et al., *Epidemiology of fetal alcohol syndrome in a South African community in the Western Cape Province.* Americal Journal of Public Health, 2000. 90(12):1905.

May, P.A., et al., *The epidemiology of fetal alcohol syndrome and partial FAS in a South African community.* Drug and Alcohol Dependence, 2007. 88(2):259-271.

McCormick, D.A., et al., *Initial localization of the memory trace for a basic form of learning.* Proceedings of the National Academy of Sciences, 1982. 79(8):2731-2735.

Medina, J.F., et al., *Mechanisms of cerebellar learning suggested by eyelid conditioning.* Current Opinion in Neurobiology, 2000. 10(6):717-724.

Meintjes, E.M., et al., *An fMRI study of magnitude comparison and exact addition in children.* Magnetic Resonance Imaging, 2010. 28(3):351-362.

Meintjes, E.M., *Tensor-based morphometry reveals brain midline tissue reduction in children with heavy prenatal alcohol exposure*. Alcoholism: Clinical and Experimental Research, 2013. 37:105A.

Miller, M.J., et al., *fMRI of the conscious rabbit during unilateral classical eyeblink conditioning reveals bilateral cerebellar activation.* Journal of Neuroscience, 2003. 23(37):11753-11758.

Molchan, S.E., et al., *A functional anatomical study of associative learning in humans.* Proceedings of the National Academy of Sciences of the United States of America, 1994. 91:8122-8126

Nagarajan, S.S., et al., *Practive-related impovements in somatosentory interval discrimination are temporally specific but generalize across skin location, hemisphere, and modality.* The Journal of Neuroscience, 1998. 18(4):1559-1570

Narum, S.R., *Beyond Bonferroni: Less conservative analyses for conservation genetics*. Conservation Genetics, 2006. 7:783-787

Nicholson, D.A. and J.H. Freeman Jr, R.F., *Selective developmental increase in the climbing fiber input to the cerebellar interpositus nucleus in rats.* Behavioral Neuroscience, 2004. 118(5):1111.

Nitschke, M.F., et al., *Somatotopic motor representation in the human anterior cerebellum A high-resolution functional MRI study.* Brain, 1996. 119(3):1023-1029.

O'Boyle, D.J. et al., *The accuracy and precision of timing of self-paced, repetitive movements in subjects with Parkinson's disease*. Brain, 1996. 119(1):51-70

Ogawa, S., et al., *Intrinsic signal changes accompanying sensory stimulation: functional brain mapping with magnetic resonance imaging.* Proceedings of the National Academy of Sciences of the United States of America, 1992. 89(13):5951-5955

Ohyama, T., et al., *What the cerebellum computes*. Trends in Neuroscience, 2003. 26(4):222-227

Oullier, O., et al., *Neural substrates of real and imagined sensorimotor coordination.* Cerebral Cortex, 2005. 15(7):975-985.

Pauling, L. and Coryell, C.D., *The magnetic properties and structure of hemoglobin, oxyhemoglobin and carbonmonoxyhemoglobin.* Proceedings of the National Academy of Sciences of the United States of America, 1936. 22(4): p. 210.

Penhune, V.B., et al., *Cerebellar contributions to motor timing: a PET study of auditory and visual rhythm reproduction.* Journal of Cognitive Neuroscience, 1998. 10(6):752-765.

Perrett, S.P., et al., *Cerebellar cortex lesions disrupt learning-dependent timing of conditioned eyelid responses.* The Journal of Neuroscience, 1993. 13(4):1708-1718.

Pouwels, P.J., et al., *Regional age dependence of human brain metabolites from infancy to adulthood as detected by quantitative localized proton MRS*. Pediatric Research, 1999. 46:474-485.

Provencher, S.W., *LCModel & LCMgui User's Manual*. Available at: http://www.s-provencher.com/pages/lcm-manual.shtml. 2008

Purcell, E.M. et al., *Resonance absorption by nuclear magnetic moments in a solid.* Physical Review, 1946. 69:37-38

Purves, D., et al., *Neuroscience 5th ed*., Sinauer Associates. 2012

Ramnani, N., et al., *Learning-and expectation-related changes in the human brain during motor learning*. Journal of Neurophysiology, 2000. 84:3026-3035.

Rickson, C., *Anatomy Picture Reference and Health News: Cerebellum Diagram*, Available at: *http://www.ehealthideas.com/2013/10/cerebellum-diagram.html*. 2013.

Rivkin, M.J., et al., *A functional magnetic resonance imaging study of paced finger tapping in children.* Pediatric Neurology, 2003. 28(2):89-95.

Rorden, C. and Brett, M., *Stereotaxic display of brain lesions*. Behavioural Neurology, 2000. 12:191-200.

Schmahmann, J.D., et al., *MRI atlas of the human cerebellum*. 2000: Access Online via Elsevier.

Schlerf, J.E., et al., *fMRI measurements of the cerebellar response to nonrhythmic movements*. In: Annual Meeting of the Society for Neuroscience; Atlanta, 2006.

Schlerf, J.E., et al., *Timing of rhythmic movements in patients with cerebellar degeneration.* The Cerebellum, 2007. 6:221-231

Schmahmann, J.D., et al., *MRI atlas of the human cerebellum*. 2000: Access Online via Elsevier

Schott, J.M., et al., *Short echo time proton magnetic resonance spectroscopy in Alzheimer's disease: a longitudinal multiple time point study*. Brain, 2010. 133:3315-3322.

Schreurs, B.G., et al., *Lateralization and behavioral correlation of changes in regional cerebral blood flow with classical conditioning of the human eyeblink response*. Journal of Neurophysiology, 1997. 77:2153-2163

Simmonds, D.J., et al., *Functional brain correlates of response time variability in children.* Neuropsychologia, 2007. 45(9):2147-2157.

Sowell, E.R., et al., *Abnormal development of the cerebellar vermis in children prenatally exposed to alcohol: size reduction in lobules I–V*. Alcoholism: Clinical and Experimental Research, 1996. 20:31-34.

Spencer, R., et al., *Disrupted timing of discontinuous but not continuous movements by cerebellar lesions*. Science, 2003. 300:1437-1439.

Spencer, R., et al., *Cerebellar activation during discrete and not continuous timed movements: an fMRI study*. Neuroimage, 2007. 36(2):378-387.

Spencer, R., et al., *Evaluating dedicated and intrinsic models of temporal encoding by varying context*. Philosophical Transactions of the Royal Society B: Biological Sciences, 2009. 364(1525):1853-1863

Stanley, J.A., et al., *Reduced N-acetyl-aspartate levels in schizophrenia patients with a younger onset age: A single-voxel ^{1}H spectroscopy study*. Schizophrenia Research, 2007. 93:23-32.

Stanton, M.E. and Goodlett, C.R., *Neonatal ethanol exposure impairs eyeblink conditioning in weanling rats.* Alcoholism: Clinical and Experimental Research, 1998. 22:270-275.

Steinmetz, J.E., *Neuronal activity in the rabbit interpositus nucleus during classical NM-conditioning with a pontine-nucleus-stimulation CS.* Psychological Science, 1990. 1(6):378-382.

Steinmetz, J.E., *Brain substrates of classical eyeblink conditioning: a highly localized but also distributed system*. Behavioral Brain Research, 2000. 110:13-24.

Stoodley, C.J., *The cerebellum and cognition: evidience from functional imaging studies*. The Cerebellum, 2012. 11(2):352-365

Stoodley, C.J. and Schmahmann, J.D., *Functional topography in the human cerebellum: a meta-analysis of neuroimaging studies.* Neuroimage, 2009. 44(2):489-501.

Stoodley, C.J. and Schmahmann, J.D., *Evidence for topographic organization in the cerebellum of motor control versus cognitive and affective processing*. Cortex, 2010. 46(7):831-844

Streissguth, A.P. and O'Malley, K., *Neuropsychiatric implications and long-term consequences of fetal alcohol spectrum disorders*. Seminars in Clinical Neuropsychiatry, 2000. 5(3):177-190.

Taylor, P.A., et al., *A DTI-based tractography study of effects on brain structure associated with prenatal alcohol exposure in newborns.* Human Brain Mapping, *in press*.

Tesche, C.D. and Karhu, J.J., *Anticipatory cerebellar responses during somatosensory omission in man.* Human Brain Mapping, 2000. 9:119-142.

Tisdall, M., et al., *MPRAGE using EPI navigators for prospective motion correction*. in *Proceedings of the 17th annual meeting of International Society of Magnetic Resonance in Medicine*. 2009.

Tsai, G.E., et al., *Increased glutamatergic neurotransmission and oxidative stress after alcohol withdrawal.* American Journal of Psychiatry, 1998. 155:726-732.

Van der Knaap, M.S., et al., *^{1}H and ^{31}P magnetic resonance spectroscopy of the brain in degenerative cerebral disorders*. Annals of Neurology, 1992. 31:202-211.

Van der Kouwe, A.J., et al., *Brain morphometry with multiecho MPRAGE.* Neuroimage, 2008. 40(2):559-569.

Voogd, J. and Glickstein, M., *The anatomy of the cerebellum.* Trends in Cognitive Sciences, 1998. 2(9):307-313.

Wang, S.S.H., et al., *Coincidence detection in single dendritic spines mediated by calcium release.* Nature Neuroscience, 2000. 3(12):1266-1273.

Watson, P., *Nonmotor functions of the cerebellum.* Psychological Bulletin, 1978. 85(5):944.

Wing, A.M., et al., *Motor disorder and the timing of repetitive movementsa*. Annals of the New York Acadedy of Sciences, 1984. 423(1):183-192

Wing, A.M. and Kristofferson, A.B., *Response delays and the timing of discrete motor responses.* Perception & Psychophysics, 1973. 14(1):5-12.

Winsberg, M.E., et al., *Decreased dorsolateral prefrontal N-acetyl aspartate in bipolar disorder.* Biological psychiatry, 2000. 47(6):475-481.

Wissmann, P. Available from: http://homepage.smc.edu/wissmann_paul/physnet/anatomynet/anatomy/neurolink.html

Witt, S.T., et al., *Functional neuroimaging correlates of finger-tapping task variations: an ALE meta-analysis.* Neuroimage, 2008. 42(1):343-356.

Woodruff-Pak, D.S. and Disterhoft, J.F., *Where is the trace in trace conditioning?* Trends in Neurosciences, 2008. 31(2):105-112.

Woodruff-Pak, D.S., et al., *MRI-assessed volume of cerebellum correlates with associative learning*. Neurobiology of Learning and Memory, 2001. 76(3):342-357

Woods, K., et al., *Poorer recruitment of intraparietal sulcus in number processing in fetal alcohol spectrum disorders.* Proceedings of the 19th Annual Meeting of the Organization for Human Brain Mapping (OHBM 2013), Seattle, WA, USA, June 16-20, 2013 (#2667).

Worsley, K.J. et al., *A three-dimensional statistical analysis for CBF activation studies in human brain*. Journal of Cerebral Blood Flow and Metabolism, 1992. 12(900)

Wright, B.A. et al., *Learning and generalization of auditory temporal-interval discrimination in humans*. The Journal of Neuroscience, 1997. 17(10):3956-3963

Yeo, C.H., *Cerebellum and classical conditioning of motor responses.* Annals of the New York Academy of Sciences, 1991. 627(1):292-304.

Yeo, C.H. and Hardiman, M.J., *Cerebellar cortex and eyeblink conditioning: a reexamination.* Experimental Brain Research, 1992. 88(3):623-638.

Yeo, C.H. and Hesslow, G., *Cerebellum and conditioned reflexes*. Trends in Cognitive Sciences, 1998. 2(9):322-330

Zelaznik, H.N., et al., *Dissociation of explicit and implicit timing in repetitive tapping and drawing movements.* Journal of Experimental Psychology: Human Perception & Performance, 2002. 28:575-588

Zelaznik, H.N., et al., *Timing variability in circle drawing and tapping: Probing the relationship between event and emergent timing.* Journal of Motor Behaviour, 2005. 37(5):395-403